

Effect of Wind Load on Various Geometrical Tall Buildings

Thesis

Submitted to the



**G. B. Pant University of Agriculture & Technology
Pantnagar -263145 Uttarakhand, India**

By

Vaibhav Saxena

ID. No. 56974

**IN PARTIAL FULFILMENT OF THE REQUIREMENTS
FOR THE DEGREE OF**

Master of Technology

In

**Civil Engineering
(Structural Engineering)**

September, 2022

ACKNOWLEDGEMENT

First of all I bow my head before 'God' who inspired me to face challenges of uneven times. All my sincere gratitude goes to him for the help he has given to me and his unfailing mercies over my life.

The author expresses his deep sense of reverence and heartfelt gratitude to Dr. Astha Verma, Assistant Professor, Department of Civil Engineering and Chairperson of Advisory Committee for her invaluable guidance, constant encouragement, abundant counsel and constructive suggestions throughout the investigation. The author is extremely indebted to her and thanks her from the bottom of his heart.

With profound sense of gratitude, the author expresses his warmest thanks to the members of Advisory Committee, Mr. S.K. Katariya, Associate Professor, Department of Civil Engineering and Dr. V.K Verma, Assistant Professor, Department Civil Engineering their inspiring and constructive suggestions at every stage of this study.

The author tenders his sincere thanks to Dr. Kiran P. Raverkar, Dean, College of Post Graduate Studies, Dr. Alaknanda Ashok, Dean, College of Technology and Dr. P. S. Mahar, Professor and Head, Department of Civil Engineering, for their ardent engrossment and assiduous efforts in providing all the necessary facilities for the completion of the research.

I am also thankful to AICTE, MHRD for providing financial assistance and support.

The author owes a very special word of thanks to his father Mr. Vinod Saxena, mother Mrs. Ragni Saxena, Brothers Pranshu Saxena and Himanshu Saxena for their boundless, generosity, everlasting inspiration, blessing abundant love and affection throughout.

This list is obviously incomplete but allow me to submit as the omissions are inadvertent and I once again record my heartfelt gratitude to all those who helped me directly or indirectly in this endeavour.

Pantnagar
September, 2022



(Vaibhav Saxena)
Author

CERTIFICATE-I

This is to certify that the thesis entitled “**Effect of Wind Load on Various Geometrical Tall Buildings**”, using Ansys CFX submitted in partial fulfilment of the requirements for the degree of **Master of Technology in Civil Engineering** with major in **Structural Engineering**, of the College of Post-Graduate Studies, G. B. Pant University of Agriculture and Technology, Pantnagar, is a record of bonafide research carried out by **Mr. Vaibhav Saxena, ID. No. 56974**, under my supervision and no part of the thesis has been submitted for any other degree or diploma.

The assistance and help received during the course of this investigation have been acknowledged.

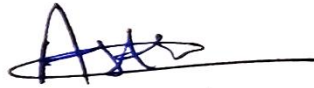
Pantnagar
September, 2022



(Astha Verma)
Chairperson
Advisory Committee

CERTIFICATE-II

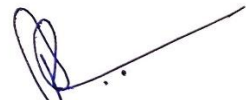
We, the undersigned, members of the Advisory Committee of **Mr. Vaibhav Saxena, ID. No. 56974**, a candidate for the degree Master of Technology in Civil Engineering with major in **Structural Engineering**, agree that the thesis entitled “**Effect of Wind Load on Various Geometrical Tall Buildings**” may be submitted in partial fulfilment of the requirements for the degree.



(Astha Verma)
Chairperson
Advisory Committee



(S. K. Katariya)
Member



(V. K. Verma)
Member

TABLE OF CONTENT

S. No.	Title	Page No.
1	INTRODUCTION	1-12
1.1	Overview	1
1.2	Loads acting on a structure	2
1.2.1	Dead loads	3
1.2.2	Live loads	3
1.2.3	Wind loads	3
1.2.4	Snow loads	4
1.2.5	Earthquake loads	4
1.2.6	Other load and Effects acting on a Structure	5
1.3	Types of Structural Systems in High Rise Buildings	5
1.3.1	Braced-frame structural system	6
1.3.2	Rigid-frame structural system	6
1.3.3	Wall-frame system (dual system)	7
1.3.4	Shear wall system	7
1.3.5	Core and outrigger structural system	7
1.4	Need of study	7
1.5	Types of Wind Design	8
1.5.1	Environmental wind studies	8
1.5.2	Wind load on the facade	9
1.6	Method of evaluation	9
1.6.1	Design wind pressure	9
1.6.2	Wind Speed	9
1.6.3	Design wind load	10
1.6.4	Determination of pressure coefficient	11
1.7	Objective and scope	11

2	LITERATURE REVIEW	13-20
2.1	General	13
2.2	Codal Provision available	13
2.2.1	Indian Standard	13
2.2.2	American Standard	14
2.2.3	Australia and New Zealand Standard	14
2.2.4	British Standard	14
2.2.5	European Standard	14
2.3	Research publications available	15
3	MATERIALS AND METHODS	21-35
3.1	General	21
3.2	Modelling and Analysis performed	22
3.2.1	Mean wind profile with height	22
3.2.2	Power law	23
3.3	Procedure	23
4	RESULT AND DISCUSSION	36-70
4.1	Pressure distribution	36
4.2	Velocity distribution	62
4.3	Pressure Coefficient	70
5	SUMMARY AND CONCLUSION	73-74
5.1	Summary	73
5.2	Conclusion	73
5.3	Future scope	74
	LITERATURE CITED	
	CURRICULUM VITAE	
	ABSTRACT	
	English	
	Hindi	

LIST OF TABLES

Table No.	Title	Page no.
3.1	Prototype and model dimension of square shaped building	22
3.2	Prototype and model dimension of triangular shaped building	22
4.1	Value of C_p for different codes	70
4.2	Pressure coefficient C_p for different faces at different angles	71
4.3	Pressure coefficient C_p for different faces at different angles	71

LIST OF FIGURES

Figure No.	Title	Page No.
1.1	Horizontal earthquake forces	5
3.1	ANSYS workbench	24
3.2	Square shaped building	25
3.3	Square shaped building with domain	25
3.4	Square cross section building with all faces	26
3.5	Triangular shaped building	27
3.6	Triangular shaped building with domain	27
3.7	Domain dimension	28
3.8	Domain (virtual wind tunnel)	28
3.9	Meshing workbench	30
3.10	Square building with meshing	31
3.11	Triangular building with meshing	31
3.12	Triangular cross section building with all faces	32
3.13	Setup workbench	34
3.14	Power law expression and plot	34
4.1	Direction of wind from 0° to 90° wind incidence angle	37
4.2	Contour plot for Face A and Face B at 0° angle of wind incidence	38
4.3	Contour plot for Face C and Face D at 0° angle of wind incidence	39
4.4	Contour plot for Face A and Face B at 15° angle of wind incidence	40
4.5	Contour plot for Face C and Face D at 15° angle of wind incidence	41
4.6	Contour plot for Face A and Face B at 30° angle of wind incidence	42
4.7	Contour plot for Face C and Face D at 30° angle of wind incidence	43
4.8	Contour plot for Face A and Face B at 45° angle of wind incidence	44
4.9	Contour plot for Face C and Face D at 45° angle of wind incidence	45
4.10	Contour plot for Face A and Face B at 60° angle of wind incidence	46
4.11	Contour plot for Face C and Face D at 60° angle of wind incidence	47

4.12	Contour plot for Face A and Face B at 90° angle of wind incidence	48
4.13	Contour plot for Face C and Face D at 90° angle of wind incidence	49
4.14	Direction of wind from 0° to 180° wind incidence angle	51
4.15	Contour plot for Face A and Face B at 0° angle of wind incidence	52
4.16	Contour plot for Face C at 0° angle of wind incidence	53
4.17	Contour plot for Face A at 30° angle of wind incidence	53
4.18	Contour plot for Face B and Face C at 30° angle of wind incidence	54
4.19	Contour plot for Face A and Face B at 60° angle of wind incidence	55
4.20	Contour plot for Face C at 60° angle of wind incidence	56
4.21	Contour plot for Face A at 90° angle of wind incidence	56
4.22	Contour plot for Face B and Face C at 90° angle of wind incidence	57
4.23	Contour plot for Face A and Face B at 120° angle of wind incidence	58
4.24	Contour plot for Face C at 120° angle of wind incidence	59
4.25	Contour plot for Face A at 150° angle of wind incidence	59
4.26	Contour plot for Face B and Face C at 150° angle of wind incidence	60
4.27	Contour plot for Face A and Face B at 180° angle of wind incidence	61
4.28	Contour plot for Face C at 180° angle of wind incidence	62
4.29	Velocity streamline at 0° angle of wind incidence	63
4.30	Velocity streamline at 15° angle of wind incidence	63
4.31	Velocity streamline at 30° angle of wind incidence	64
4.32	Velocity streamline at 45° angle of wind incidence	64
4.33	Velocity streamline at 60° angle of wind incidence	65
4.34	Velocity streamline at 90° angle of wind incidence	65
4.35	Velocity streamline at 0° angle of wind incidence	66
4.36	Velocity streamline at 30° angle of wind incidence	67
4.37	Velocity streamline at 60° angle of wind incidence	67
4.38	Velocity streamline at 90° angle of wind incidence	68
4.39	Velocity streamline at 120° angle of wind incidence	68
4.40	Velocity streamline at 150° angle of wind incidence	69
4.41	Velocity streamline at 180° degree of wind incidence	69

1.1 Overview

Due to the rapid-fire increase in population, the land area around the world getting more congested day by day which increases the demand for high structures. To meet the gruelling ultramodern construction demand, expert engineering designs are required. The Wind is caused by pressure differences on the earth's surface. It changes over time and space. Because of the variable nature of wind, it is necessary to design altitudinous structures while keeping the critical goods of wind on the structure in mind. The higher the erecting, the more vulnerable to wind loads in comparison to earthquake loads. Contrivers are concerned with selecting structural systems that can withstand side loads as well as utility and inhabitant comfort conditions. These wind-related complications and the loads they impose on structures should be considered when designing a structure.

High-rise buildings are viewed as a representation of progress and civilization. From a structural standpoint, these are the constructions whose side forces generated by earthquake and wind loads will have an impact on height to the point that they will be heavily considered throughout the design phase. High-rise structure construction is a gruelling design accepted by experts and masterminds. To make a high-rise structure, one should suppose a construction design whose design depends completely on logical analysis and gauged modelling.

The structural designer must be sure that the structure is safe and serviceable for the duration of its expected life, even when subjected to wind loads. In altitudinous free-standing structures, wind is the primary source of cargo. Wind loads on a single altitudinous structure or a group of high-rise structures are critical for profitable design.

The mastermind's job is to ensure that the performance of wind-exposed structures is reasonable over their expected lifetime. The goal of structural control in building structures is to reduce climate caused by external stressors such as earthquakes and wind loading through a variety of methods such as stiffness, mass, damping, or shape revision. **(Javed and Satish 2020).**

In the design of tall structures, wind loading is one of the prime important lateral loads that need to be considered while designing. In general, occupant comfort needs to be

considered along with structural safety. A mean and a fluctuation component make up the two components of wind, a time-varying force. Eddies of various sizes and rotational features make wind a complex phenomenon. These eddies cause the wind to be turbulent and gusty in nature. Wind Loading initially was viewed as estimating the dynamic pressure of wind at the structure and then just multiplying it by some shape factor and area of a structure to obtain the wind force. However, it was later discovered that wind dynamics in nature, as well as dynamic responses such as galloping, flutter, vortex excitement, ovaling, and so on, needed to be investigated. The building shape is a well-known topic in aerodynamics optimization that has a significant impact on the behaviour of high structures under wind loads. Wind response can be reduced by optimizing the geometry of supertall structures for aerodynamics during the design stage.

1.2 Loads acting on a structure

Safety and economy are two which are taken into consideration when building a structure. The economy is impacted if the loads are appraised and taken higher. Safety is jeopardized if loads are carried at a lower rate in the interest of the economy. It is necessary to calculate the estimation of different active loads precisely. The American Standard Code ASCE 7: Minimum Design Loads for Buildings and Other Structures and the Indian Standard Code IS:875-1987 provide information on the various design loads for buildings and other structures.

Types of loads acting on a structure are

1.2.1 Dead Loads (DL)

Dead load is the initial vertical load to be taken into account. Dead loads are constant or immobile loads that are applied to a structure over its lifetime. The self-weight of structural parts, permanent partition walls, fixed permanent equipment, and the weight of various materials are the main causes of dead load. It majorly consists of the weight of roofs, beams, walls and columns, etc. which are otherwise the permanent parts of the building. In **IS 875 (part 1)-1987** The volume of each segment is multiplied by the unit weight to determine the dead loads of each construction. Plain Cement Concrete (PCC) = 24 kN/m², Reinforced Cement Concrete (RCC) = 25 kN/m².

1.2.2 Live Loads (LL)

Imposed loads, also known as living loads, are the second vertical load that is considered while designing a building. Live loads are anything that can move or is moving but not accelerating or impacting. These loads which can include the weights of mobile furniture and walls, among other things are presumptively generated by the building's planned usage or occupancy. Live loads are always fluctuating. The designer must appropriately assume these loads. One of the main loads in the design is it. In **IS 875 (part 2)-1987**, the minimum live load values that must be assumed are listed.

1.2.3 Wind Loads (WL)

Wind load is mostly a horizontal load brought on by air movement with respect to the earth. In structural design, wind load must be taken into account, especially when the building's height exceeds the dimensions transverse to the exposed wind surface.

For low-rise structures, such as those with four to five stories, the wind load is not essential since the continuous floor systems and walls between columns provide an adequate moment of resistance to withstand the effects of these forces. Further, in the limit state technique, the factor for design load is decreased to 1.2 (DL+LL+WL) when the wind is taken into account as opposed to 1.5 (DL+LL) otherwise. When designing the structure, it is important to consider the horizontal forces that the wind's various components will impose. The two variables—wind velocity and building size—have an impact on how wind loads are calculated. The **IS-875 (Part 3)-2015** provides detailed instructions for calculating wind load on structures in the sections below. The walls, roof and foundation must be strong, and the attachments between them must be strong and secure. For a structure to resist hurricane and weak tornadic winds, it must have a continuous load path from the roof to the foundation -- connections that tie all structural parts together and can resist types of wind loads that could push and pull on the building in a storm

The design wind pressure is given by

$$P_z = 0.6 V_z^2$$

where P_z is the pressure which is in N/m^2 at height z and V_z is velocity which is in m/sec . To the height of 30 m, the wind pressure is considered to act uniformly. Above 30 m height, the wind pressure also increases.

1.2.4 Snow Loads (SL)

Snow loads are another building's vertical loads. But these kinds of loads of burdens are taken into account only in areas with heavy snowfall are these kinds of loads of burdens taken into account. The **IS 875 (part 4) - 1987** addresses snow loads on building roofs. The term for the minimal snow load on a roof area or any other surface above ground that is subject to snow accumulation

$$S = \mu S_0$$

Where,

S = Design snow load on plan area of the roof.

μ = Shape coefficient

S_0 = Ground snow load.

1.2.5 Earthquake Loads (EL)

A building is subject to both vertical and horizontal forces during an earthquake. Three mutually perpendicular directions—typically regarded as the vertical and two horizontal directions—can be used to decompose the overall vibration induced by an earthquake. Vertical movement does not significantly increase the forces acting on the superstructure. But while designing, it is important to taken into account the building's horizontal movement during an earthquake.

The kind of foundation soil, the size, and method of construction, as well as the duration and severity of ground motion, all affect how the building reacts to ground

vibration. The details of these estimates for structures standing on soils that would not significantly settle or slide because of an earthquake.

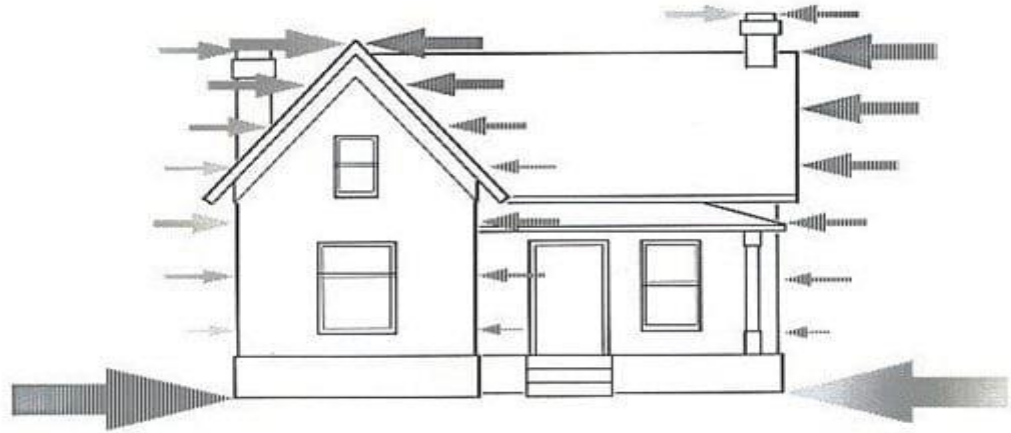


Fig. 1.1- Horizontal earthquake forces (Muffassir and Kalurkar 2016)

The seismic accelerations for the design can be calculated using the seismic coefficient, which is the ratio of seismic acceleration to gravitational acceleration. Seismic pressures are not important for monolithic reinforced concrete structures in seismic zones 2 and 3 that are no taller than 5 storeys and have a significant factor below 1.

1.2.6 Other load and effects acting on a Structure

According to IS 456 - 2000 clause 19.6, in addition to the load already mentioned, consideration must be given to the following forces and effects if they have the potential to seriously impair the structure's safety and serviceability: (a) The foundational motion (See IS 1904) (b) Elastic axial shortening (c) Pressure of the soil and fluid (See IS 875, Part 5) (d) Impact (e) Fatigue (f) Vibration (g) Erection loads (see IS 875, Part 2), and (h) The effect of stress concentration brought on by point loads and similar things.

1.3 Types of Structural Systems in High Rise Buildings

Today, skyscrapers, or high-rise buildings, are common in many cities across the globe. The first buildings over 137 feet tall to be built in Chicago in 1885 were referred to as skyscrapers. Generally speaking, it is one that requires mechanical vertical transportation for humans and is taller than the highest height. The majority of the time, these structures are only intended to serve as residential apartments, hotels, and office buildings, while they are occasionally also used in house retail and educational

establishments. Due to the fact that high-rise structures are among the largest ever constructed, their commercial and office use necessitate a great level of flexibility.

Because of this, structural systems or structural frames the collection of interconnected or dependent pieces that constitutes a complex structure are crucial for high-rise buildings. These structural systems were created and planned to withstand various loads. Consider the human body as a comparison to better comprehend the operation of structural systems. Human bones must be strong and properly positioned in order for the human body as a whole to function. Similar to how structural systems would not be able to support loads if improperly constructed. After all, nobody wants a skyscraper that collapses. This article will go through a few of the structural systems found in high-rise structures so that readers can learn more about them.

1.3.1 Braced-frame structural system

Cantilevered vertical trusses, which form the web of the vertical truss and withstand lateral loads along with girders, are the subject of this structural arrangement. This is most frequently utilized in steel buildings and is appropriate for multi-storey buildings that are between low and mid-height. The lateral stiffness and resistance of a rigid-frame system can be improved effectively and economically using this type of technology. A braced frame has the unique advantage of being affordable to design and fabricate, and it may be repeated up to the height of the building. Unfortunately, there is also a chance of making internal planning difficult and changing where doors and windows are placed.

1.3.2 Rigid-frame structural system

To endure moments produced by loads, beams and columns in this type of structure are built monolithically. For structures made of reinforced concrete, a rigid-frame system is preferable. Despite the possibility of using this method in steel buildings, the connections will be expensive. The open rectangular form does have the advantage of making window planning and installation more likely. A rigid-frame system's members can also endure shear force, axial loads, and bending moments. Just a fun fact The Burj Khalifa, the tallest building in the world, was built utilizing a rigid-frame method.

1.3.3 Wall-frame system (dual system)

A wall and frame interact horizontally to create the wall-frame or dual system, which is stronger and more rigid. In this arrangement, the walls are typically solid and located near stairwells, the building's exterior, and elevator shafts. Additionally, the walls might improve the performance of the frames by, for example, preventing a soft-story collapse.

1.3.4 Shear wall system

A continuous vertical wall made of masonry or reinforced concrete constitutes this type of system. Shear walls function as narrow-deep cantilever beams and are excellent at withstanding lateral stresses and gravity. This is frequently built into the centre of structures. This method is ideal for bracing tall buildings made of steel or reinforced concrete since shear walls have a significant amount of strength and plane stiffness. A shear wall system is also suited for residential and hotel structures with repetitive floor-by-floor planning that enables the walls to be vertically continuous. Shear walls between rooms and flats can be great acoustic and fire insulators.

1.3.5 Core and outrigger structural system

This structural structure joins the core or spine to the closely spaced outside columns, increasing the stiffness and strength of the building during overturning. Outrigger systems essentially work by joining two structural systems—a core system and a perimeter system—and causing the structure to respond similarly to a composite cantilever. The outriggers are the walls of a reinforced concrete structure and the trusses of a steel structure, respectively. Due to the increased effectiveness attained in resisting forces, this type of structural system is practically employed for structures up to 70 floors and more.

1.4 Need of study

Housing and humanity are the basic primary needs, along with food and clothing, with clean air and potable water being crucial for survival. On the other hand, most existing houses and those that will be built up in the coming decades are likely to be non-engineered, with thatched roofs that are vulnerable to wind. Strong winds are causing massive losses among rural residents by causing their houses to collapse completely or

partially due to roof lifting. Wind is the movement of air relative to the Earth, driven by several different forces, mainly pressure differences in the atmosphere, which themselves arise from the differential solar heating of different parts of Earth's surface due to which forces generated by the rotation of the Earth. Differences in solar radiation between the poles and the equator create temperature and pressure differences. Together with the effects of the earth's rotation, they create extensive circulation systems in the atmosphere with both horizontal and vertical orientations.

Strong tropical cyclones, such as hurricanes and typhoons, generate extremely strong winds over some parts of tropical oceans and coastal areas both north and south of the equator. In these types of severe storms, the wind is highly turbulent or gusty. Turbulence is produced by eddies or eddies in an air stream that is created by frictional interaction at ground level or shearing action between air moving in opposite directions relative to altitude. The two most important forces operating in the free atmosphere i.e. ground effects boundary layer, are the pressure gradient and the Coriolis force.

Though the problem of wind loadings on buildings and structures is common throughout the world, and it is expected that the solution will be similar from country to country, research in this field should be conducted by taking into account the climatic conditions and problems of this country in to obtain a clear picture of the nature of wind loading. The findings of these studies should help Indian architects, engineers, and town planners design more efficient buildings and structures.

1.5 Types of Wind Design

For wind-sensitive structures, there are usually three basic effects of wind to consider.

1.5.1 Environmental wind studies

Examine the effects of wind on the surrounding environment caused by the construction of a structure (e.g. tall buildings). This study is particularly important to assess the effect of wind on pedestrians, motor vehicles, and architectural features such as fountains, etc. that use public space in the vicinity of the proposed structure.

1.5.2 Wind load on the facade

It is used for the assessment of the design wind pressures in the entire area of the structure for the design of the cladding system. Because of the significant cost of typical facade systems relative to the total cost of very tall buildings, engineers cannot afford the luxury of conservatism while assessing design wind loads. Even the most sophisticated wind codes typically cannot adequately measure design loads due to the intricacy of building designs and the dynamic properties of wind and building structures. Wind tunnel testing to assess design loads for cladding is now common industry practice to minimize initial capital costs and more significantly avoid expensive maintenance costs related to failures due to leaks and/or structural failure. (Mendis. P *et al.* 2017).

1.6 Method of evaluation

Different methods of evaluation of building structure as given below.

1.6.1 Design wind pressure

Design wind pressure at any height above normal will be found in the next relationship between air pressure and wind speed

$$P_z = 0.6 V_z^2$$

Where,

P_z = Air pressure designing at N/m^2 at altitude 'z' m.

V_z = design wind speed in m/s

1.6.2 Wind Speed

Above the surface of the earth, where drag effects are negligible, air movements are controlled by pressure gradients in the atmosphere, which is gradually the physical consequence of variable stellar heating of the world. This upper-level wind speed is considered the gradient wind speed. From the lofty abodes of the earth, when the effects of resistance are indifferent, air movement is presently driven by pressure gradients in the atmosphere.

The basic wind speed (V_z) of any site is provided by

$$V_z = V_b \cdot k_1 \cdot k_2 \cdot k_3 \cdot k_4$$

Where,

V_z = wind speed per hour per m/s at a height of z .

V_b = the basic wind speed of the region in m/s.

k_1 = probability factor (risk coefficient).

k_2 = terrain roughness and height factor.

k_3 = topography factor.

K_4 = cyclonic region importance factor.

1.6.3 Design wind load

The operation of the incoming wind's characteristics, the regarded structure's pure mathematics, and the pure mathematics and closeness of upwind structures are all measured by the characteristics of wind pressures on a square structure. The pressures do not appear to be constant, but however extremely unstable, due to gusts of wind and jointly due to natural eddies on the perimeters of the structures themselves. Unsteady pressures can result in fatigue and dynamic excitation damage to the structure if the structure is dynamically sensitive to wind. The pressures are also not uniformly distributed over the surface of the structure, but vary with position. Once you use a style document, the complexity of wind loads must be kept in mind. Due to the many uncertainties involved, the largest wind loads known to the structure during its lifetime may differ significantly from those assumed at design.

As a result, it is not possible to determine whether or not normal wind loading is conservative or unconservative based on whether a structure fails or does not fail during a windstorm. Buildings and constructions with unusually shaped or placed square measurements are exempt from the criteria. Some forms of constructions, such towering skyscrapers and thin towers, are shaped by wind stresses. It often becomes tempting to formulate using wind tunnel experimental information in situ the coefficients given in the wind load code for these structures.

1.6.4 Determination of pressure coefficient

The pressure coefficient is defined as

$$C_p = \frac{\Delta P}{\frac{1}{2} \rho U_\infty^2}$$

Where,

$$\Delta P = P - P_o$$

P is the static pressure on the surface of the cylinder

P_o is the ambient pressure

ρ is the density of the air

U_∞ is the free stream velocity

ΔP is obtained from

$$\Delta P = -\Delta h_w \times \gamma_w$$

Where,

Δh_w is the manometer reading

γ_w is the specific weight of manometer liquid, that is water

1.7 Objective and Scope

The flow around buildings in the actual environment is very complex and the formulation of a mathematical model to predict the flow is almost impossible. Thus, the model study is a must and the results obtained under the simulated condition in the software are found to be quite satisfactory for practical purposes.

The objectives of the present study are as follows:

- a) To measure the static pressure distribution around an isolated square and triangular plan building at various wind incidence angles.

- b) To measure the pressure distributions for different side face dimensions of square and triangular plan buildings.
- c) To determine the Pressure coefficient of square and triangular plan shaped building.
- d) To determine the wind velocity around the square and triangular cross-section shape building.

CHAPTER 2

REVIEW OF LITERATURE

2.1 General

In this section, an elaborate study of the literature is essential for any expressive and fruitful research on any topic. This work is not a special case, and therefore a committed and serious investigation of the form involving various aspects related to the shape and size of the structures was completed. In a literature review, researchers studied the effect of wind forces on differently shaped models placed in a wind tunnel. Varying various parameters, the drag and lift coefficients were calculated using experimental setups as well as numerical simulation using ANSYS fluent and other related software. Using the basic knowledge gained from reading these literary works, a further study of improvisation was carried out.

2.2 Codal Provision available

There are wind regulations available for the construction of wind-resistant buildings, and they are used by designers all around the world. Different nations, like India, Australia, and New Zealand, each have a unique wind code for the design of wind-resistant structures within their borders. The evaluation of wind load and the impact of wind on high rise structures is outlined in all international wind loading regulations and standards.

2.2.1 Indian Standard (IS: 875, Part-3, 2015)

According to IS: 875 (Part 3), while designing buildings, structures, and components, wind loads must be taken into consideration. By averaging the peak gust speed across a limited window of time of around three seconds, this method creates a single wind map with the highest wind speed in meters per second. Using the most recent wind data, the wind speeds were calculated for a 50-year return period. To account for geography, local terrain, structure size, and other factors, the fundamental wind speed was modified using modification parameters. Coefficients of force and pressure were given for a variety of clad and unclad buildings as well as for certain structural components. For frames, lattice towers, walls, and hoardings, force coefficients (or drag coefficients) were calculated.

2.2.2 British Standard (BS 6399 2, 1997)

The rules established by this code of practice specify how to account for natural wind activities in the structural design of buildings and other civil engineering projects for each loading scenario. Up to a specific height, this rule of practice is applicable to projects and buildings. bridges with a maximum span of 200 meters and buildings taller than 200 meters. The regular wind behaviours on land-based constructions are also predicted by this algorithm. Members of the group For formations with irregular cross sections, there is no wind data. Pressure dispersion Information on various skews of wind must also meet this criterion.

2.2.3 American Standard (ASCE 07, 2007)

The ASCE-7 is a thorough manual on wind loads on low-rise structures with various roof types. This standard also applies to low-rise structures with different aspect ratios. Data on wind loads on high-rise structures with various cross-sectional shapes, however, are scarce. In the event of skew wind, there is no information provided.

2.2.4 Australia and New Zealand Standard (AS/NZS-1 170-2, 2021)

This code of practice applies to structures that meet the following criteria: a roof height of 200 meters or less and a span of less than 100 meters. This regulation covers wind loads for projects other than offshore ones, like transmission towers and bridges. The only cross-sectional shapes mentioned in this code of practice are square and rectangular. The pressure distribution that occurs when a building is hit by a skew wind angle is seldom ever studied.

2.2.5 European Standard (EN 1991-1-4:2005)

EN 1991-1-4 can only be used for structures and civil engineering projects up to a height of 200 m, as well as for bridges with a maximum span of 200 m. The main focus of EN 1991-1-4 is the wind loading on the total number of structures. This encompasses the entire structure, individual structural components, and any attached elements, such as safety and sound barriers, cladding pieces, and their fasteners.

2.3 Research Publications

Murakami *et al.* (1988) authors studied the k- ϵ two-equation turbulence model-based numerical simulation of the airflow around a cubic model in three dimensions. Numerous factors influence the consequences of the numerical modelling of wind flow around the building model. To determine the effect of work separating framework and boundary conditions on simulated outcomes, seven scenarios of numerical replication of the wind flow around a cubic model were examined. The accuracy of these reproductions has been analyzed by the company contrasting with expected results and controlled wind tunnel tests. That was confirmed by a numerical recreation using the k- ϵ sample accurately mimics the speed of a mass field with a fine determination of work around the model.

Tamura and Kawai (1997) author studied wind loading on buildings and other structures was researched using computational fluid dynamics (CFD). Ten working group participants in the AIJ project calculated the flows and pressures around a low-rise building (width: depth: height=1: 1: 0.5), primarily using the k-model or the large eddy simulation for turbulent flows.

Meroney *et al.* (1999) authors studied the flow and dispersion of gases emitted by various sources located near different building shape studied separately in different wind tunnels were determined using the commercial forecasting model fluent using standard k- ϵ , and the calculations are compared with wind tunnel measurements, but no special effort was made to match the forces, numerical and experimental data after adjustment, coefficients, surface roughness, initial conditions.

Liu (2012) studied a numerical flow model in combination with a realizable k- ϵ turbulence model for a compressible viscous fluid to simulate flow perpendicular to one wall of a cube in a straight rectangular duct, and the equations are solved by the finite volume method. The calculated distribution of the velocity field shows that the proposed model is reliable and can be used for the numerical simulation of turbulent pipe flow.

Sevaliaa *et al.* (2012) studied was made to study the effect of different geometric plan configurations such as square, circle, hexagon and octagon of a tall building with the same floor plan area on the force coefficient. A Computational Fluid Dynamics (CFD) Code called Fluent / Gambit was used to create 3-D wind flow conditions around a tall

building in order to analyse the impact of the wind. Numerical computations were then carried out to determine the pressure coefficient and wake area surrounding the building. According to this study, tall buildings with circular plans have the lowest wind pressure coefficient and those with square plans have the highest. The octagonal plan shape tall building with a sharp windward edge is more effective in reducing the wind pressure coefficient than the hexagonal plan shape of a tall building with a sharp windward edge.

Tang *et al.* (2013) authors studied wind resistance on tall buildings of different shapes using computational fluid dynamics. With the increase in sides of the polygon, the drag coefficient of the extruded tower decreases, and eventually it converged with the circular tower. The results also show consistent reducing wind resistance while using rounded corners on a polygonal cross-section and as the radius of the round corner gradually increases. This paper too investigates the effect of twisting on a structure to reduce wind. Design Experiments have shown that wind resistance can be reduced if the building is twisted appropriately.

Raj and Ahuja (2013) studied an experimental study on a rigid model of tall buildings with varying cross-sectional shapes, but with equal floor area, in an open circuit boundary wind tunnel to calculate the wind forces acting on them. It was observed that the base shear, base moment, and twisting moments developed due to wind loads are not only influenced by wind directions but also highly affected by cross-sectional shapes.

Verma *et al.* (2013) authors studied a rigid Perspex model of a square floor plan of a tall building sheet in the closed circuit of the wind tunnel under the boundary layer flow. Wind pressure coefficient calculated from wind pressure values measured at many pressure points on all 4-wall surfaces of the model. Results of an experimental study were presented in the form of pressure contours.

Chakraborty *et al.* (2013) authors studied the pressure exerted on the various surfaces of the "+" floor plan tall building. The Computational Fluid Dynamics (CFD) technique was used to evaluate the pressure on the various model faces for wind incidence angles of 0° and 45° . The analysis was performed using ANSYS FLUENT with the k- ϵ viscosity model and the obtained results were compared with the wind tunnel test results. Generally, good agreement between the results was observed for both wind angles. In addition, a square plan model for a normal angle of incidence was analyzed to verify the

reliability of the code. The face of the "+" model has the shape of a plan and shows a different pressure distribution compared to the square-shaped model with a large difference observed in the case of the side surfaces. The flow pattern around the model was also studied to understand the various phenomena occurring around the building. Numerical analysis together with experimental data can provide useful data for calculating wind loads on such structures.

Arya et al. (2014) authors studied the wind speed and structural response of building frames on sloping terrain was studied and analysed. Considering different frame geometries and terrain slopes. A combination of static and wind loads is considered. There are many types of sloping terrain for a combination of 60 cases in different wind zones and three different heights of a building frame were analysed. STAAD-Pro software was used for analysis purposes. The results are collected in terms of storey drift, shear force, moment, axial force, support reaction, and displacement, which were critically analysed to account for the effects of different terrain slopes.

Dagnew and Bitsuamlak (2014) authors studied the aerodynamic wind load on a conventional tall building. The authors employed open terrain flow parameters to specify the transient inlet boundary of the LES simulations, which were recorded downstream of an empty boundary layer wind tunnel (BLWT). To determine if they were suitable for LES, three distinct numerically generated inflow boundary conditions were examined.

Reddy (2015) authors investigated the wind analysis of tall reinforced concrete stacks by random vibration approach and codal methods from India (IS 4998 (Part 1)), America (ACI 307) and Australia (AS/NZS1170.2). For analysis based on the random vibration approach, the RC chimney is modelled as a multi-degree-of-freedom system subjected to static loading due to the mean wind speed component and dynamic loading due to the variable velocity component. The variable component of the wind speed at a point is cautious as a temporal random process. subsequently, code procedures for downwind analysis of tall RC stacks from Indian, American and Australian codes are reviewed. Four RC stacks were analysed using these methods to obtain their response. It was found that the codal methods of analysis along the wind are basic, they were not ready to estimate the deflection of chimneys and produce mixed results. Simplifying assumptions used in the codes were also discussed.

Bhattacharyya and Dalui (2015) authors studied the force and pressure coefficients of an unsymmetrical shape of a tall building under wind excitation. The floor plan of the building is asymmetrical in both directions (downwind and across the direction of the wind). The experimental and numerical study is carried out by wind tunnel boundary layer wind tunnel test and Computational Fluid Dynamics (CFD) technique using ANSYS software, respectively to study the above model under wind excitation.

Yadav and Jignesh (2016) authors studied CFD simulation performed for a specific arrangement of a group of tall buildings. The pressure coefficients on the same were studied using the Computational Fluid Dynamics (CFD) technique. Buildings of different heights were taken into account by the authors. The effect of different wind incidence angles on the pressure coefficients on all walls of the main building was investigated. Also, pressure coefficient contours on all faces of all buildings are plotted for wind incidence angles of 0° , 30° , 60° , and 90° . ANSYS CFX was used to perform CFD simulation.

Muffassir and Kalurkar (2016) author studied that high-rise structure or building is a must for metro cities. RC multi-storey high-rise buildings were inherently larger and less elastic composite structures. This study investigates the similarity or comparison between RCC and composite structure under the effect of wind, in addition, the composite structure also includes different plan configurations. This study has a total of 15 buildings models arranged and was analyzed for wind load using ETABS 2015 software. Different software is working on wind and earthquake analysis but they chose ETABS 2015 software. Wind analysis is done for different heights like 20 m, 50 m, and 80 m, in this order. Summing up the comparative study, it was concluded that the structure of the compounds was more elastic in nature and at risk compared to the RCC structure and the composite option is better than RCC for multi-storey structures. The entire study were monitored in software analysis. In addition, the comparison of different design configurations shows the response of parameters such as story displacement, story stiffness, base response and time period under wind action. The reason for this analysis is to reach a conclusion about the most effective shape of the structure in the horizontal zone.

Mendis *et al.* (2017) authors studied urban habitats around the world which become increasingly congested with growing populations, and the need for tall buildings

is as high as ever. Sri Lanka is currently experiencing this reality as Colombo's skyline is expanding rapidly with a large number of up-and-comers complex high-rise buildings. The response of tall buildings to wind forces is a critical design criterion and which requires both conventional force-based designs and performance-based solutions. This paper discusses these challenges and the technical solutions required to successfully design a tall building which were not only stable, safe, and strong under wind loads, but also performs well and provides a usable and highly functional design.

Kumar and Reddy (2017) studied an experiment to evaluate the distribution of wind pressure on all four sides of a rectangular tall building with a ratio of 1:1.5:7. The model is made of an acrylic plate on a geometric scale of 1:300 with floor plan dimensions of 10 cm × 15 cm and a height of 70 cm. The model is to be tested using boundary layer wind twelve angles are taken given in bracket (0°,5°,10°,15°,25°,33.5°,45°,56.5°,60°,75°,87.5°, and 90°) of wind incidence under steady flow conditions. The mean and standard deviation of pressure coefficients, drag and lift coefficients downwind and perpendicular to the wind direction, and mean moment coefficient were calculated as pressure measurements on the model.

Li et al. (2018) Although relevant design programmes included empirical methods for calculating wind loads and wind-induced responses on square high-rise structures, it is still necessary to quantify how corner alteration procedures affect these variables. In order to establish spatial-temporal changing pressure distributions, wind pressure measurements for a benchmark square high-rise building and three corner modified square high-rise structures were first carried out. Furthermore, full-scale finite element models were created in ANSYS software to obtain dynamic properties. Wind loads and wind-induced responses of four square high-rise buildings were calculated and compared using wind tunnel test results and modal analysis to design the best aerodynamic treatment for reducing wind effects on square buildings.

Javed and Kumar (2020) studied the population is rising veritably fleetly has forced to emphasis on the design and construction of multilevel altitudinous structures. Civil Engineering is an abecedarian element of our society. The altitudinous structures of structures were designed to persist the rigid loads still, they may be exposed to dynamic cargo similar to wind effects, cyclones, earthquakes, etc. The impact of wind loads is to consider in the design of high-rise structures as there were numerous failures of structures

that have appeared in India due to wind. From the present study, it can be concluded that wind goods are significant compared to the graveness effect. The author examines these difficulties and the engineering solutions that were necessary to create an altitudinous structure which were not only stable, safe, and robust under wind loads but also performed superbly, providing a useful and mainly functional design structure.

Sanyal and Dalui (2021) author studied the Y-shaped building which was usually a symmetrical building where three separate branches are bridged in the central part of the core. Due to some technical or architectural requirements, the symmetry between the wings were not properly maintained and the modification of the arm angle is unavoidable. By changing the internal angles between the arms by 30° for various wind incidence angles (WIA) from 0° to 180° at 30° intervals, this work presents a thorough investigation of the mean pressure, force, and moment coefficients of several types of tall buildings with a "Y" plan shape. The size of the limbs was adjusted somewhat in order to preserve the same projected area. Numerical analysis was performed to generate a similar flow type as per IS:875 (Part 3) –2015 terrain category II. ANSYS CFX is used for simulation. To verify the current computational setup, a graphical comparison is made on the Commonwealth Advisory Aeronautical Research Council (CAARC) building model. Some previous wind tunnel results on a "Y" shaped building were also compared with our numerical data. For each 'Y' building model, the surface pressure distribution, mean pressure coefficients, and force coefficients was evaluated and the results were graphically displayed to understand the extent of discrepancies caused by these angular adjustments in the plan.

Raj et al. (2022) author studied the use of CFD (Computational Fluid Dynamics) and the k-turbulence model in ANSYS: CFX, this study has been conducted to understand the wind flow characteristics of an isolated tall building (Model A) (Analysis of Computational Fluid Dynamics program). Model A is 192 metres tall and has two different cross sections: plus and square, each of which is 96 metres tall. It is exposed to winds of 10 m/s strength at four different incidence angles: 0° , 30° , 60° , and 90° . According to pressure contours derived from simulation, all lateral faces of the Model A (suggested design model) exhibit a similar pressure impact for incident wind angles of 0° and 90° . While the pressure impact on wind ward faces (A and C) is lessened at incidence wind angles of 30° and 60°

CHAPTER 3

MATERIALS AND METHODS

Currently, both studies with models and full-scale buildings are being created performed to compare the result for different validity of the first. But full scale experiments are costlier and difficult to perform. Current around buildings in the real environment is very complex and the formulation of the mathematical model predicting the flow is almost impossible. So, a model study is a must and the results obtained by simulation are found to be quite satisfactory for practical purposes.

3.1 General

The following design criteria must be met while designing a tall building for lateral wind loads using force methods. The strength of the building's structural elements, must be maintained without failure throughout the structure's lifetime. Serviceability is achieved when storey and total deflections are within acceptable limits. Tall buildings require deflection and displacement control to limit damage and cracking of non-load bearing elements such as the facade, internal partitions, and ceiling

In this study, two different shapes i.e. square and triangular with fillet end corners having sides of square 25 m and height is 175 m and side of triangular shaped building is 25m and heights is 125 m. The prototype building has been considered to be situated in Terrain Category The free mean wind velocity is taken as 10 m/s and each model is studied at various wind incidence angle.

This study has also been validated with wind pressure distribution of an isolated square. The wind effects of typical shape buildings were compared to those of plan shape tall buildings using CFD simulation. IS: 875 (Part- 3), 2015.

Dimension of square and triangular shaped building under the scale as shown in the table 3.1 and table 3.2

Table 3.1: Prototype and model dimension of square shaped building

Parameter	Prototype Dimension(m)	ANSYS Model Dimension(mm)	Scale of Model
Length	25	100	1:250
Height	175	700	

Table 3.2: Prototype and model dimension of triangular shaped building

Parameter	Prototype Dimension(m)	ANSYS Model Dimension(mm)	Scale of Model
Length	25	100	1:250
Height	125	500	

3.2 Modelling and Analysis performed

Engineering analysis software for a variety of fields, such as heat transfer, computational fluid dynamics, finite element analysis, and structural analysis, is published by ANSYS. The models can be simulated using a variety of turbulence models. Points were indicated on various sides of variously shaped models that were placed in a subsonic wind tunnel. It is necessary to compute and compare the forces acting on various places. Use of ANSYS is used to perform and analyse the results and mesh the model into finite elements. The forces of drag, lift, and pressure must be determined. Different turbulence models, such as the $k-\epsilon$, $k-$, and RSM (Reynolds Stress Models) models, might have been applied. However, $k-\epsilon$ is employed since it assumes that the viscosity is isotropic and that all that is required are the beginning or boundary conditions (k is the turbulent kinetic energy and is the eddy dissipation). When there are wall effects, the k -model is applied. RSM couldn't be employed since it offers an incredibly high concentration which cannot be measured experimentally.

3.2.1 Mean wind profile with height

The roughness of the earth's surface creates a drag force which affects flow of wind close to the ground. As the height rises, this effect steadily diminishes, and at a certain gradient (about 400m), this drag-force disappears. The amount of surface

roughness and drag produced by nearby projections which obstruct the wind flow define the vertical profile of wind speed. At a certain height, the effects of drag start to minimizing, this velocity is known as the gradient velocity. The atmospheric boundary layer is the height at which terrain affects wind speed.

3.2.2 Power law

As per Power Law, the atmospheric boundary layer's wind speed profile is provided by,

$$\frac{V}{V_o} = \left[\left(\frac{Z}{Z_o} \right)^{\frac{1}{\alpha}} \right]$$

Where,

V = wind velocity at height Z .

V_o = wind velocity at reference height Z_o .

Z = height above ground.

Z_o = Boundary layer nominal height (also called gradient height).

alpha = coefficient of power law.

3.3 Procedure

There are the five steps involving in the analysis of different building and workbench is shown below in Fig. 3.1.

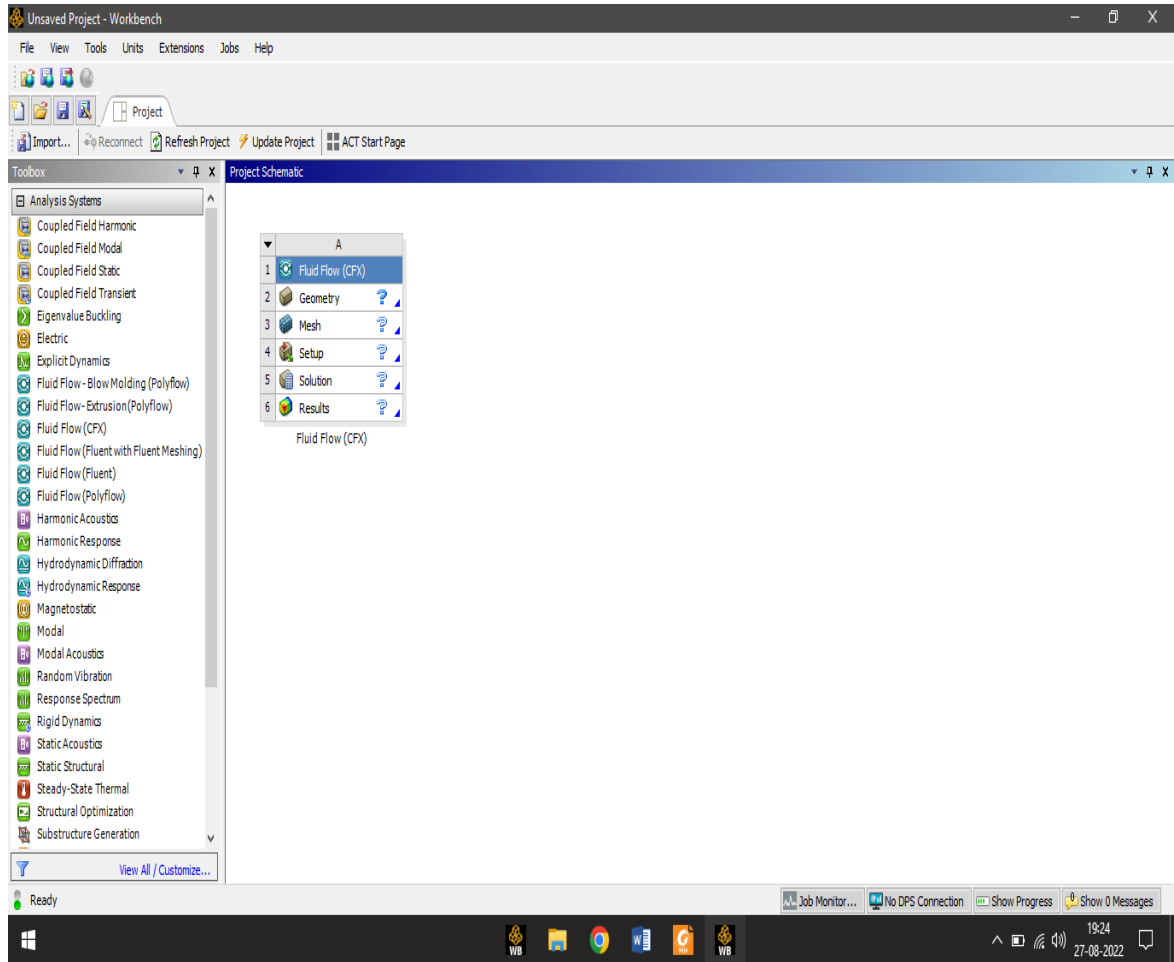


Fig. 3.1 ANSYS workbench

a) Geometry

Model 1 – Square shaped building

The dimension of square shaped building (100x100) mm as shown in Fig. 3.2 and with height 700 mm and building with domain as shown in Fig. 3.3. To prevent wind backflow, such a broad domain is suitable for vertex creation on the leeward side of the building. Heights of the domain 6H and leewards face of building from the domain is 15H and windward face is 5H and left and right side of building is also 5H from the domain side walls. Square cross section building with all the faces Face A, Face B, Face C and Face D as shown in Fig 3.4.

Where,

H = height of building

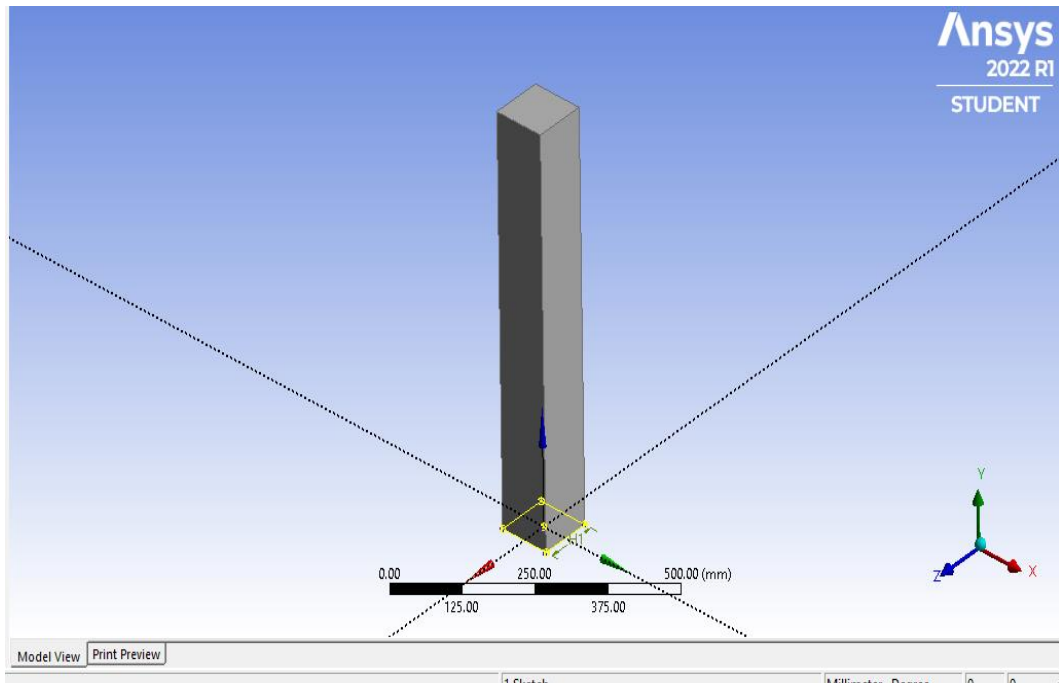


Fig. 3.2 Square shaped building

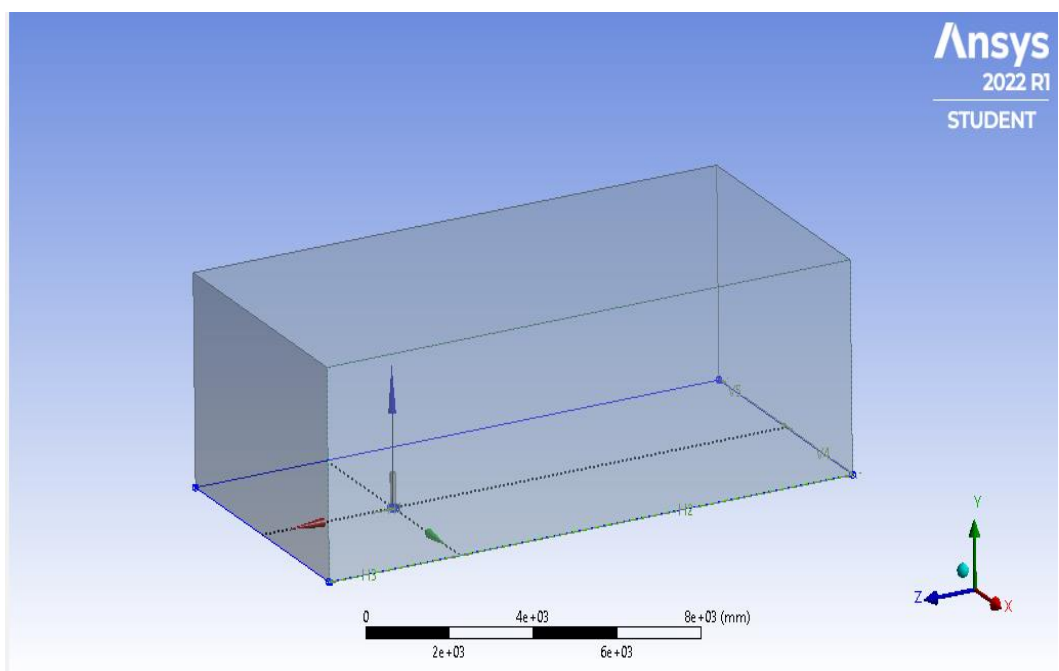


Fig. 3.3 Square shaped building with domain

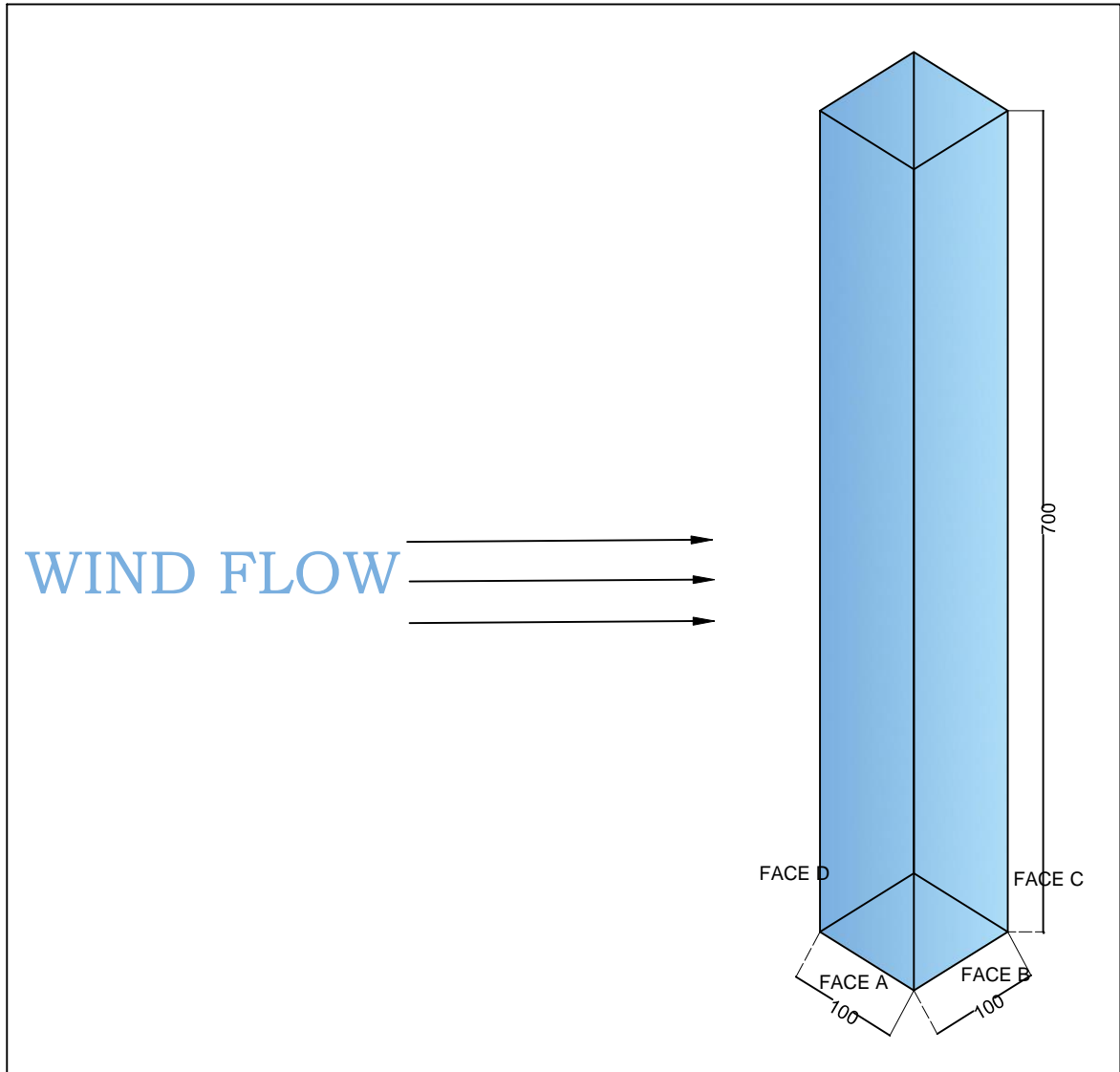


Fig. 3.4 Square shaped building with all faces

Model 2 – Triangular shaped building

The dimension of triangular shaped building considered in present research work are 100 mm for each side with fillet corners with height 500 mm as shown in Fig. 3.4 and building with domain as shown is Fig. 3.5. To prevent backflow of wind, such a broad domain is suitable for vertex creation on the leeward side of the building.

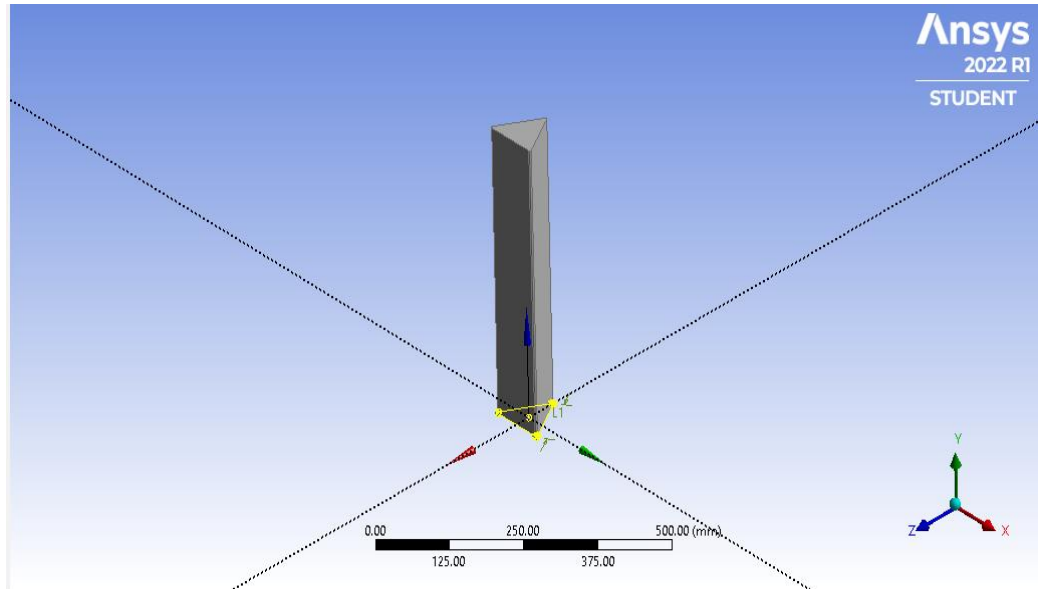


Fig. 3.5 Triangular shaped building

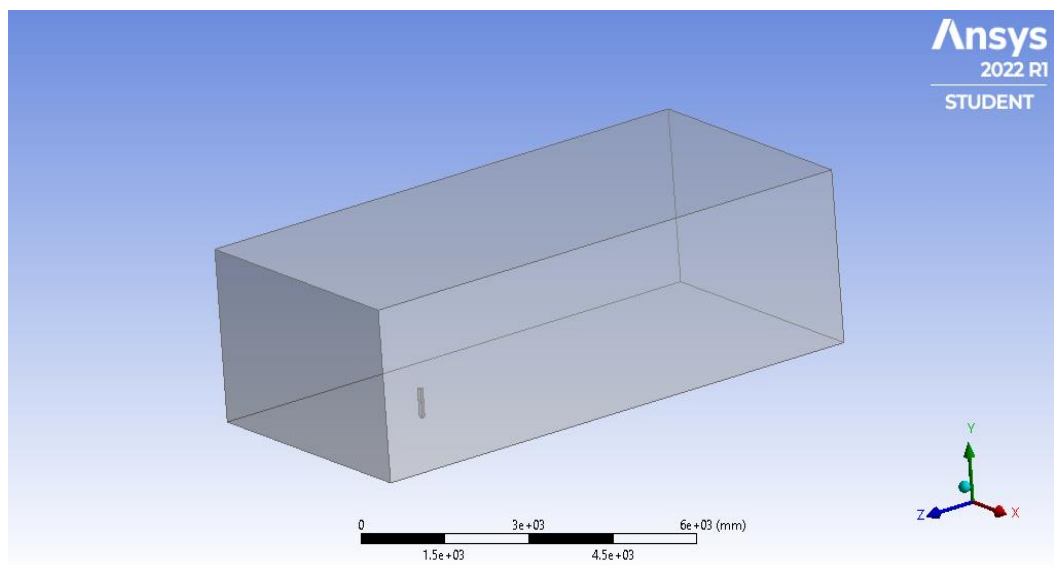


Fig. 3.6 Triangular shaped building with domain

Domain

High-rise buildings having a domain size mostly determined by their height, allows the formation of a huge number of cells, many of which are used in areas distant from the wake region.

The domain's inlet and outflow distances from the building position are estimated as $5H$ and $15H$, respectively, according to the definition of the domain size chosen for

modelling provided by (Frank *et al.* 2004). Assuming that H is the building's height, the top clearance and side aspect are both calculated as $5H$. Graphical representations of the domain setups are provided which are as shown in Fig. 3.6

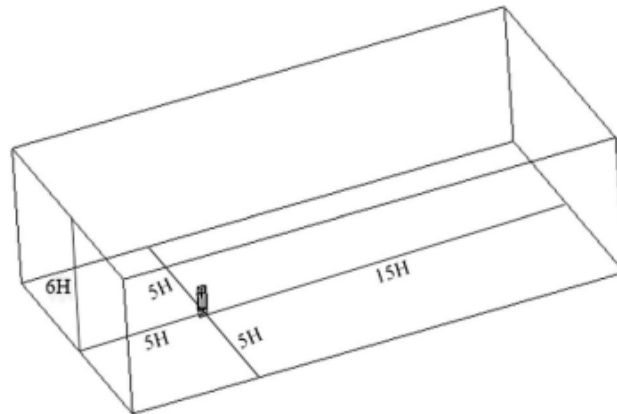


Fig. 3.7 Domain dimension

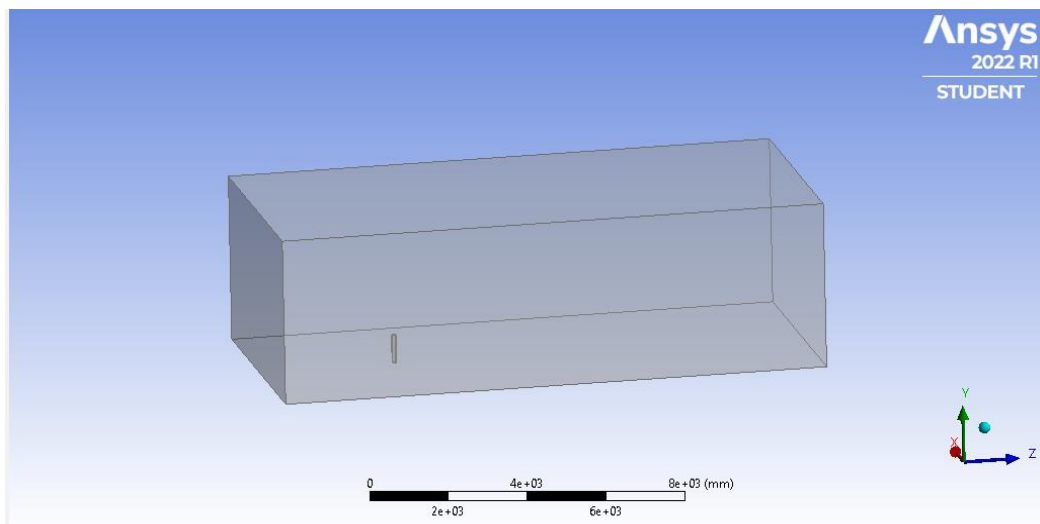


Fig. 3.8 Domain (virtual wind tunnel)

Meshing

As part of the engineering simulation process, complex geometries are broken down into basic pieces called meshes, which can be used as discrete local approximations of a larger domain. Meshing affects the simulation's precision, convergence, and performance. The accuracy increases with the mesh fineness.

Types of Mesh :-

1. Tetrahedron Meshing.
2. Pyramid Meshing.
3. Hexahedron Meshing.
4. Polyhedron Meshing.
5. Prism Meshing.

1. Tetrahedron Meshing

Tetrahedrons have four vertices, six edges, and four triangular faces enclosing them. A tetrahedral volume mesh typically can be produced automatically.

2. Pyramid Meshing

A pyramid with a quadrilateral base has five vertices, eight edges, and four triangular and one quadrilateral face enclosing it. In hybrid meshes and grids, these are used as transitional elements between square and triangle faced elements and other elements.

3. Hexahedron Meshing

The topological cube known as a hexahedron has six quadrilateral faces and eight vertices. It also has twelve edges. It is also known as a brick. Hexahedral meshes have the maximum accuracy of solutions for the same number of cells.

Scientists can think of the pyramid and triangular prism zones as degenerate hexahedrons with part of their edges reduced to zero. There may also be representations of additional hexahedral degenerate forms.

4. Polyhedron Meshing

Any number of vertices, edges, and faces can be found on a polyhedron (dual) element. Due to the amount of neighbours, it frequently requires more computations per cell (typically 10).

5. Prism Meshing

Six vertices, nine edges, and two triangular and three quadrilateral faces define a triangular prism. This kind of layer has the benefit of effectively resolving boundary layer.

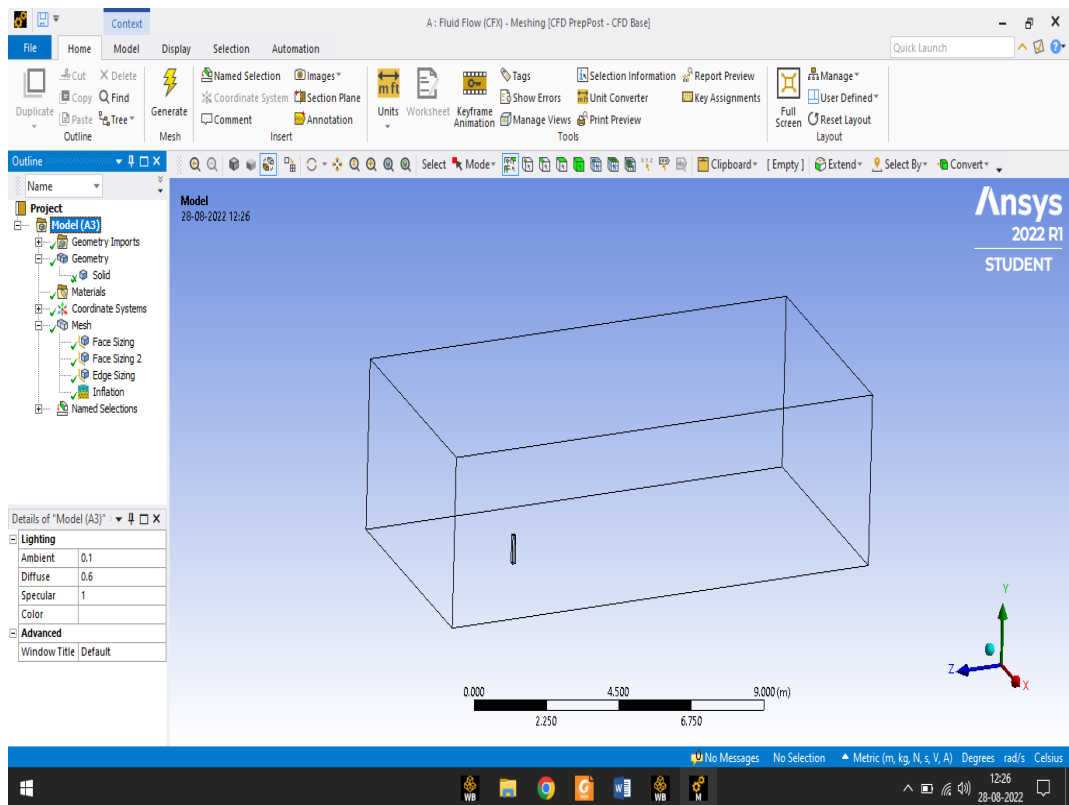


Fig. 3.9 Meshing workbench

Tetrahedral mesh elements are used to mesh the domain. To improve results accuracy, meshing is done somewhat finer in the vicinity of structures. It is assumed that the inflow velocity is 10 m/s. For side walls and the ground, there is a no slide criterion established, Fig. 3.9 shows the work bench for meshing.

Model 1 – Square plain building with meshing

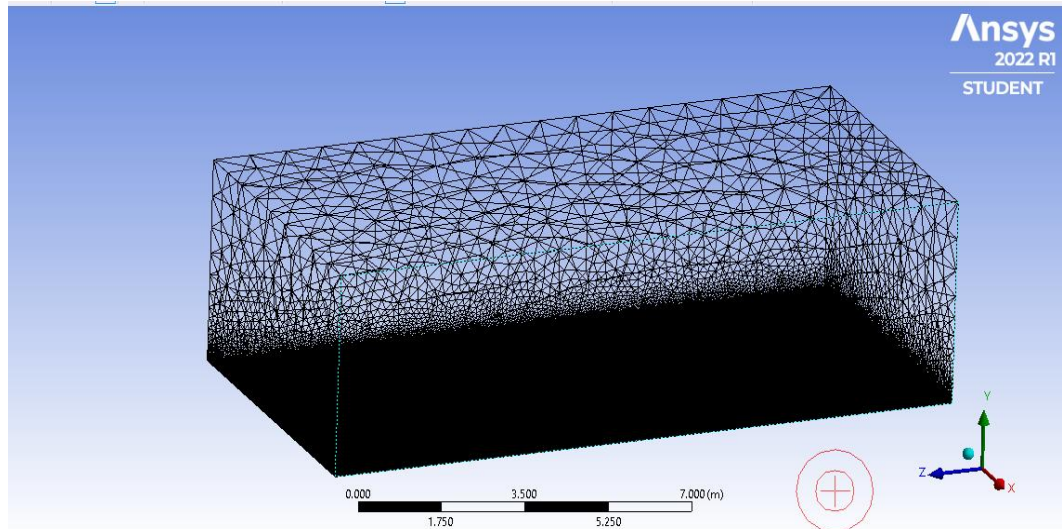


Fig. 3.10 Square building with meshing

Model 2 - Triangular shape building with meshing

ANSYS CFX is used for purpose of analysis since it mainly focuses to study aerodynamic applications. Meshing of the domain is done using tetrahedral elements. Meshing is done finer near surfaces of building in order to get good results on surface of building as shown in Fig. 3.10. It is assumed that the inflow velocity is 10 m/s. For side walls and the ground, there is a no slide criterion established.

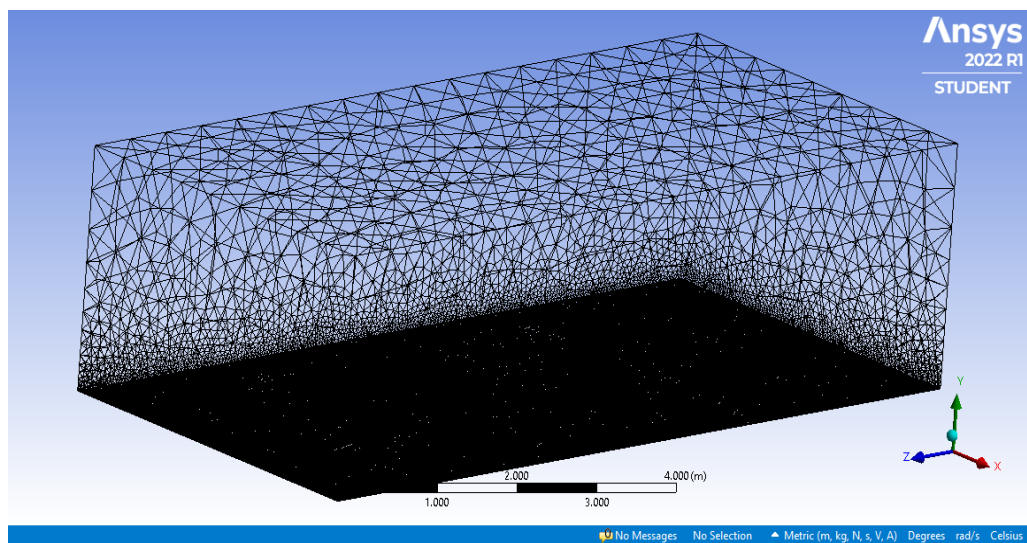


Fig. 3.11 Triangular building with meshing

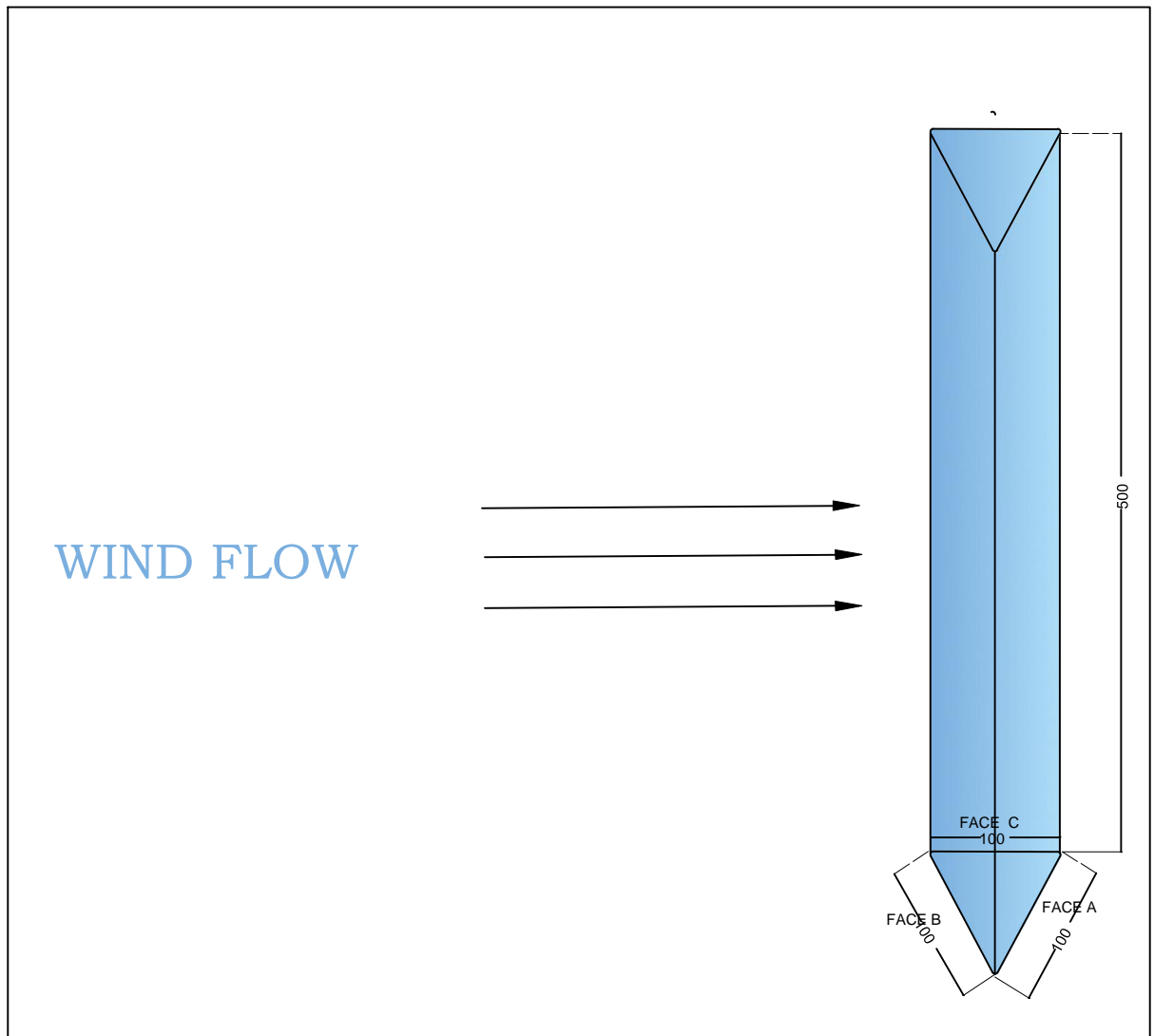


Fig 3.12 Triangular cross section building with all faces

- Triangular cross section building with all the faces Face A, Face B, Face C and Face D as shown in Fig 3.12

b) Setup

Using ANSYS, drags of several polygonal towers have been estimated while maintaining the same base area and volume. We discovered the drag coefficients of various n-shaped polygons. A domain of this size also aids in preventing backflow of wind and vortex formation on the leeward side of the flow.

For the purpose of performing numerical simulation, several boundary conditions must be imposed to a domain. The flow parameters are set at the surface body, walls, input, and output. Below are the boundaries that have been established for the study area.

1. Inlet boundary condition

One significant inlet condition is the flow velocity. To establish a consistent starting point for all the models, the flow velocity is assumed to be 10 m/s. The velocity is in the direction of positive Z.

2. Outlet boundary condition

In order to maintain a steady pressure outflow, the outflow was set to pressure outlet. To ensure that it will have no impact on the inflow, the pressure taken for the current scenario is zero (i.e., the pressure is assumed to be atmospheric).

3. Side wall of domain

The wall is considered to be a stationary wall for all types of models free slip walls condition is applied at all these domain side walls

4. Ground of domain

Ground of domain is considered to be stationary and no slip wall and smooth wall condition are applied

5. Walls of building

No slip wall and smooth wall condition are applied to all building walls.

Fig. 3.12 showing the setup workbench inside the Ansys under which we applied the different boundary condition for building and domain, we can also apply power law for the analysis of building by using Ansys setup under expression option given in setup workbench

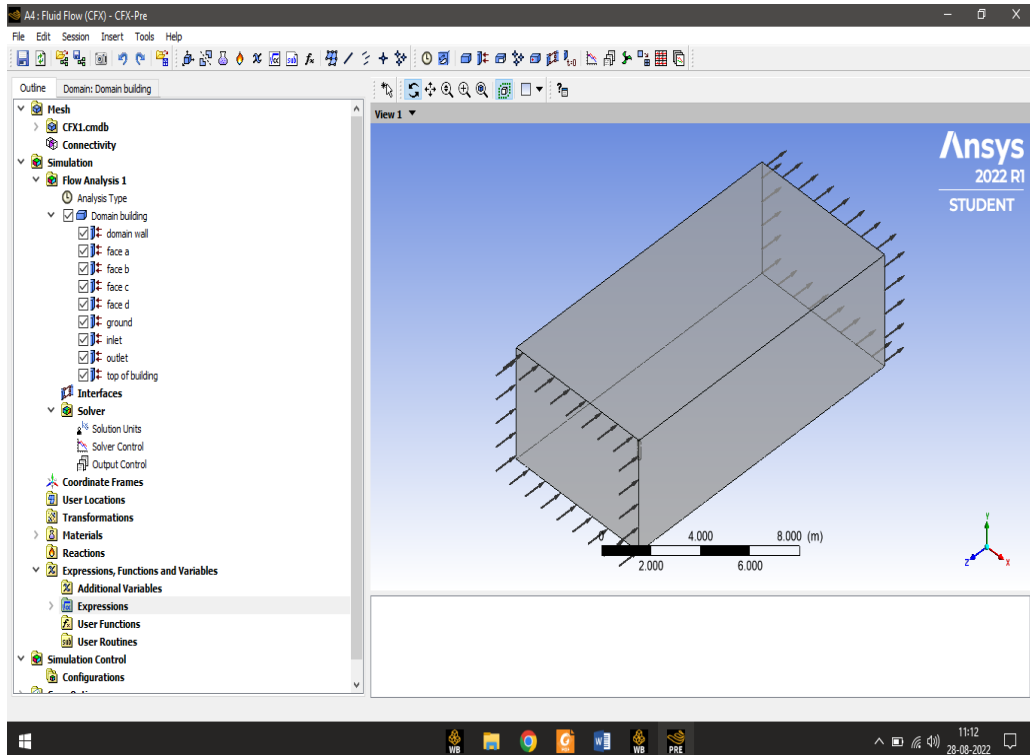


Fig. 3.13 Setup workbench

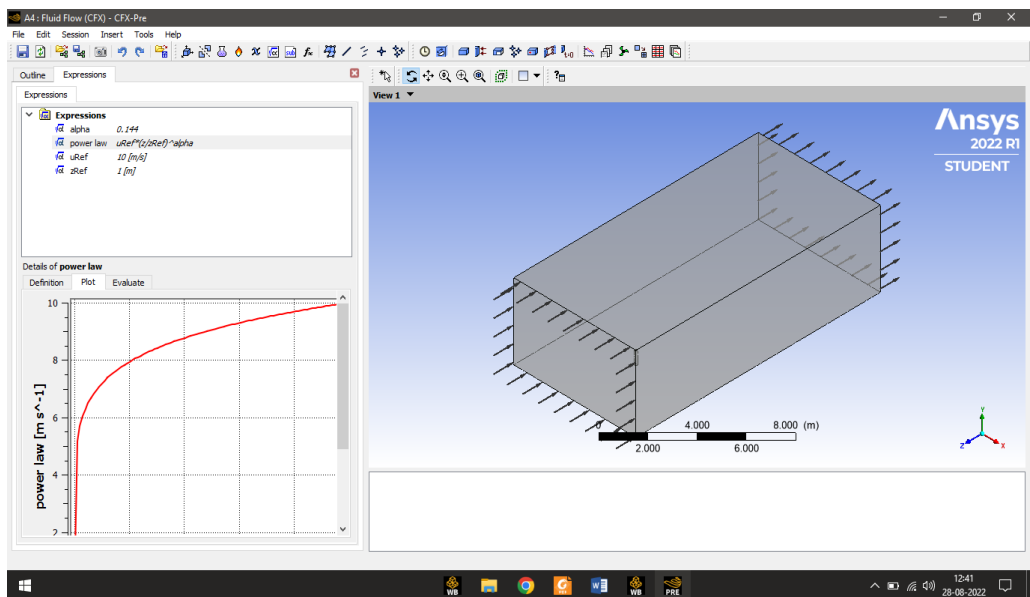


Fig. 3.14 Power law expression and plot

Power law expression is given below

$$u_{Ref} \times \left[\left(\frac{z}{z_{ref}} \right)^\alpha \right]$$

where,

$$\alpha = 0.144$$

$$Z_{\text{ref}} = 1 \text{ m}$$

$$u_{\text{Ref}} = 10 \text{ m/s}$$

Fig. 3.13, Power law is defined under expression option and plot is also shown in the Fig. 3.13

4.1 Pressure distribution

Model 1 - Square cross-section building

- The pressure contours for different faces for different angle of incidence depicts the pressure distribution on faces and are as shown in Fig. 4.1 - Fig.4.12.
- Analysis of model were conducted using ANSYS CFX 2022 R1. Meshing is done using tetra-hedron method and the size square cross section high rise building (100x100) mm. Based on above data, ANSYS produces results in terms of relative pressure, global pressure, eddy viscosity and temperature etc. Different slip conditions are used no slip wall are used for all the faces of building as well as ground and free slip walls for all the walls of domain (inlet, outlet, side walls).
- Initially, at 0° wind incidence, Face A shows a positive pressure being the windward face of the square shaped building whereas Face B, Face C and Face d depicts a negative pressure distribution along the leeward and side wall face of the building.
- At 15° angle of incidence, Face A of the square-shaped building demonstrate a positive pressure distribution on the windward face, while Faces B, C, and D exhibit a negative pressure distribution on the leeward and side wall faces of the building.
- Face A of the square-shaped building shows a positive pressure distribution at angles of incidence of 30° and 45°, whereas Faces B, C, and D show a negative pressure distribution at 30° and 45° angles of incidence respectively.
- As the angle of incidence changes so the pressure distribution also changes and a positive pressure distribution at Face A become slightly less as compared with 15°, 30° and 45° wind angle of incidence where in 0° wind incidence angle suction pressure increases in side face and leeward face of building.
- It was found that the value of pressure is positive on the top i.e. 88.86 N/m² and negative as we go centre to bottom of building and at the bottom 131.42 N/m². When compared the results with IS 875 (Part 3):2015. Pressure contours for the isolated square shaped building for the different faces of building i.e. Face B, Face

C and Face D were observed as when compared the result with (Roy and Kumar 2016) whose values are at top 45.492 N/m^2 and at bottom -56.874 N/m^2 .

- Wind flow incidence from 0° to 90° for square shaped building is also shown Fig.4.1.

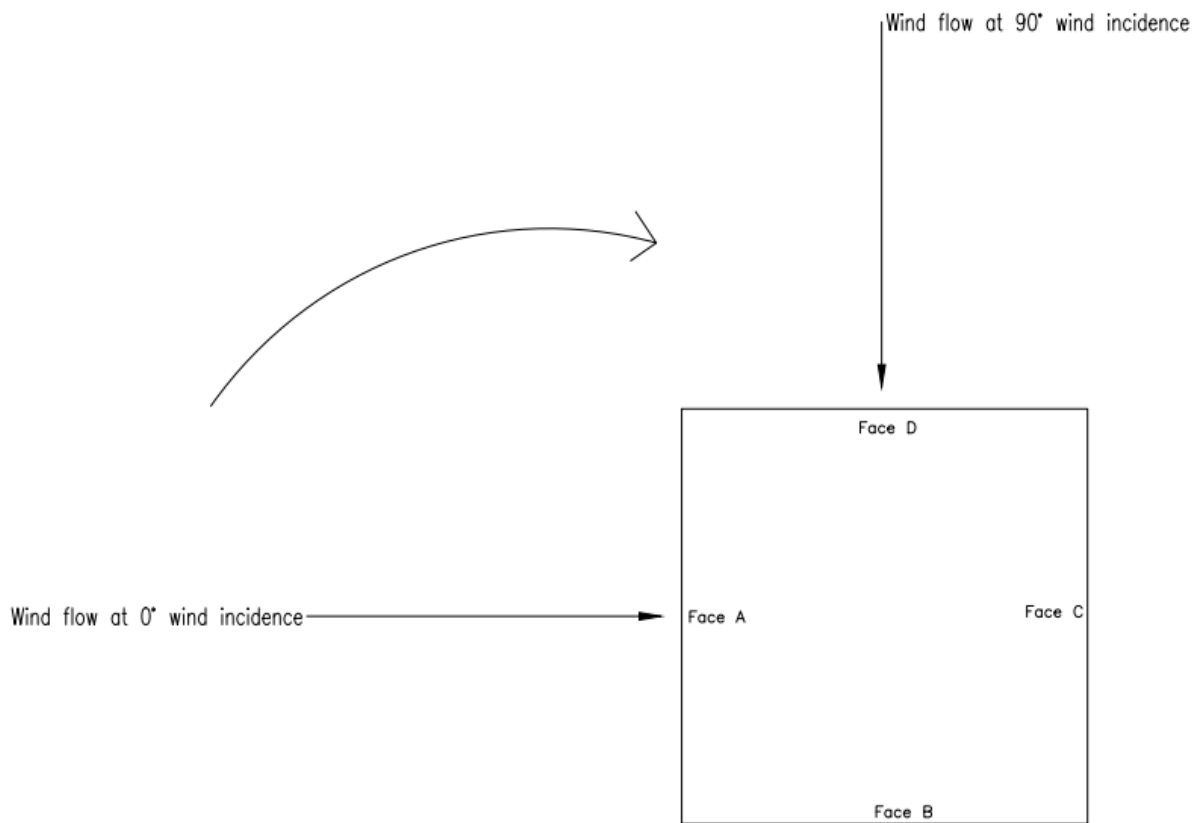


Fig. 4.1 Direction of wind from 0° to 90° wind incidence angle

1. 0° degree contour plot

Pressure contour of Square cross-section at 0° wind incidence angle for Face A, Face B, Face C and Face D shown in Fig. 4.2 and Fig 4.3.

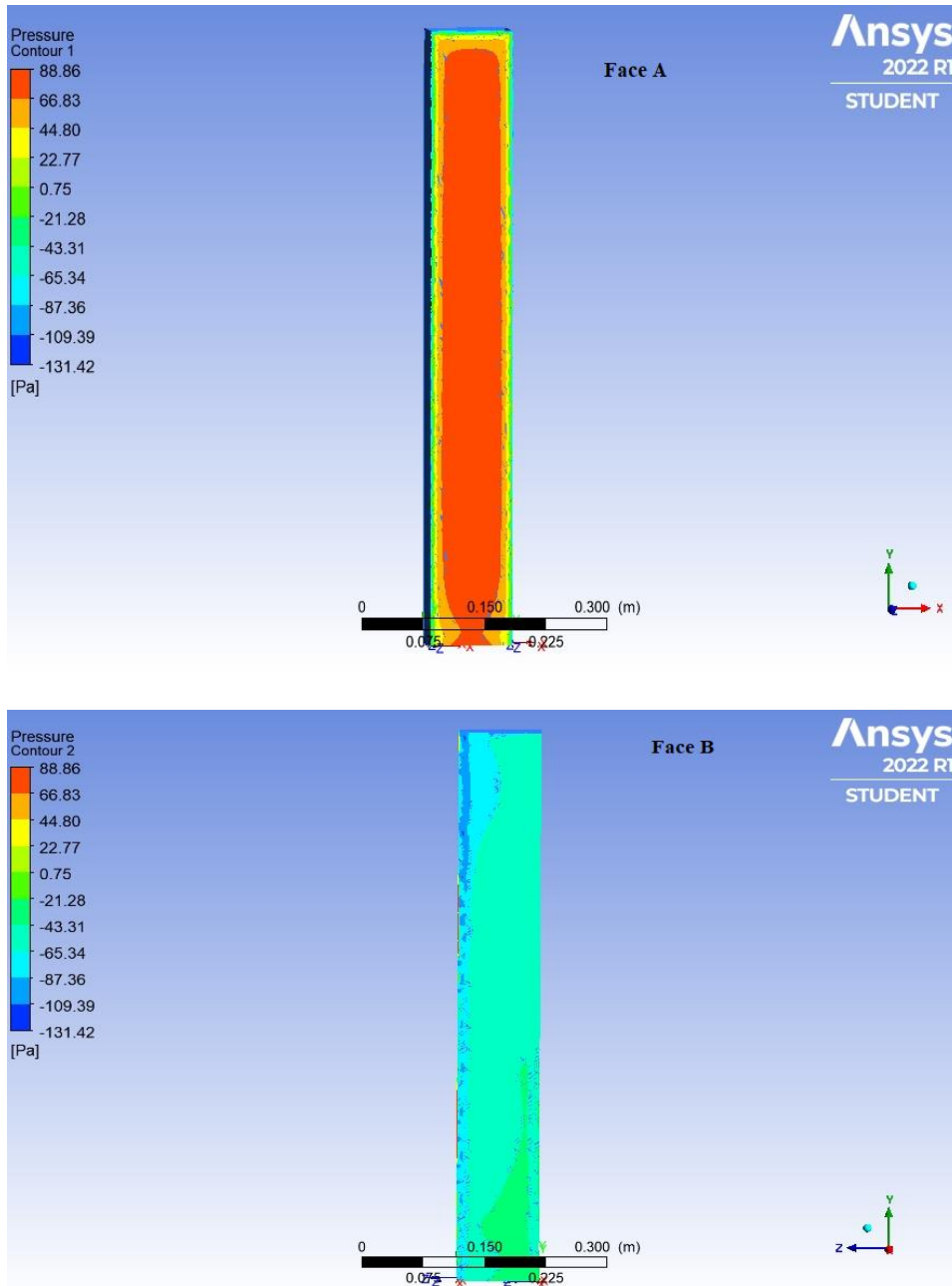


Fig. 4.2 Contour plot for Face A and Face B at 0° angle of wind incidence

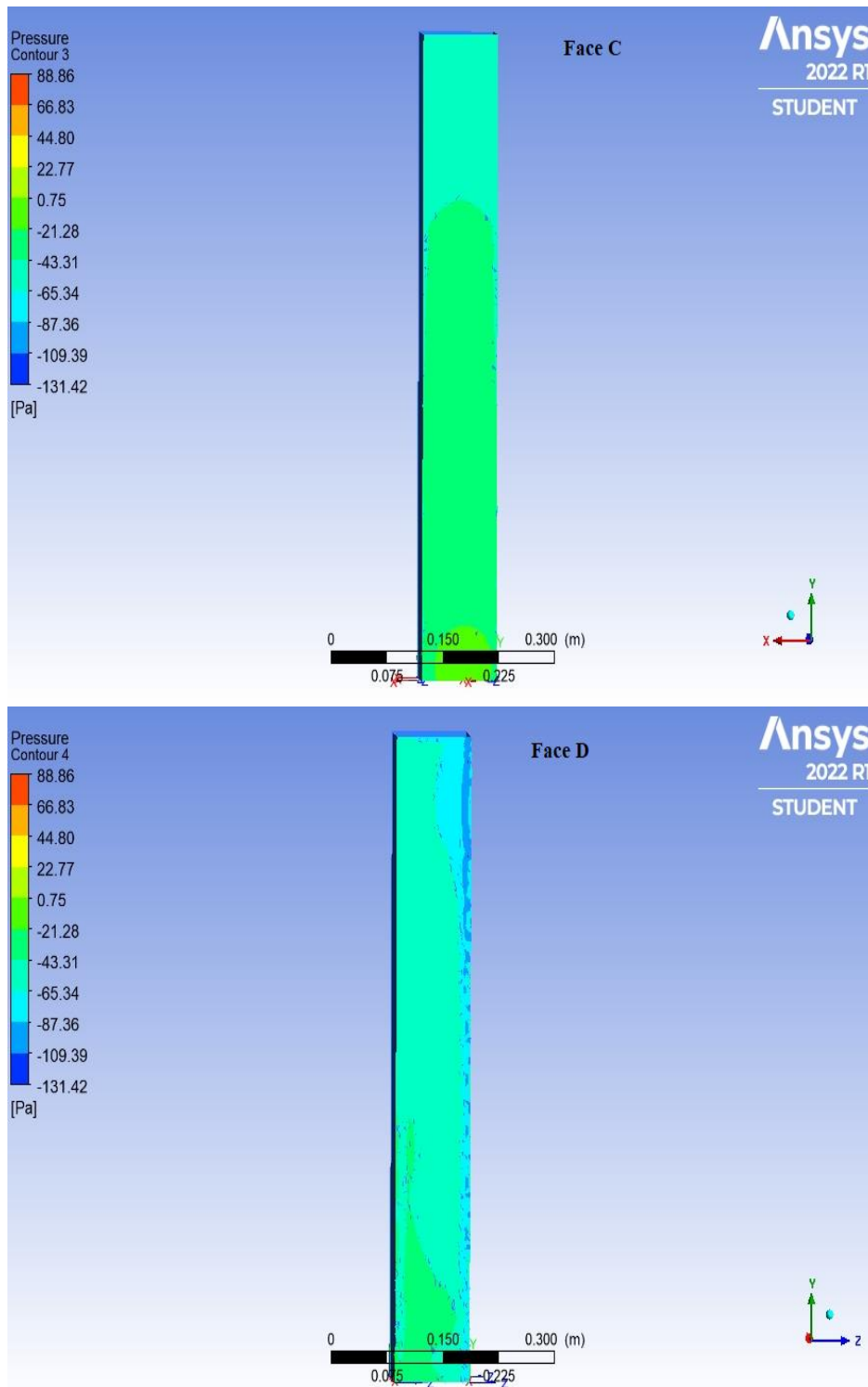


Fig. 4.3 Contour plot for Face C and Face D at 0° angle of wind incidence

2. 15° contour plot

Pressure contour of Square cross-section at 15° wind incidence angle for Face A, Face B, Face C and Face D shown in Fig. 4.4 and Fig 4.5.

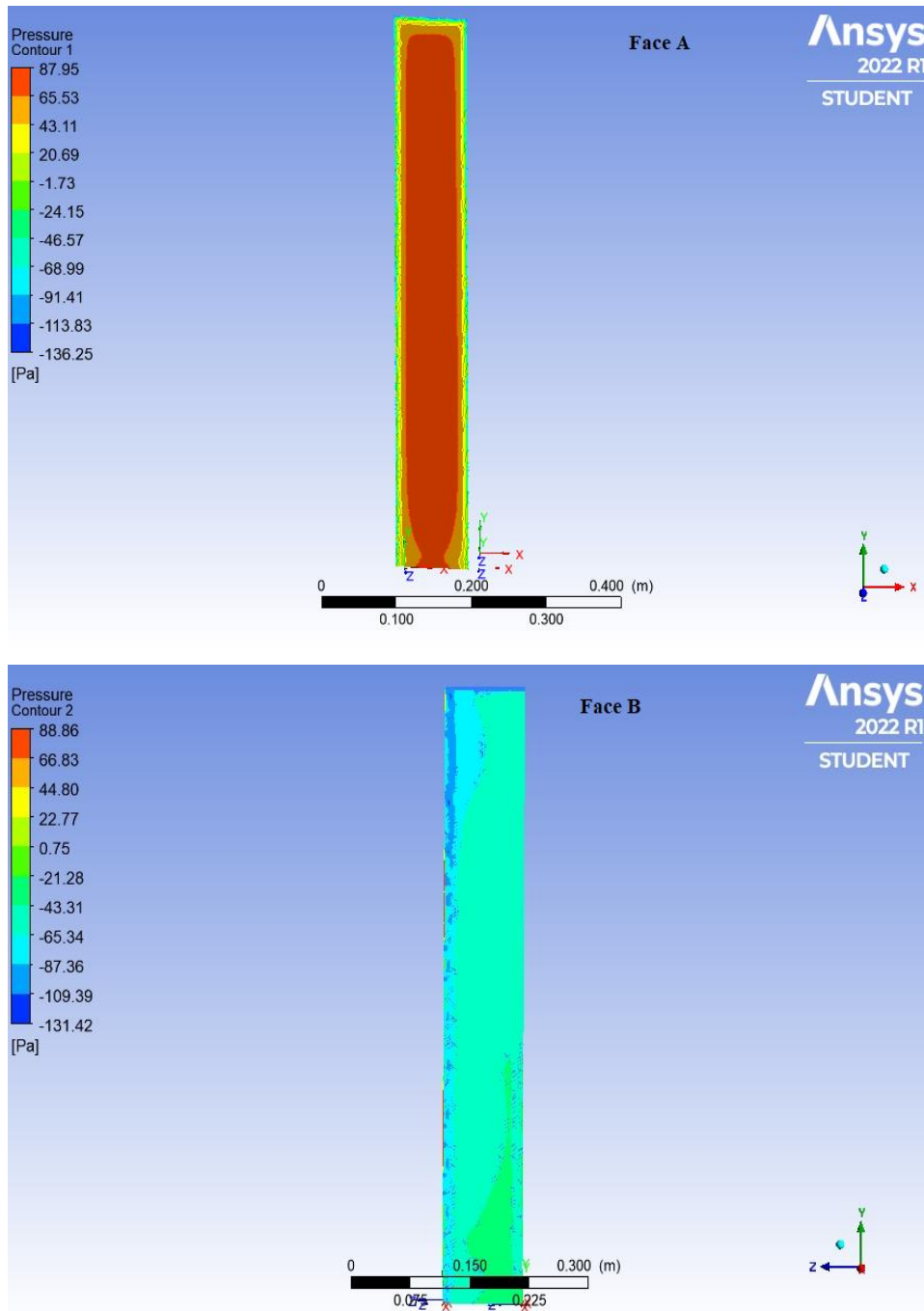


Fig. 4.4 Contour plot for Face A and Face B at 15° angle of wind incidence

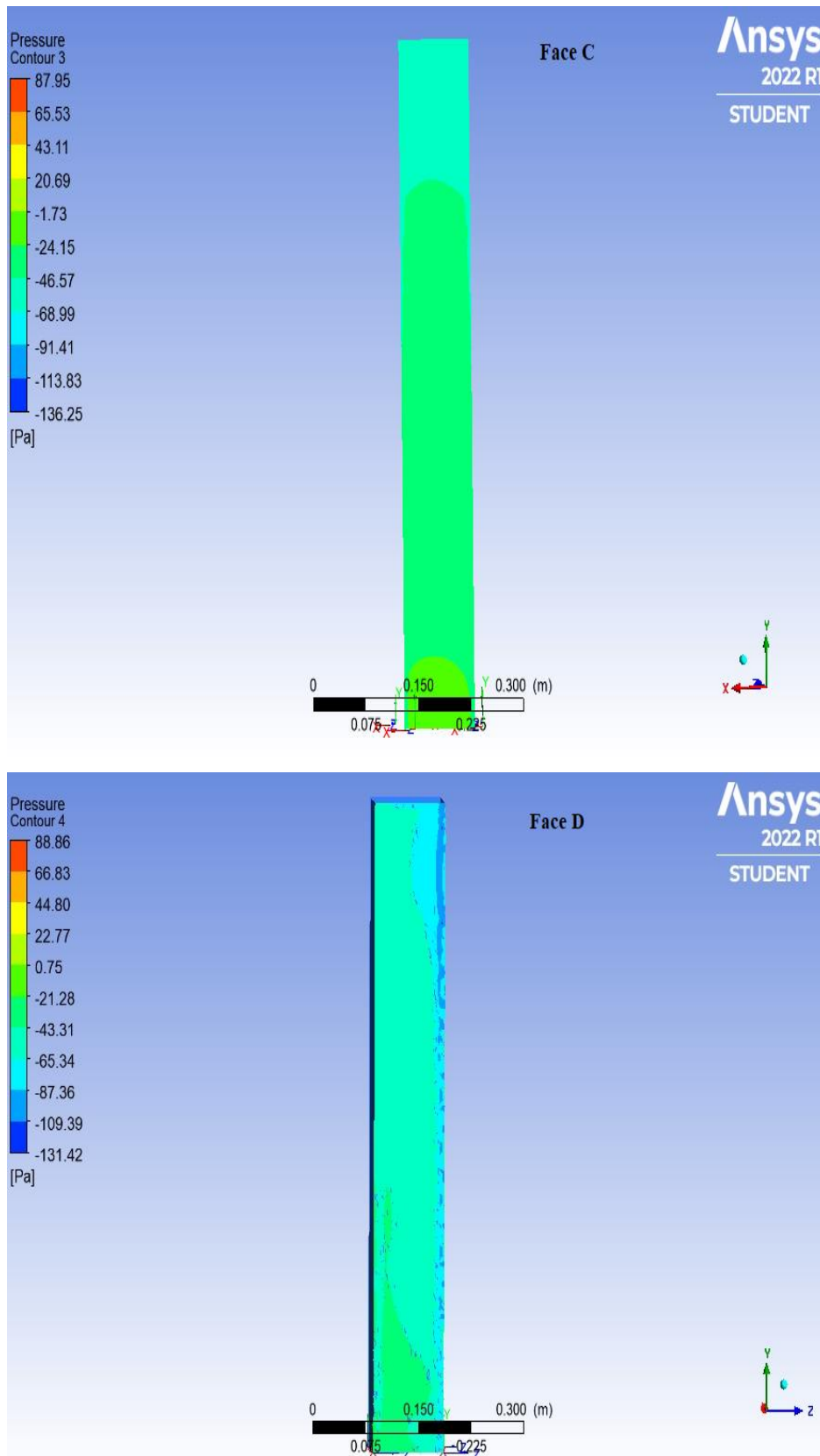


Fig. 4.5 Contour plot for Face C and Face D at 15° angle of wind incidence

3. 30° contour plot

Pressure contour of Square cross-section at 30° wind incidence angle for Face A, Face B, Face C and Face D shown in Fig. 4.6 and Fig 4.7.

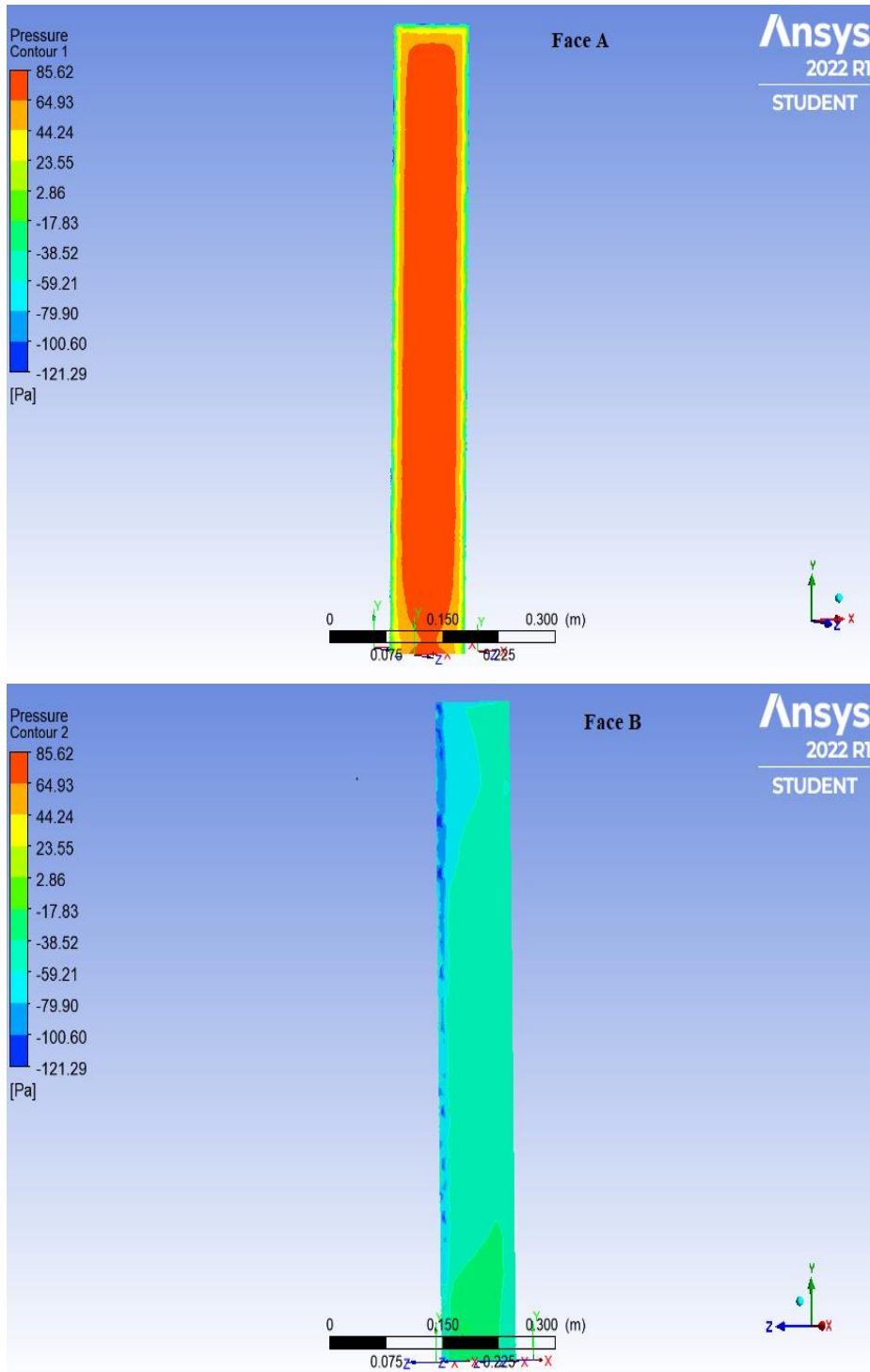


Fig. 4.6 Contour plot for Face A and Face B at 30° angle of wind incidence

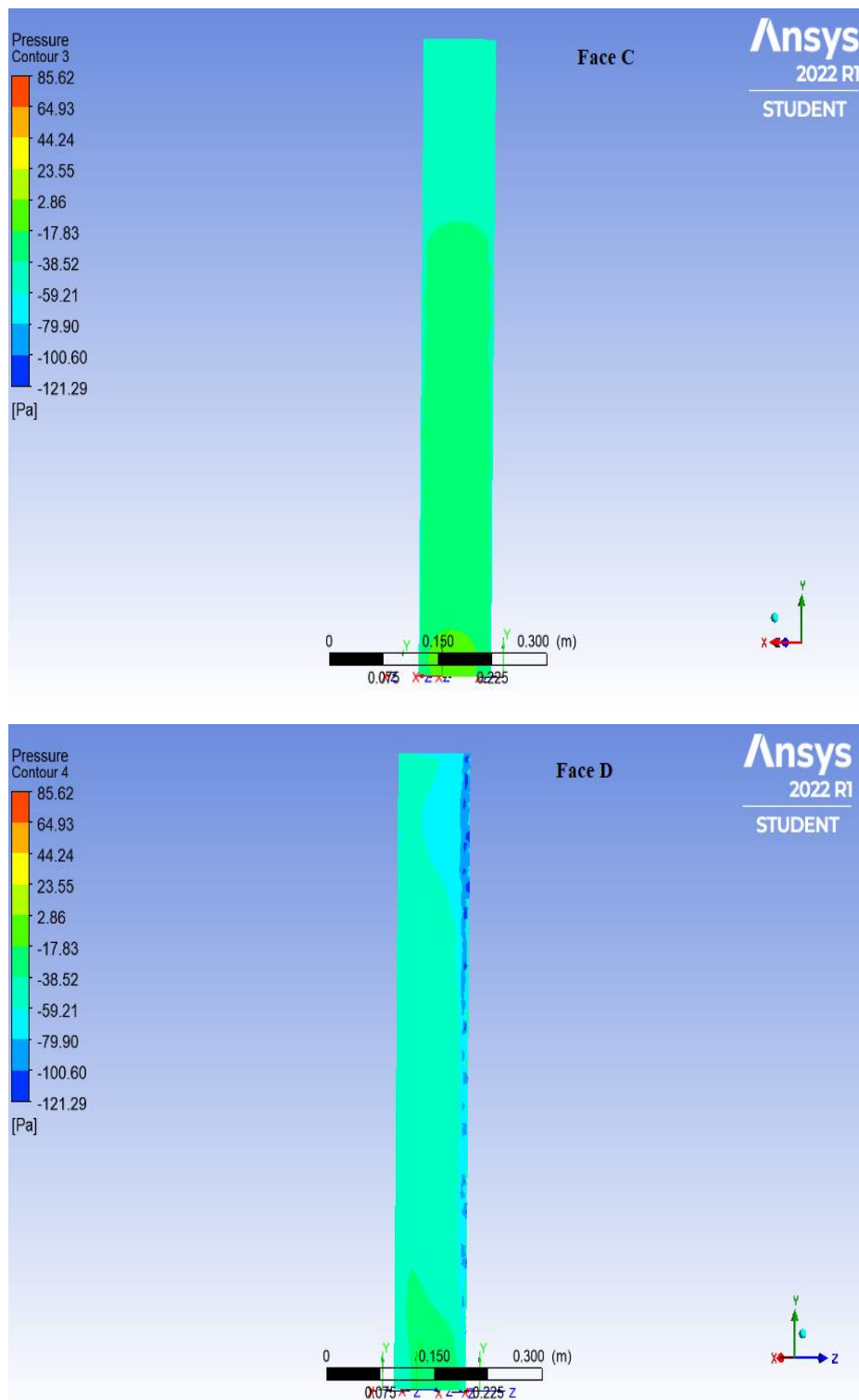


Fig. 4.7 Contour plot for Face C and Face D at 30° angle of wind incidence

4. 45° contour plot

Pressure contour of Square cross-section at 45° wind incidence angle for Face A, Face B, Face C and Face D shown in Fig. 4.8 and Fig 4.9.

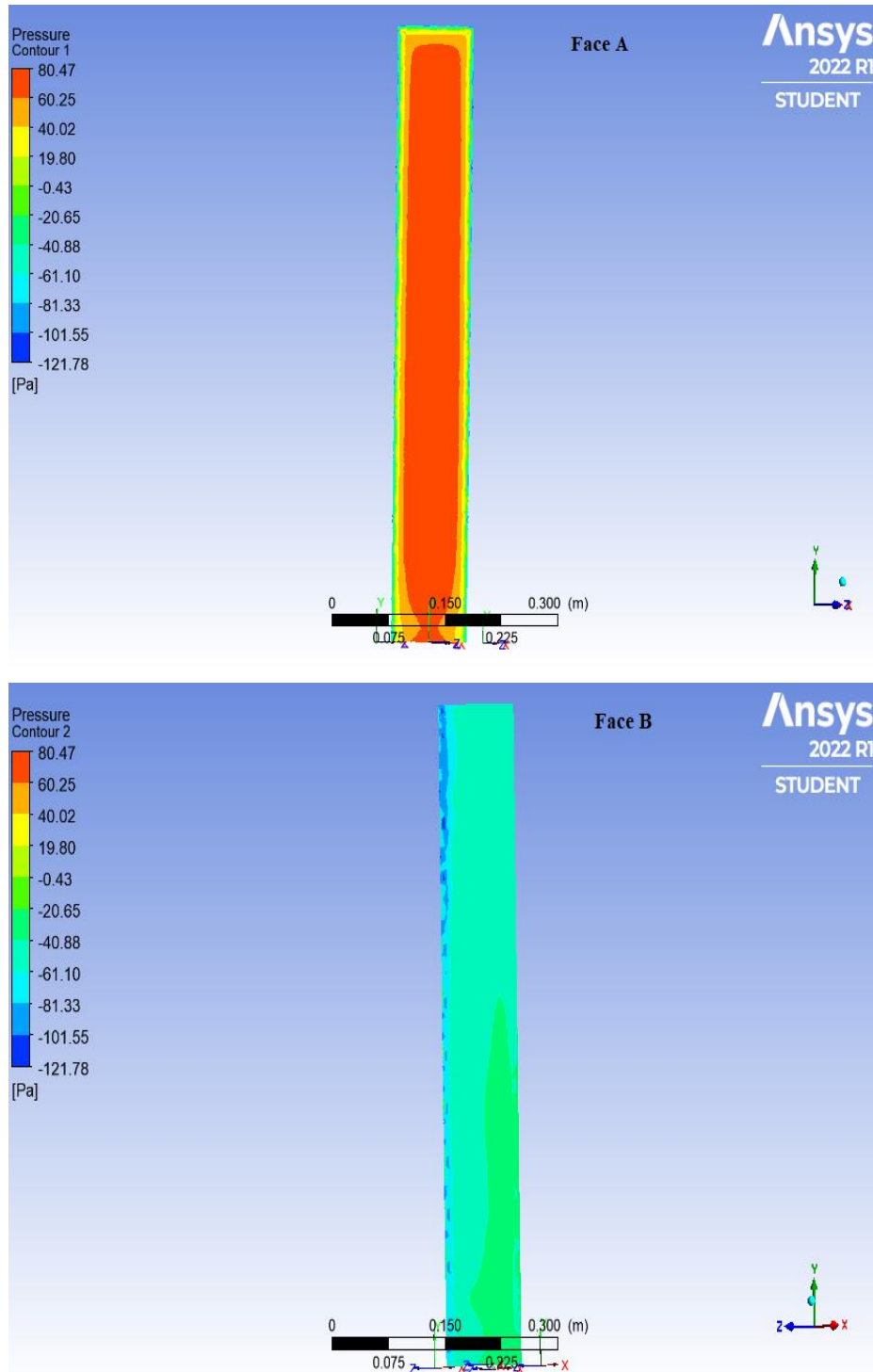


Fig. 4.8 Contour plot for Face A and Face B at 45° angle wind of incidence

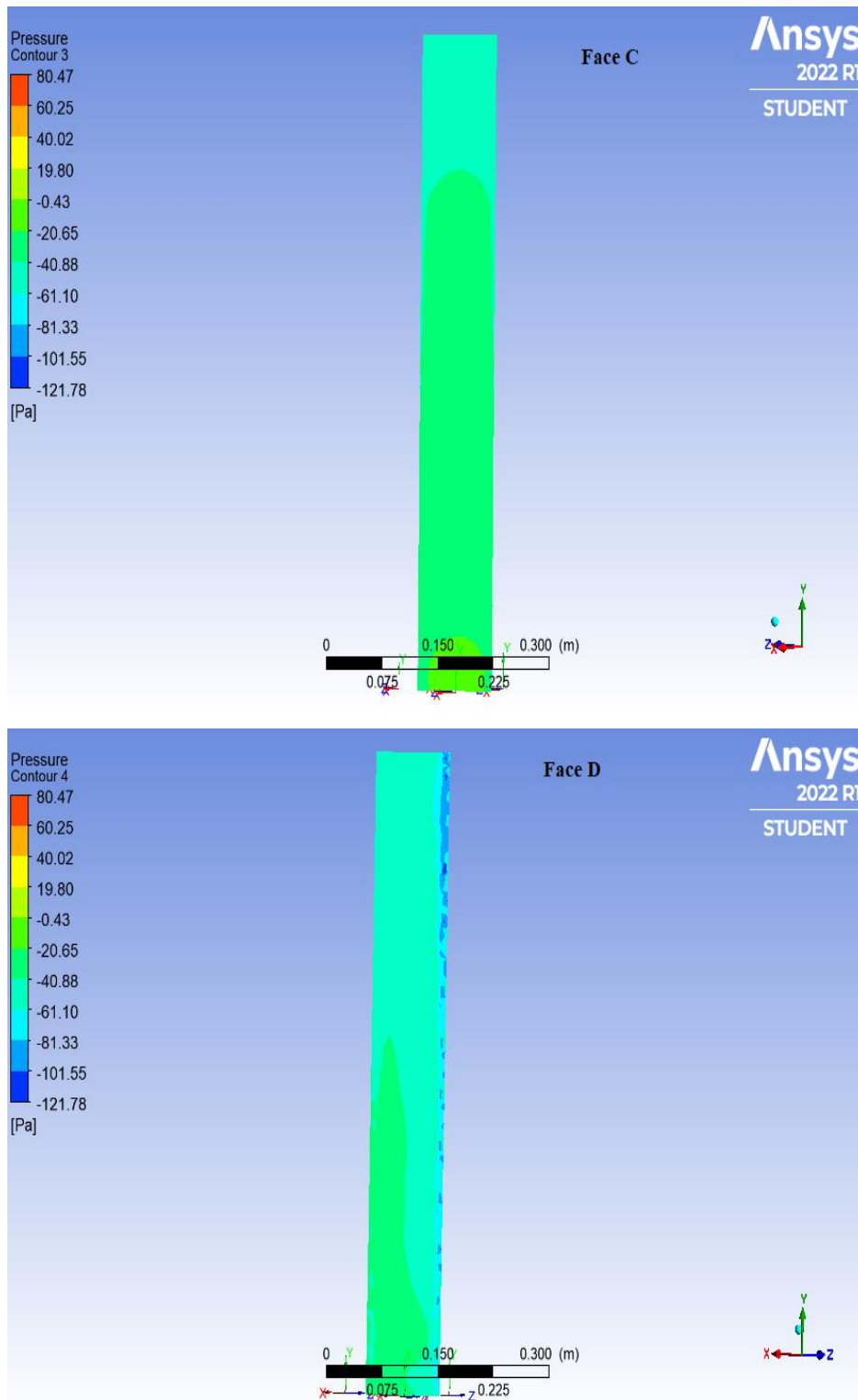


Fig. 4.9 Contour plot for Face C and Face D at 45° angle of wind incidence

5. 60° contour plot

Pressure contour of Square cross-section at 60° wind incidence angle for Face A, Face B, Face C and Face D shown in Fig. 4.10 and Fig 4.11.

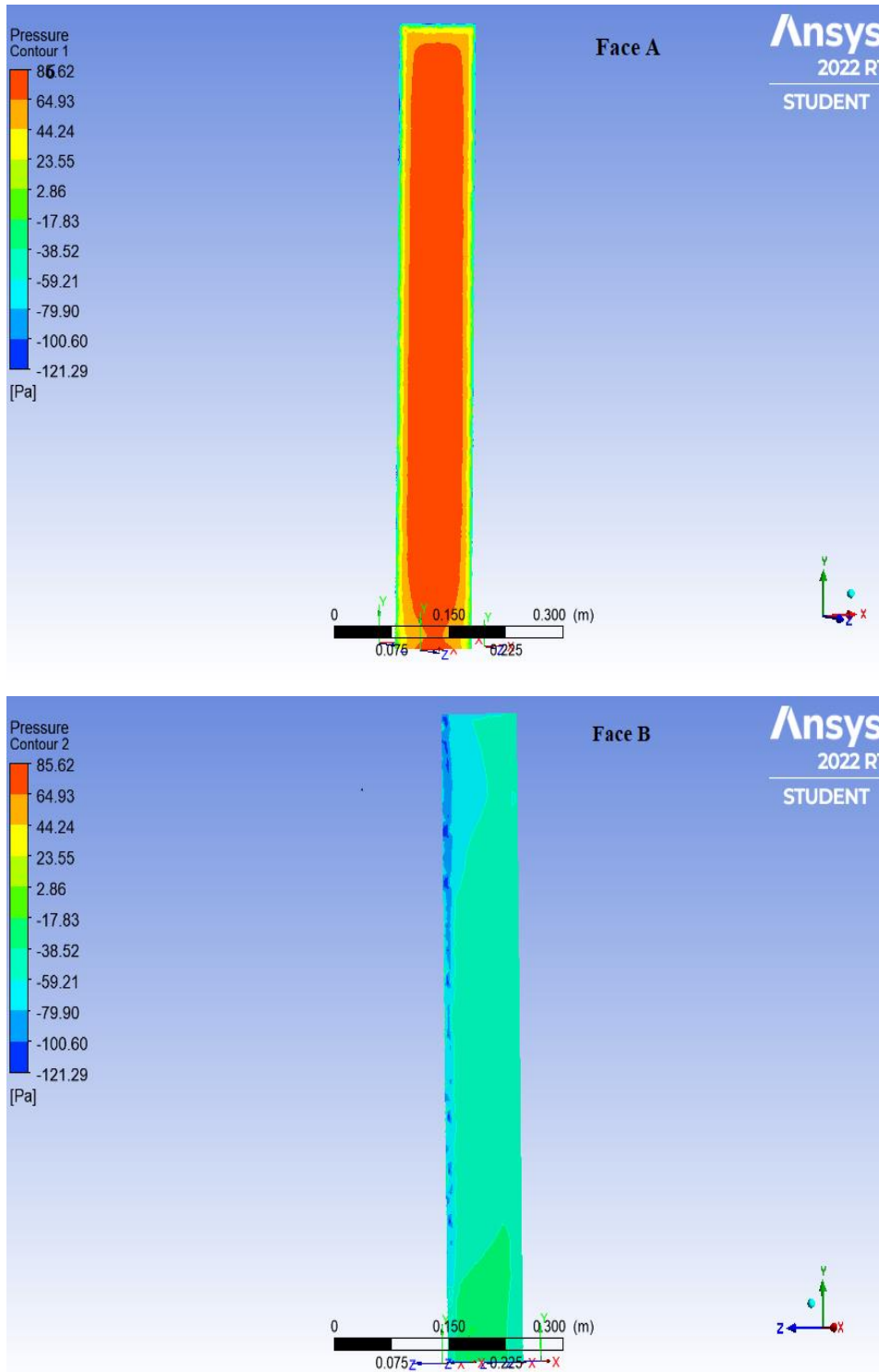


Fig. 4.10 Contour plot for Face A and Face B at 60° angle of wind incidence

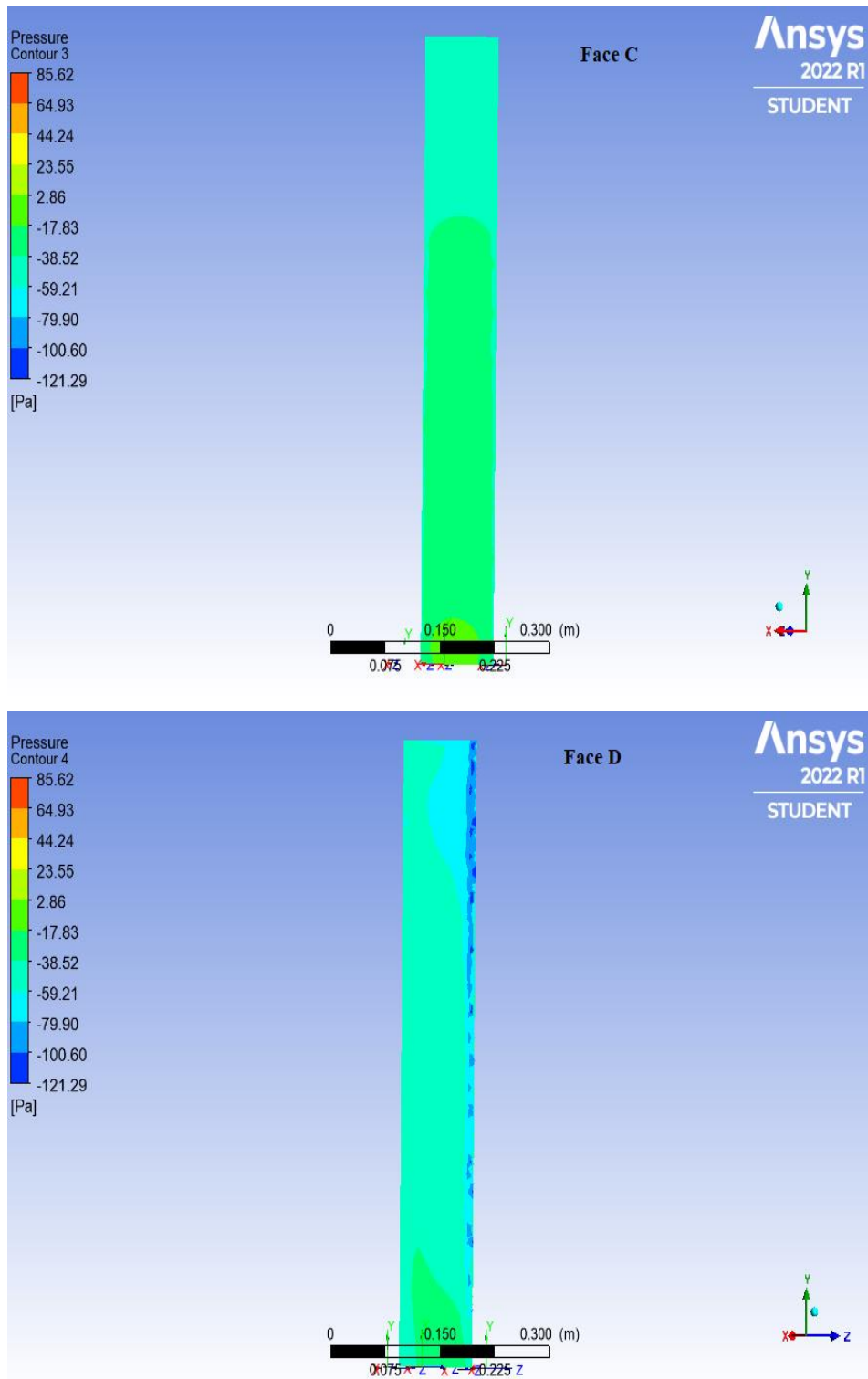


Fig. 4.11 Contour plot for Face C and Face D at 60° angle of wind incidence

6. 90° contour plot

Pressure contour of Square cross-section at 90° wind incidence angle for Face A, Face B, Face C and Face D shown in Fig. 4.12 and Fig 4.13.

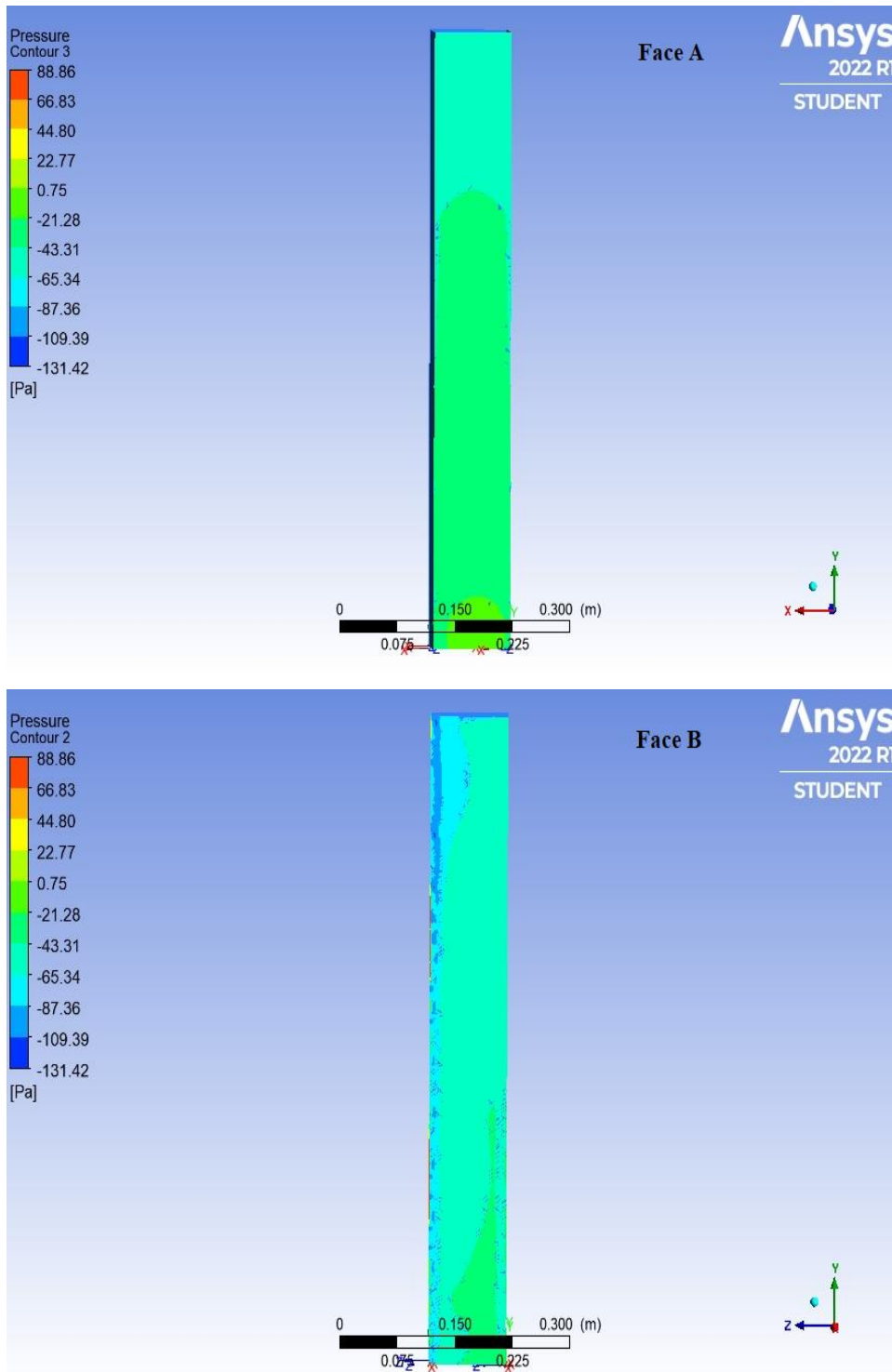


Fig. 4.12 Contour plot for Face A and Face B at 90° angle of wind incidence

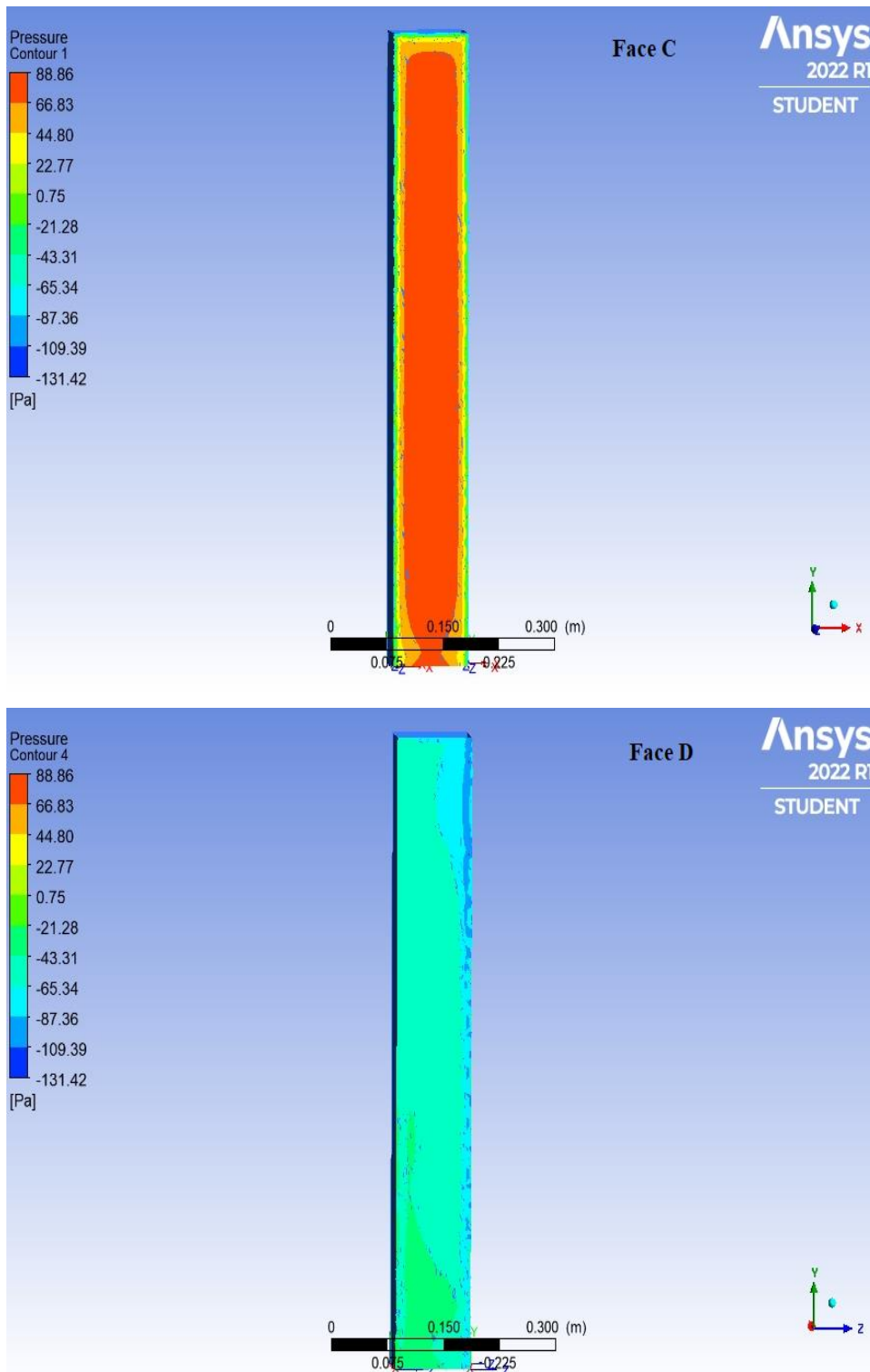


Fig. 4.13 Contour plot for Face C and Face D at 90° angle of wind incidence

Model 2- Triangular cross-section building

- The pressure contours for different faces at various angle of incidence depicts the different pressure distribution on different faces and are shown in Fig. 4.14 - Fig. 4.27.
- Analysis of model were conducted using ANSYS CFX 2022 R1. Meshing is done using tetrahedron method on a triangular cross section high rise building 100 mm each side. Based on above data in ANSYS results were produced in terms of relative pressure, global pressure, eddy viscosity and temperature etc. Different slip conditions are used and no slip wall used for all the faces of building and ground where as free slip walls were used for all the walls of domain (inlet, outlet, side walls)
- Initially, at 0° wind incidence Face A shows a positive pressure along the windward face of the triangular shaped building whereas Face B and Face C shows a negative pressure distribution along the leeward and side wall face of the building.
- It was found that the value of pressure is positive on the top i.e. $+80.93 \text{ N/m}^2$ and negative as we move towards centre to bottom of building and at the bottom -204.5 N/m^2 and the results are compared their results with IS 875(Part 3):2015. Pressure contours are also plotted for the isolated square shaped building for the different faces of building i.e. Face B, Face C also the results are compared with **(Roy and Kumar 2016)** and their values for pressure is positive at top 45.493 N/m^2 and negative at the bottom -56.874 N/m^2 , as we can see that change in magnitude is obtained because of different size of building but nature is same.
- For 30° and 60° angle of wind incidence, it is observed positive pressure distribution is obtained at Face A and it became slightly less when compared. 0° wind incidence angle along with suction pressure increase at Face C.
- For 90° , 120° and 150° wind incidence angle the positive pressure obtained at Face B and negative pressure is obtained at Face A and Face C.
- For 180° negative pressure obtained at Face A and positive pressure is obtained at Face B and Face C where as at the edges negative pressure is obtained.
- Wind incidence angle is also shown in Fig 4.14 from 0° to 180°

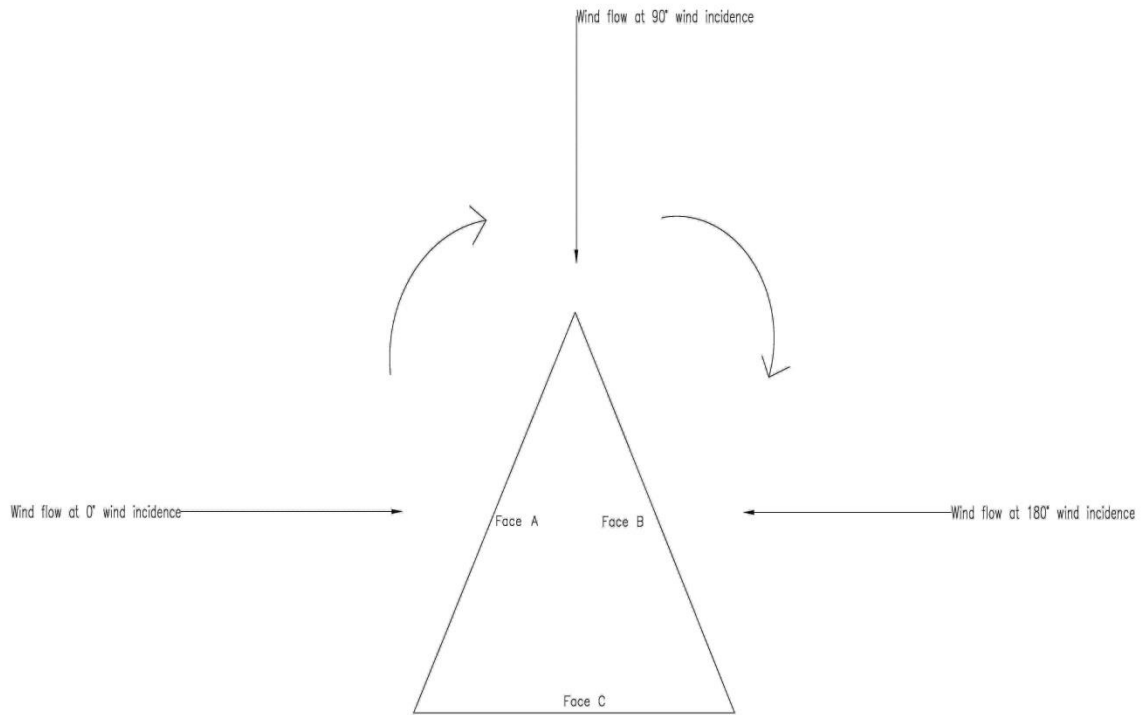


Fig. 4.14 Direction of wind from 0° to 180° wind incidence angle

1. 0° contour plot

Pressure contour of Triangular cross-section at 0° wind incidence angle for Face A, Face B and Face C shown in Fig. 4.15 and Fig 4.16.

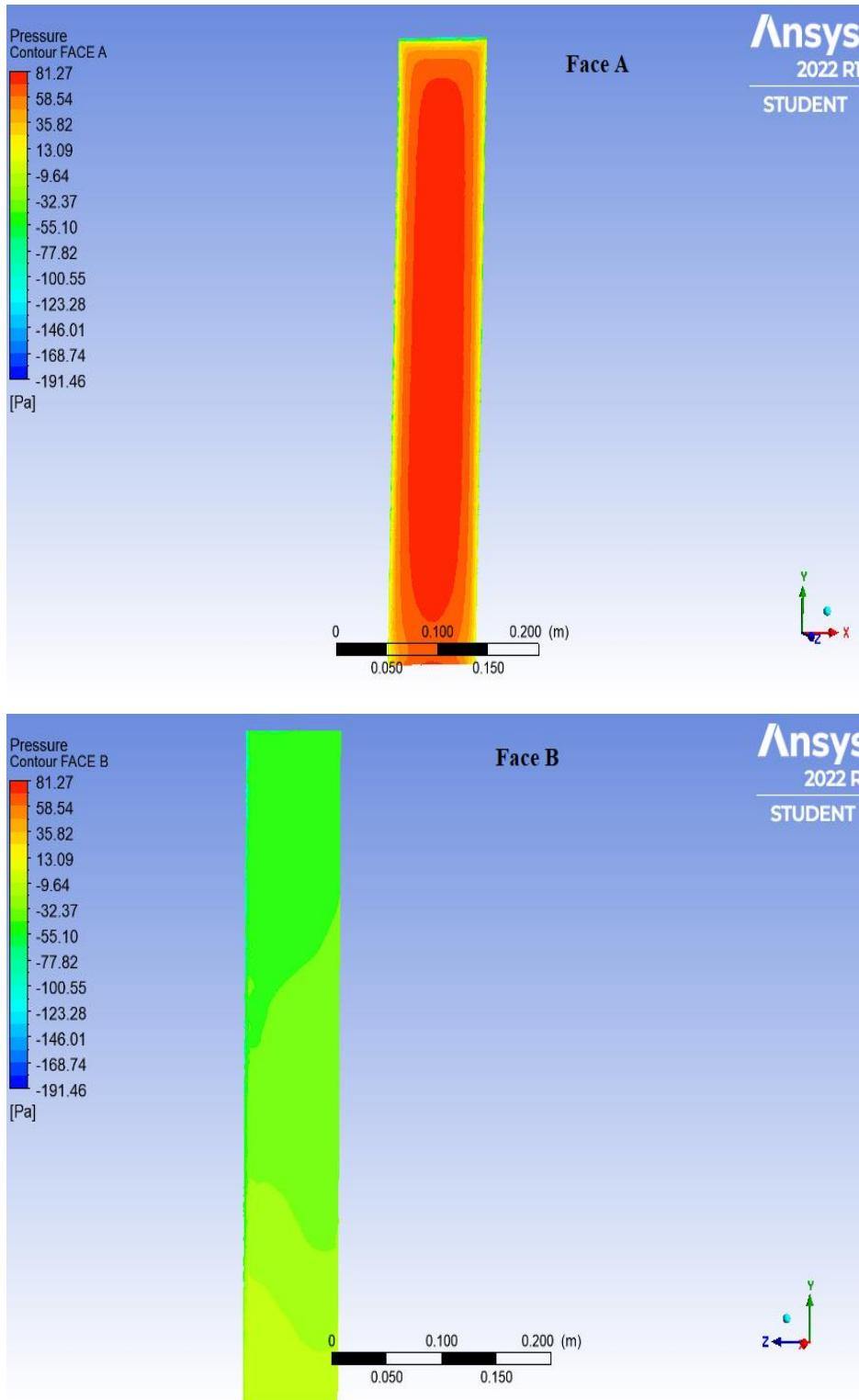


Fig. 4.15 Contour plot for Face A and Face B at 0° angle of wind incidence

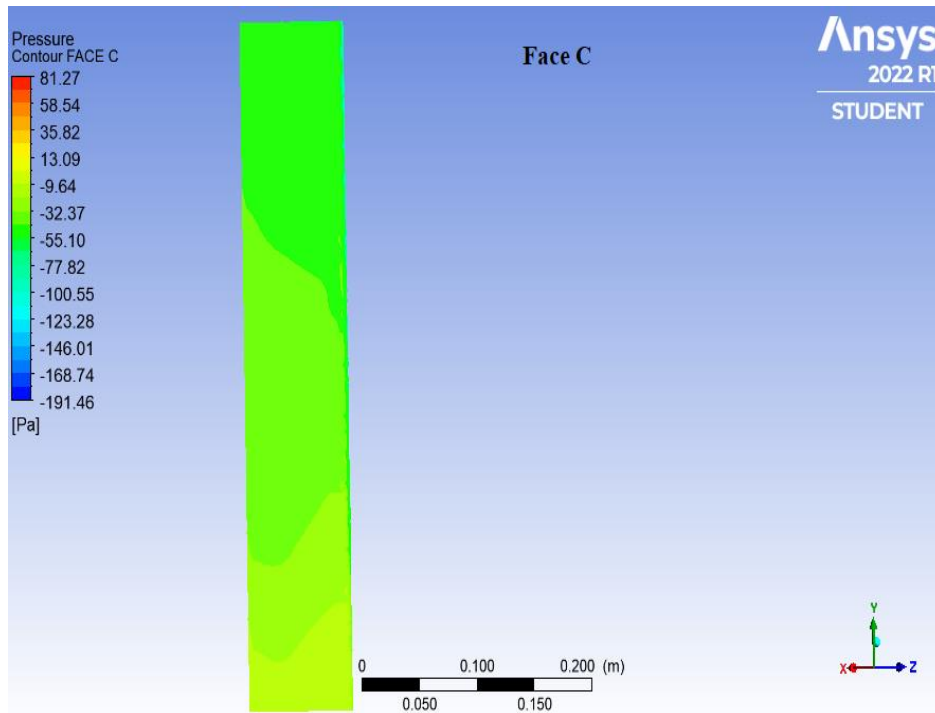


Fig. 4.16 Contour plot for Face C at 0° angle of wind incidence

2. 30° contour plot

Pressure contour of Triangular cross-section at 30° wind incidence angle for Face A, Face B and Face C shown in Fig. 4.17 and Fig 4.18.

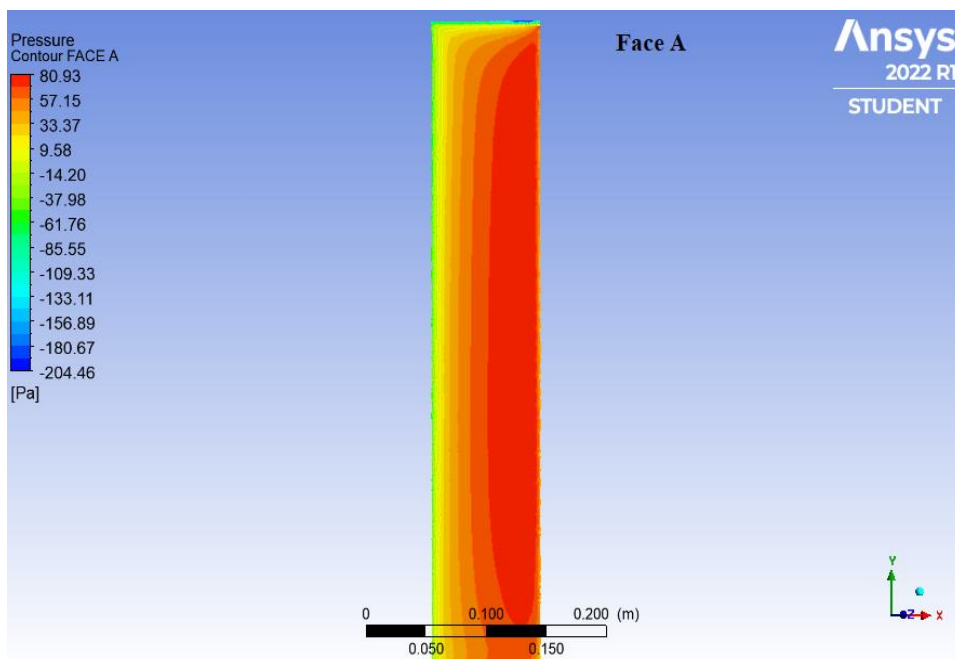


Fig. 4.17 Contour plot for Face A 30° angle of wind incidence

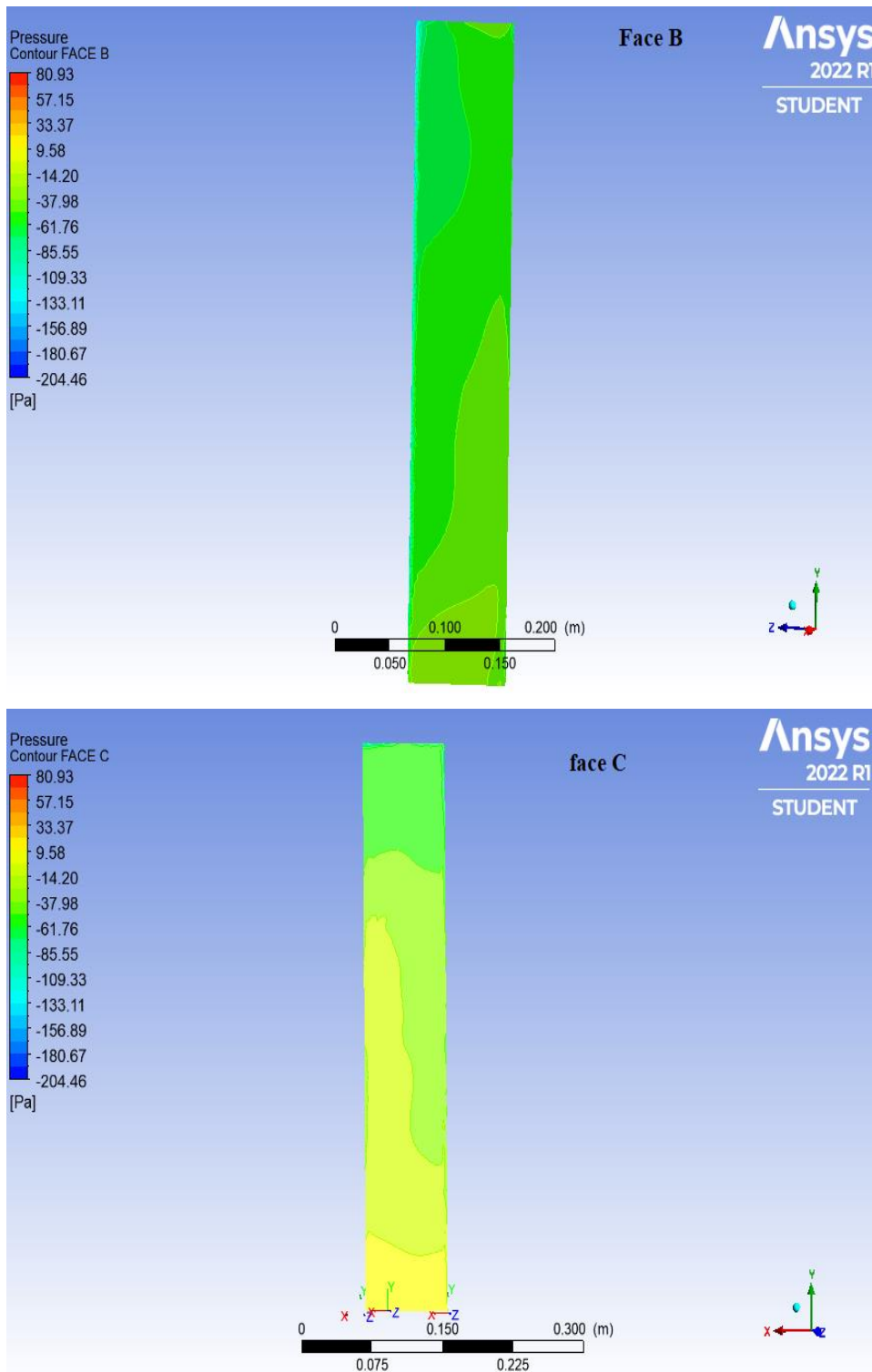


Fig. 4.18 Contour plot for Face B and Face C at 30° angle of wind incidence

3. 60° contour plot

Pressure contour of Triangular cross-section at 60° wind incidence angle for Face A, Face B and Face C shown in Fig. 4.19 and Fig 4.20.

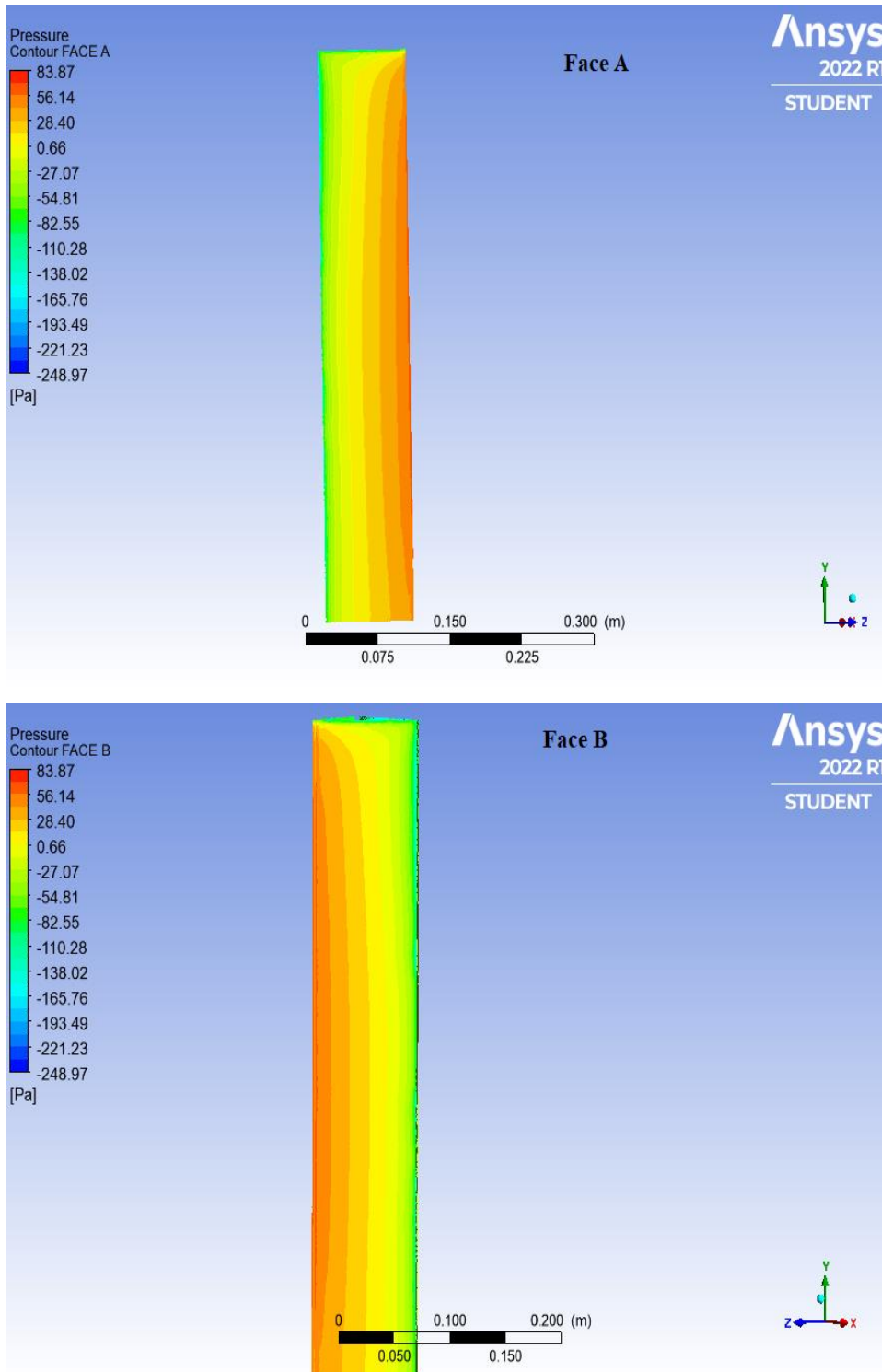


Fig. 4.19 Contour plot for Face A and Face B at 60° angle of wind incidence

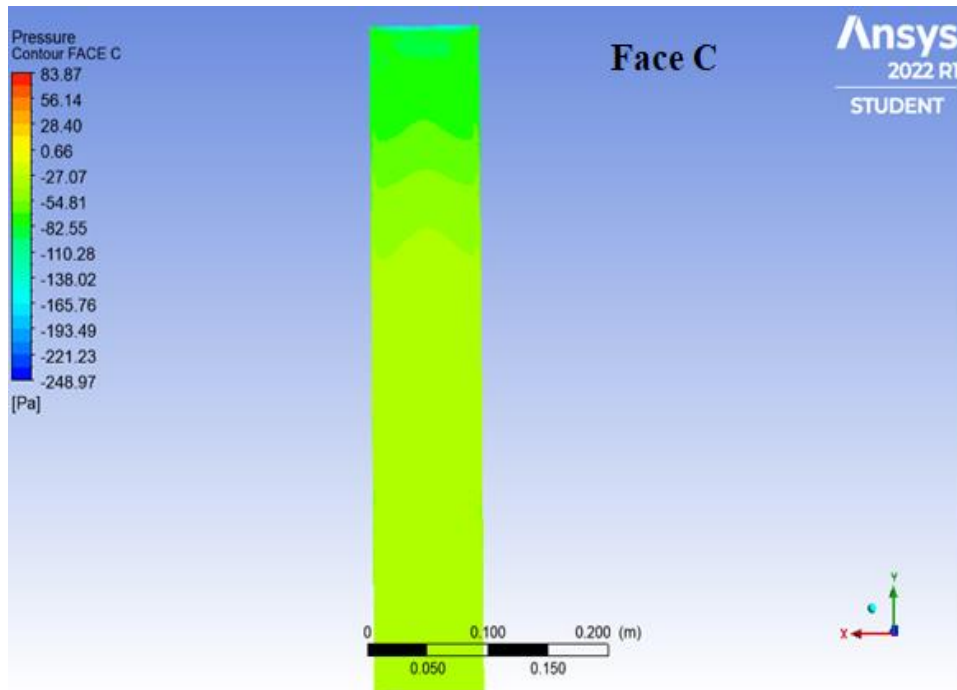


Fig. 4.20 Contour plot for Face C at 60° angle of wind incidence

4. 90° contour plot

Pressure contour of Triangular cross-section at 90° wind incidence angle for Face A, Face B and Face C shown in Fig. 4.21 and Fig 4.22.

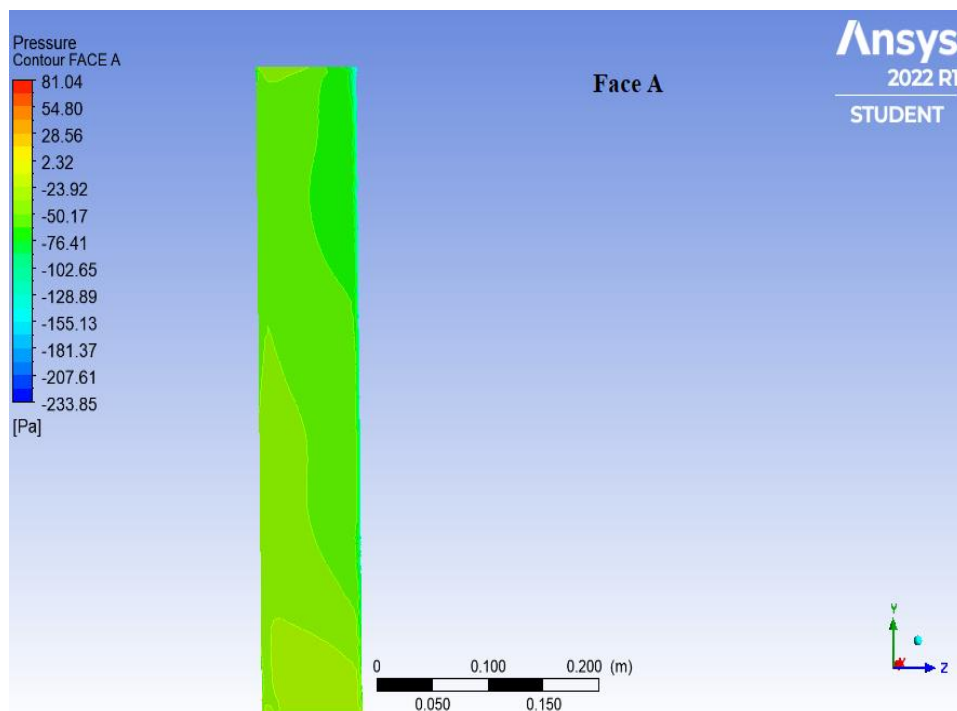


Fig. 4.21 Contour plot for Face A at 90° angle of wind incidence

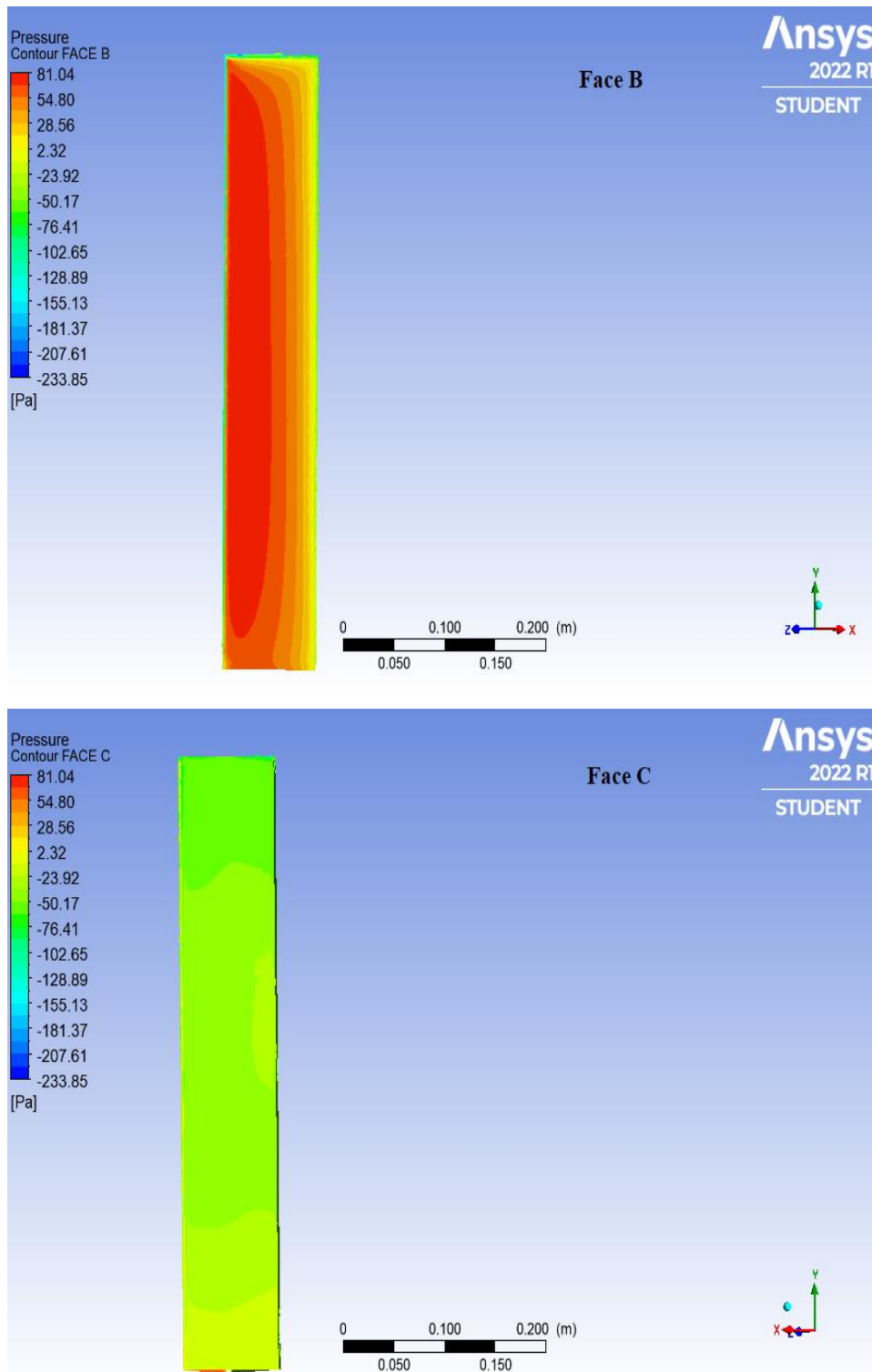


Fig. 4.22 Contour plot for Face B and Face C at 90° angle of wind incidence

5. 120° contour plot

Pressure contour of Triangular cross-section at 120° wind incidence angle for Face A, Face B and Face C shown in Fig. 4.23 and Fig 4.24.

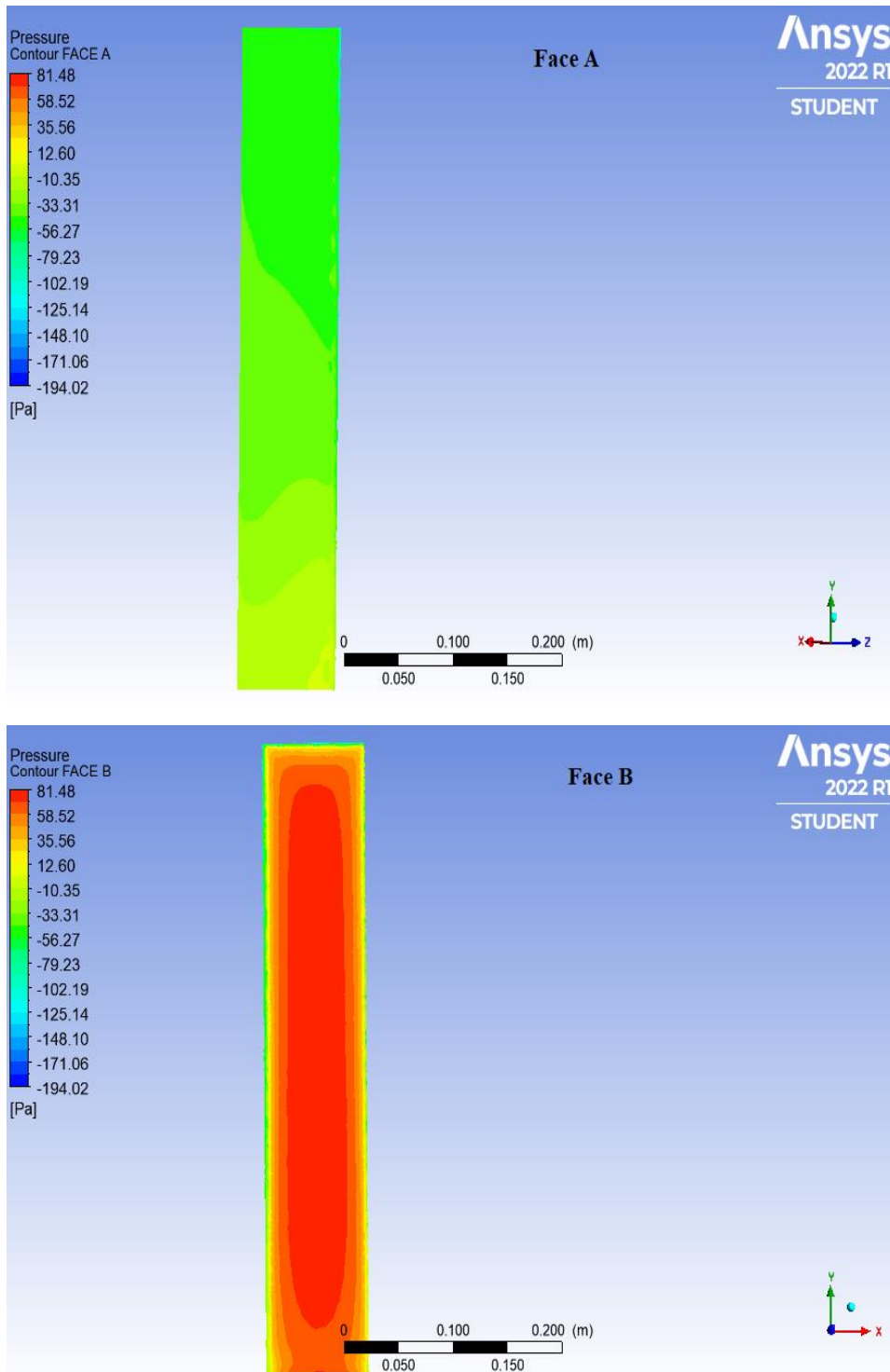


Fig. 4.23 Contour plot for Face A and Face B at 120° angle of wind incidence

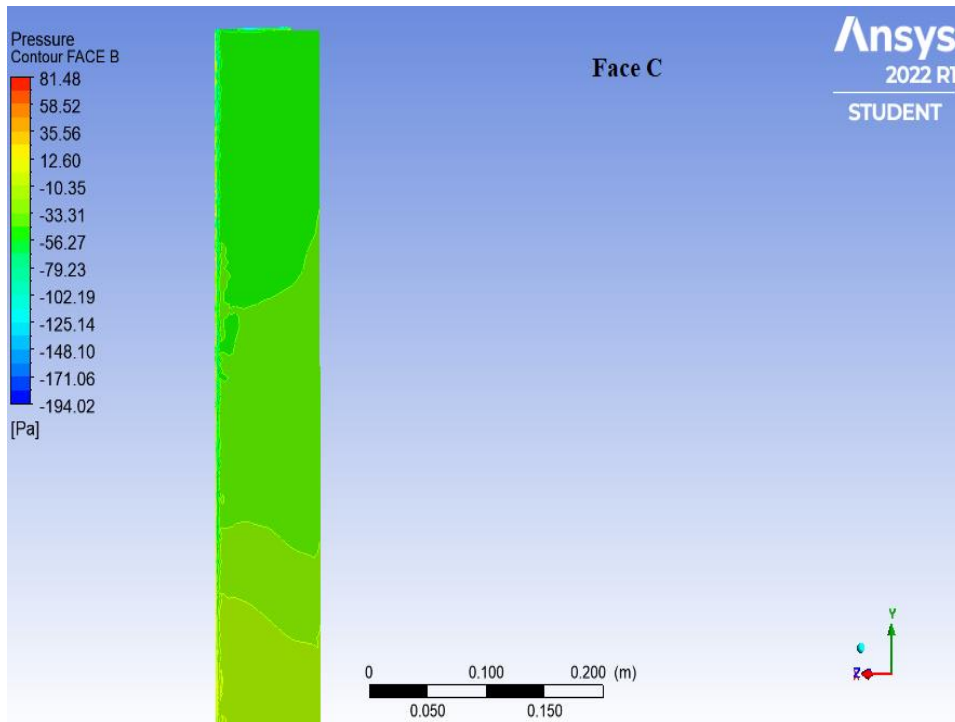


Fig. 4.24 Contour plot for Face C at 120° angle of wind incidence

6. 150° contour plot

Pressure contour of Triangular cross-section at 150° wind incidence angle for Face A, Face B and Face C shown in Fig. 4.25 and Fig 4.26.

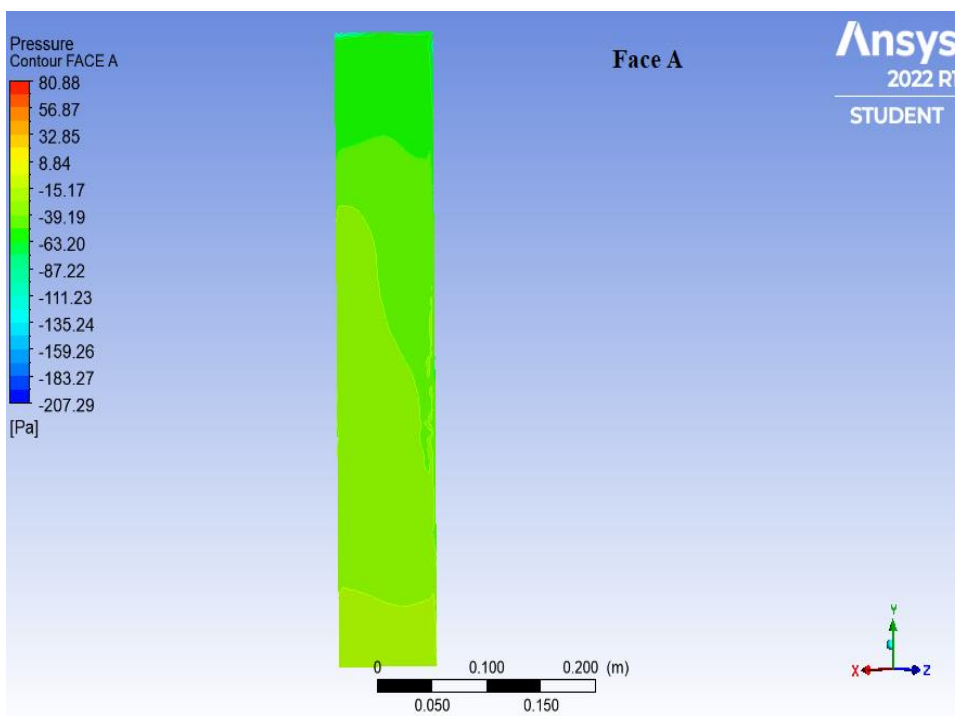


Fig. 4.25 Contour plot for Face A at 150° angle of wind incidence

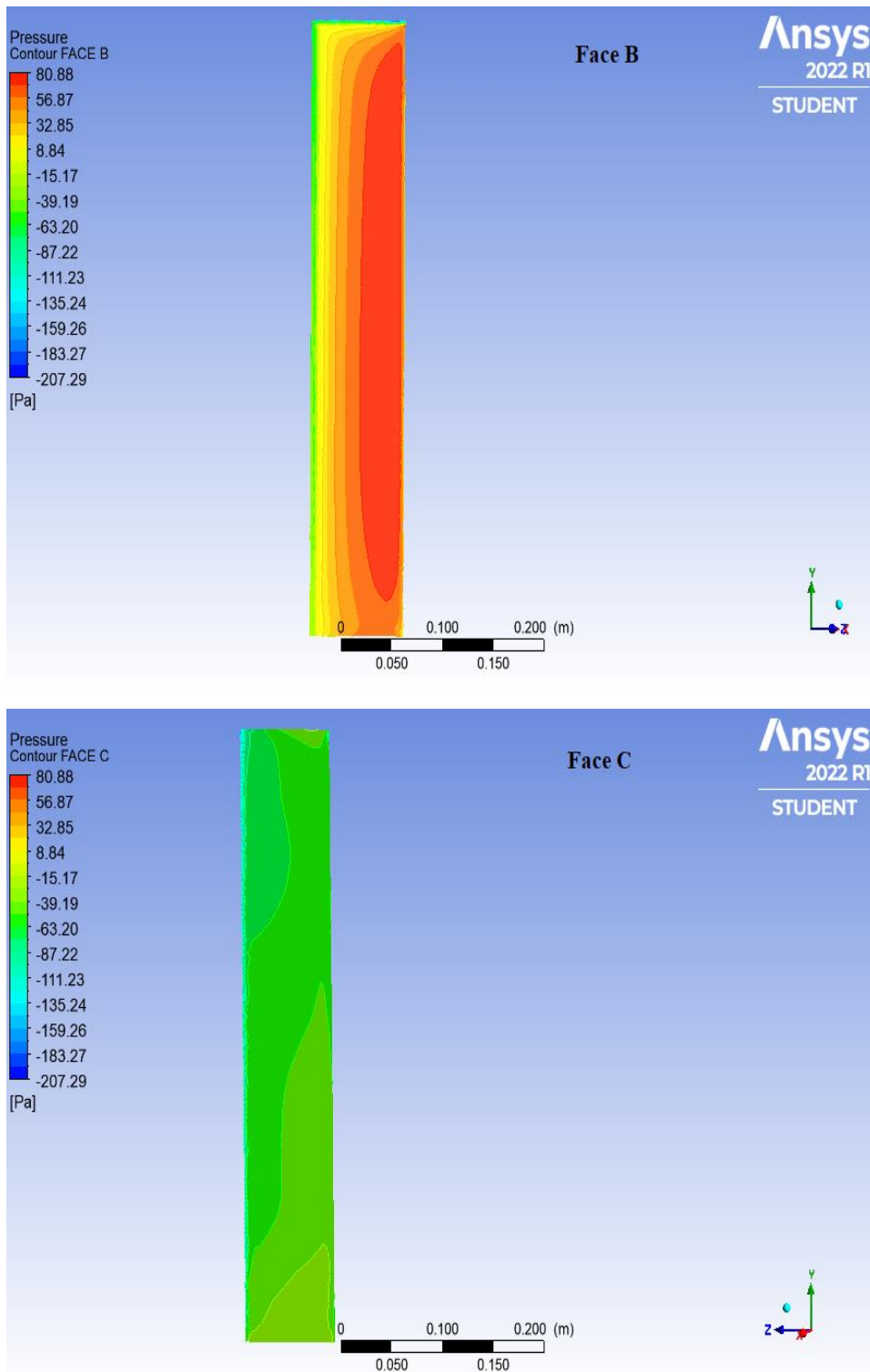


Fig. 4.26 Contour plot for Face B and Face C at 150° angle of wind incidence

7. 180° contour plot

Pressure contour of Triangular cross-section at 180° wind incidence angle for Face A, Face B and Face C shown in Fig. 4.27 and Fig 4.28.

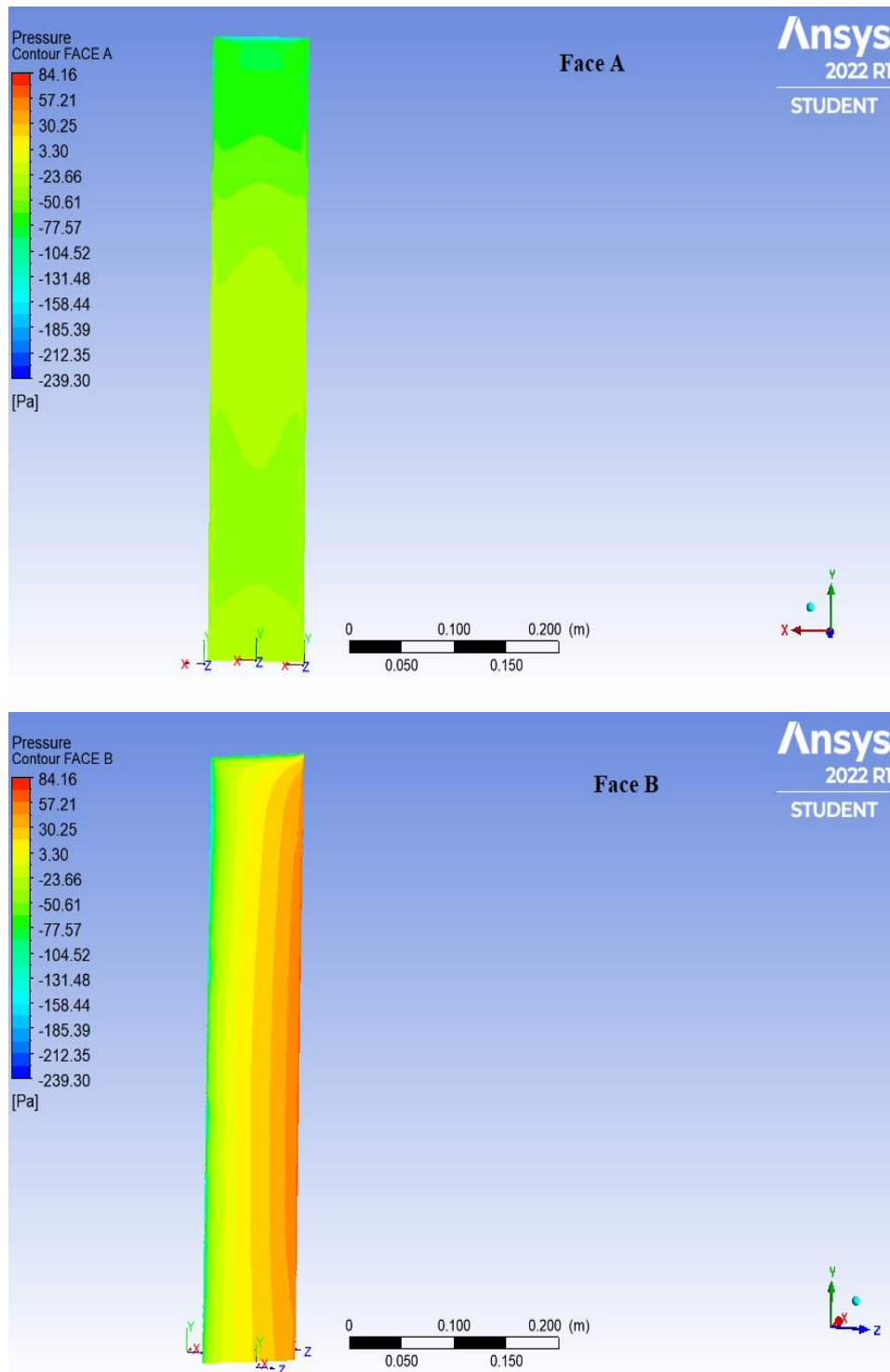


Fig. 4.27 Contour plot for Face A and Face B at 180° angle of wind incidence

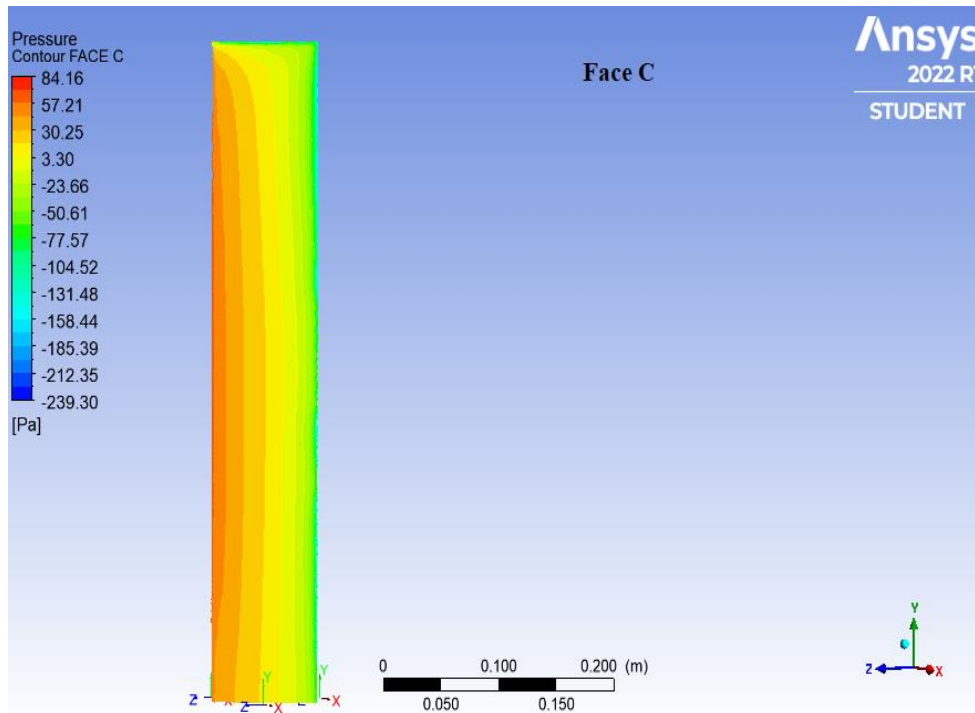


Fig. 4.28 Contour plot for Face C at 180° angle of wind incidence

4.2 Velocity distribution

The velocity variation at various faces of buildings at different angles are as shown in Fig. 4.29- Fig. 4.34 contour plots.

Model 1 – Square cross-section building

- Velocity distribution on different faces at different angles of incidence.
- Wind velocity and pressure are highest on the building's windward side.
- Wind velocity and pressure is varying at different angle of incidence.
- The red line represents the maximum wind velocity and speed, while the blue line represents the minimum wind velocity and speed
- Velocity is maximum at the top i.e. 16.16 m/s and minimum at the bottom of the building.
- Initially, at 0° velocity is maximum as compared to the 15°, 30° and 45° which are having slightly lesser velocity as compared to zero degree of incidence.

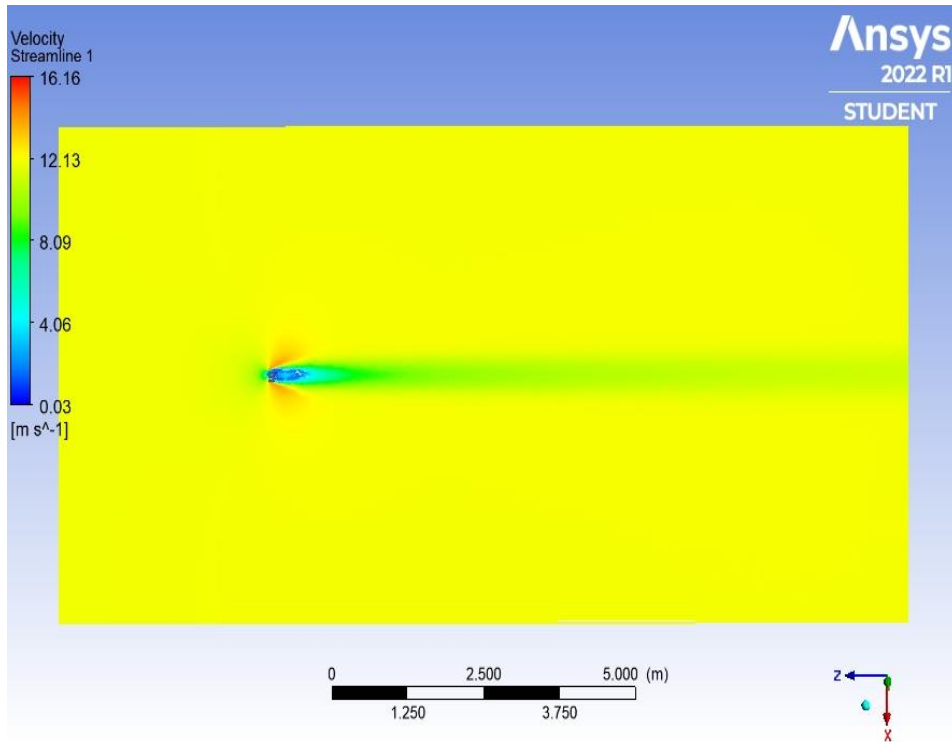
1. 0° wind incidence

Fig. 4.29 Velocity streamline at 0° angle of wind incidence

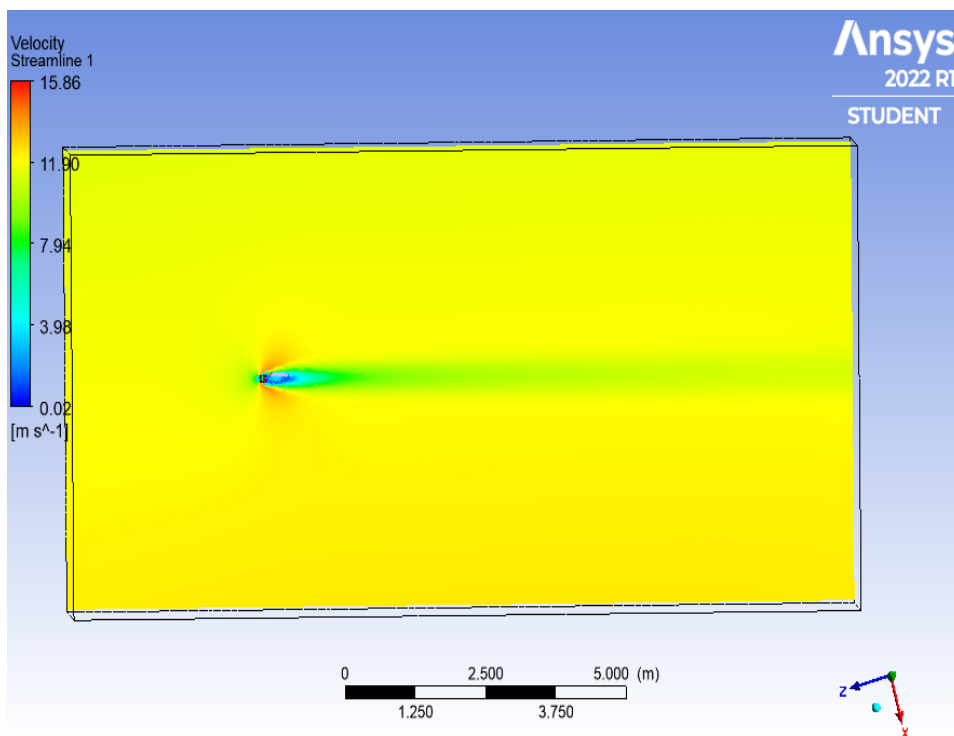
2. 15° wind incidence

Fig. 4.30 Velocity streamline at 15° angle of wind incidence

3. 30° wind incidence

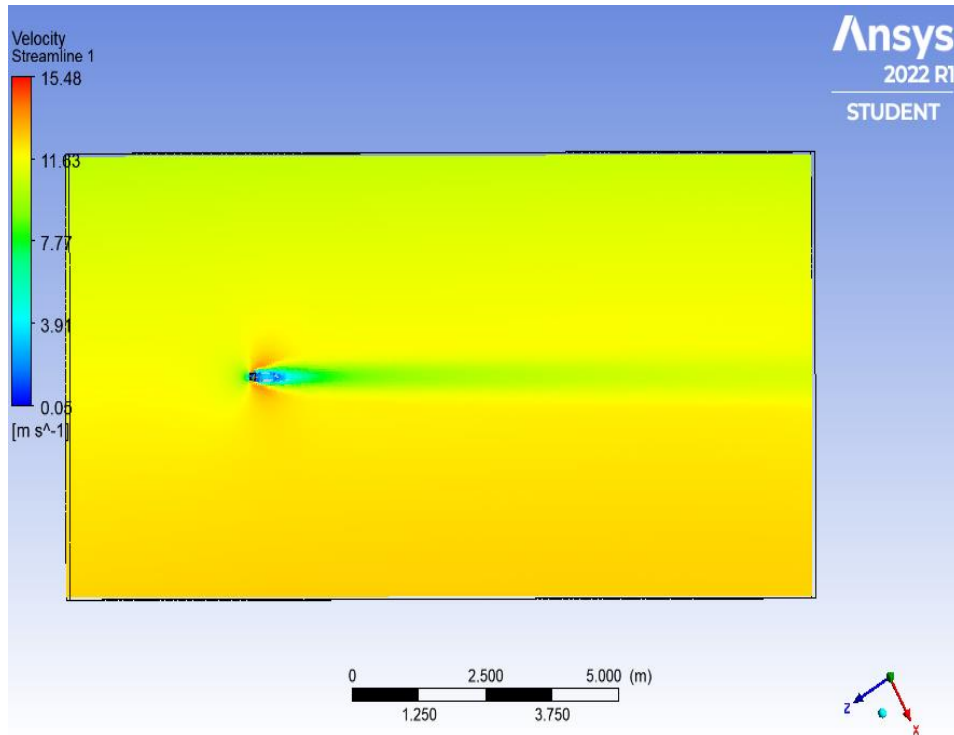


Fig. 4.31 Velocity streamline at 30° angle of wind incidence

4. 45° wind incidence

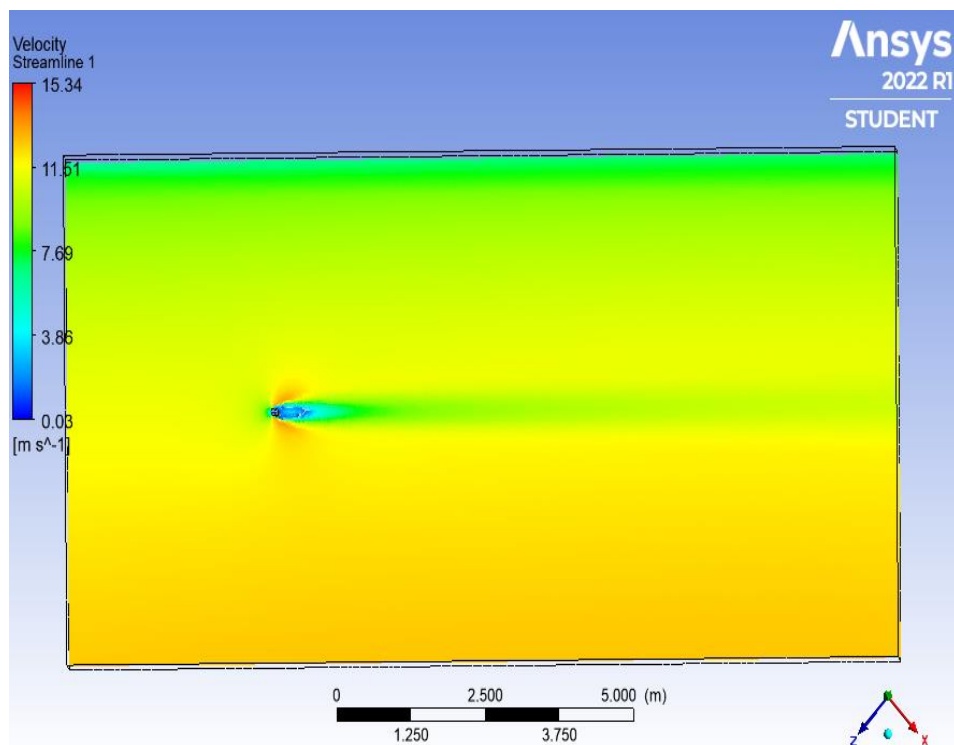


Fig. 4.32 Velocity streamline at 45° angle of wind incidence

5. 60° wind incidence

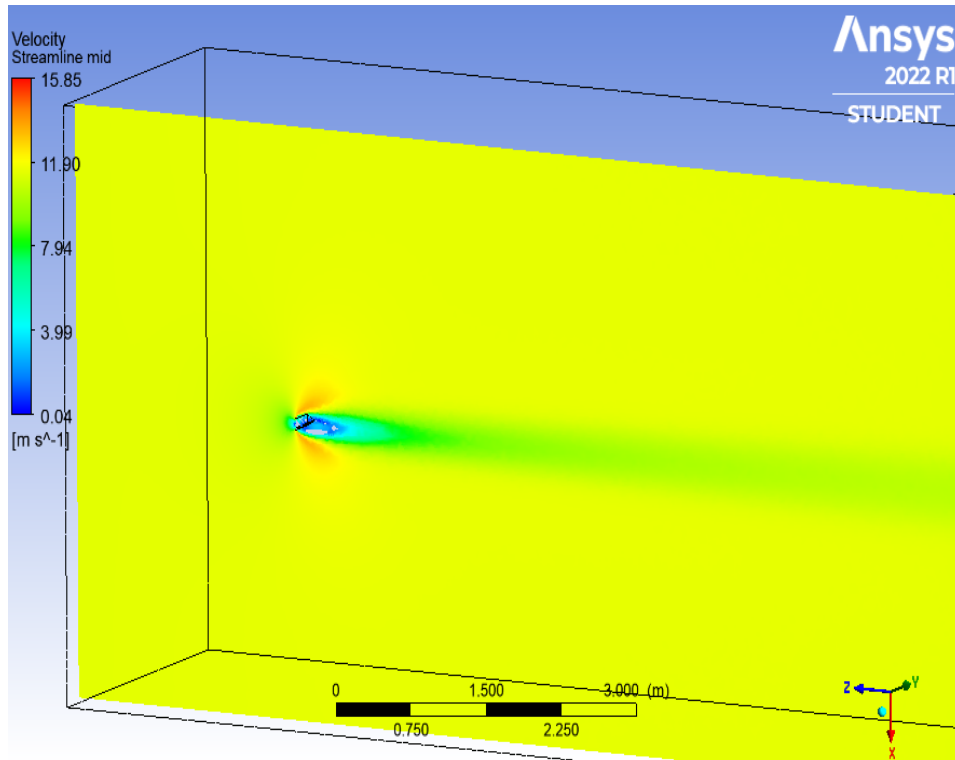


Fig. 4.33 Velocity streamline at 60° angle of wind incidence

6. 90° wind incidence

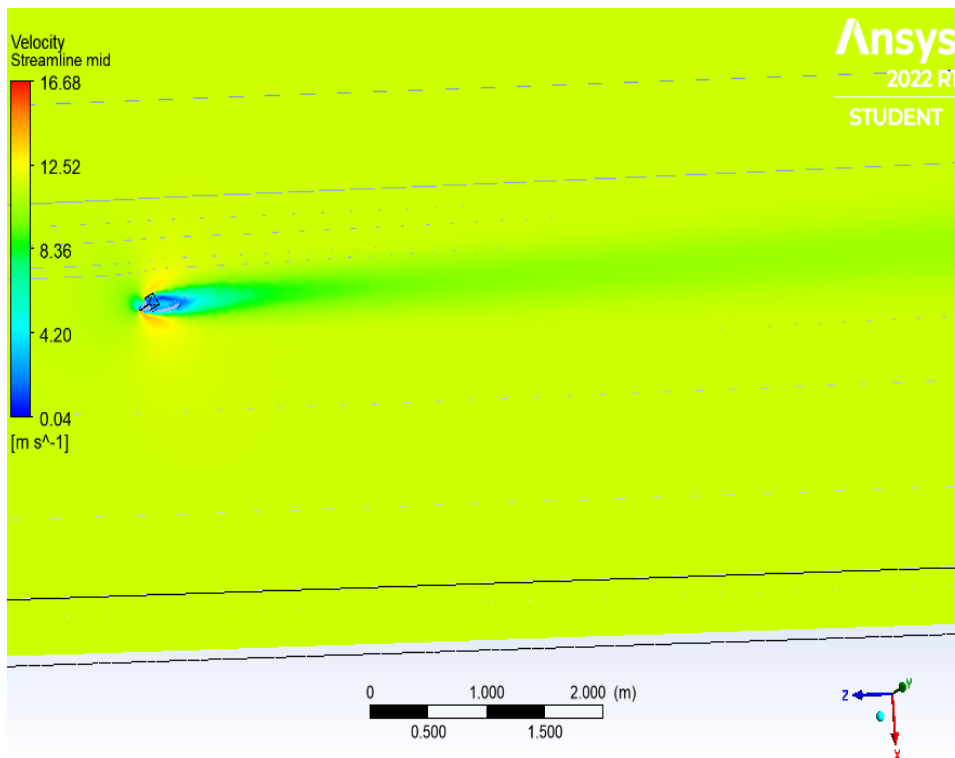


Fig. 4.34 Velocity streamline at 90° angle of wind incidence

Model 2- Triangular-cross section building

- Wind velocity and pressure are highest on the building's windward side.
- Wind velocity and pressure is varying at different angle of incidence.
- The red line in Fig. 4.35- Fig. 4.41 represents the maximum wind velocity and speed, while the blue line represents the minimum wind velocity and speed
- Initially, up to 60° maximum velocity of velocity streamline increases but at 90° , decreases and then again maximum velocity again starts increases up to 180° .

1. 0° wind incidence

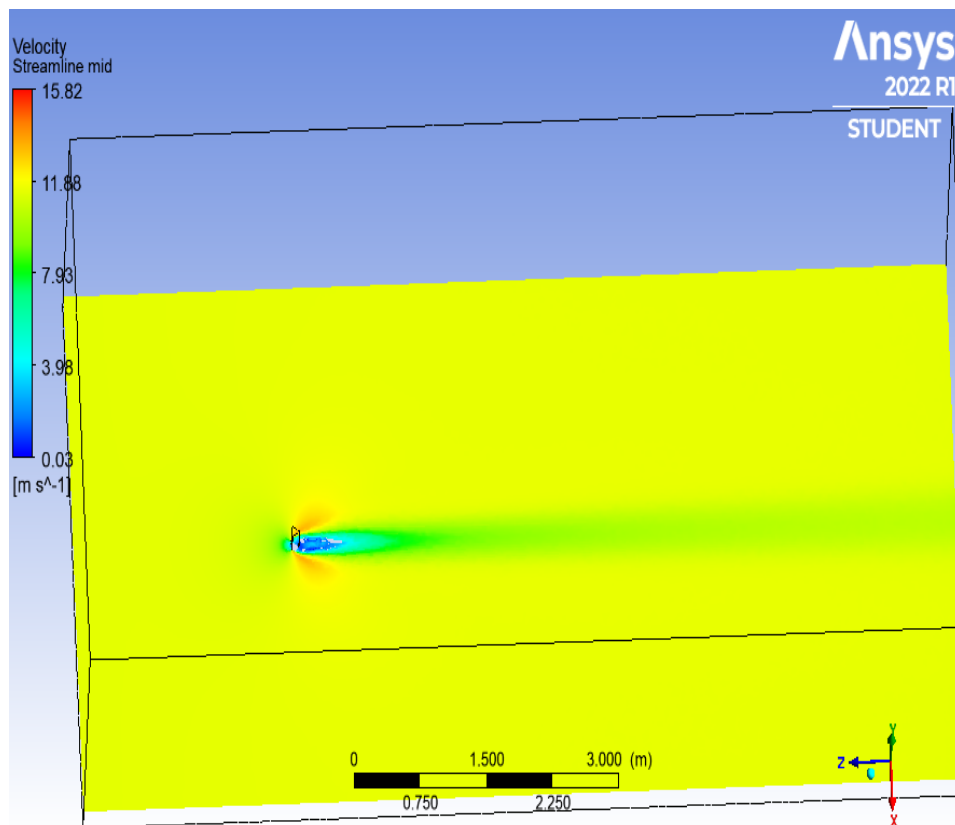


Fig. 4.35 Velocity streamline at 0° angle of wind incidence

2. 30° wind incidence

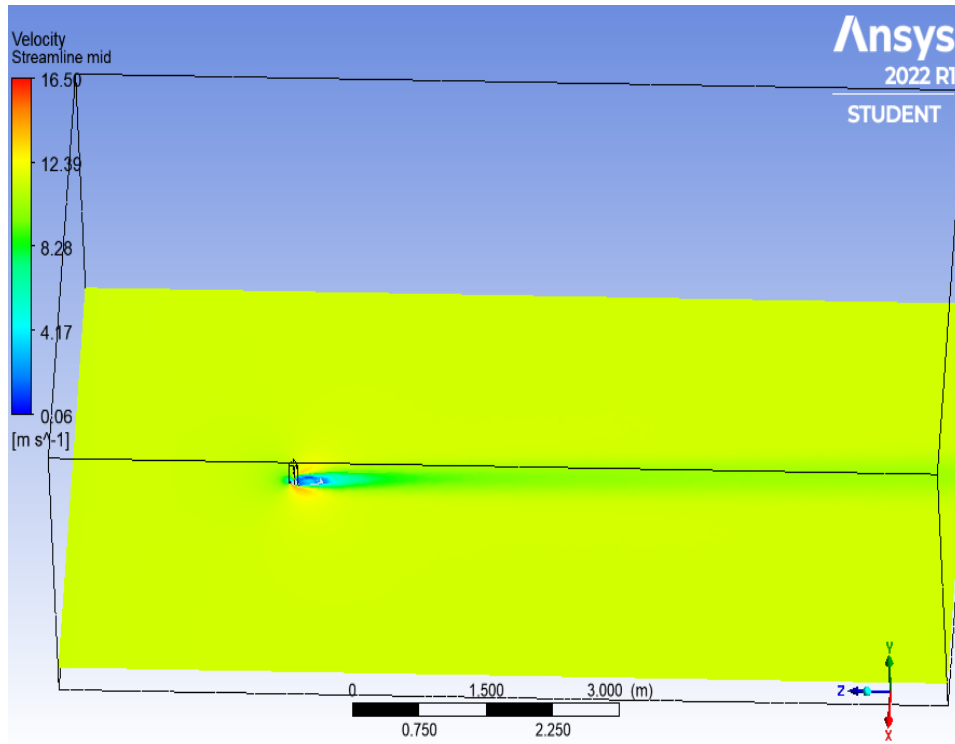


Fig. 4.36 Velocity streamline at 30° angle of wind incidence

3. 60° wind incidence

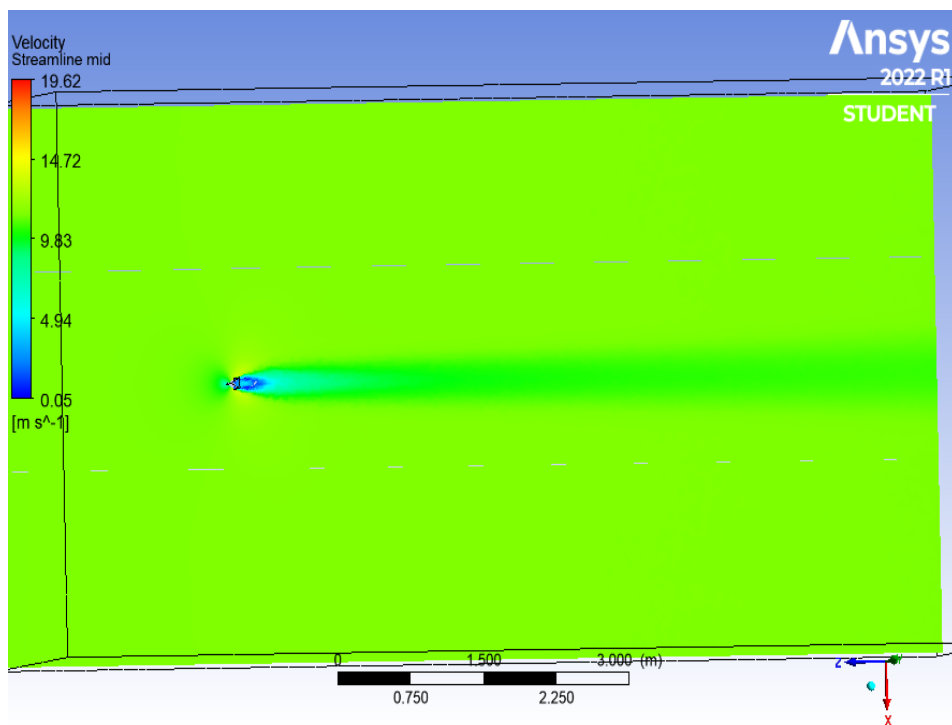


Fig. 4.37 Velocity streamline at 60° angle of wind incidence

4. 90° wind incidence

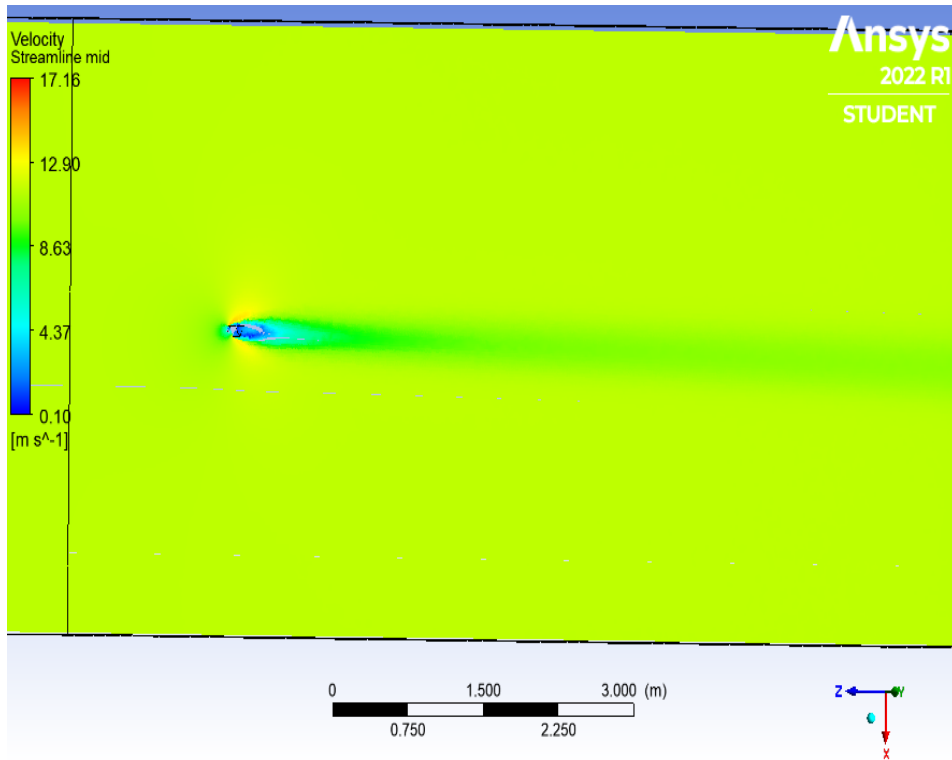


Fig. 4.38 Velocity streamline at 90° angle of wind incidence

5. 120° wind incidence

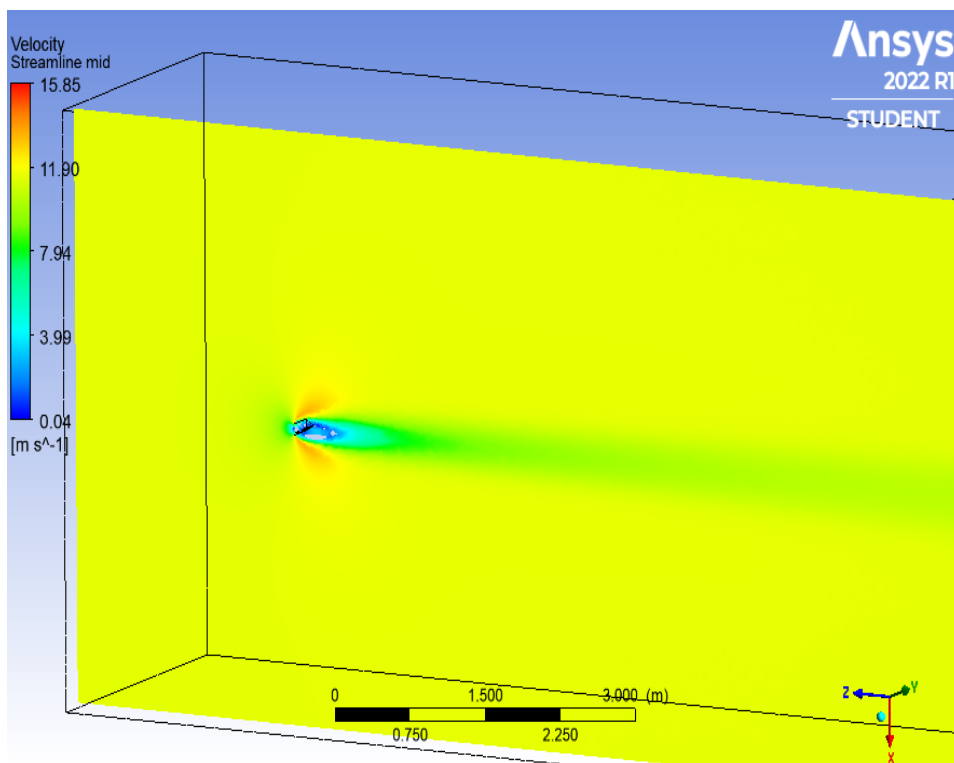


Fig. 4.39 Velocity streamline at 120° angle of wind incidence

6. 150° wind incidence

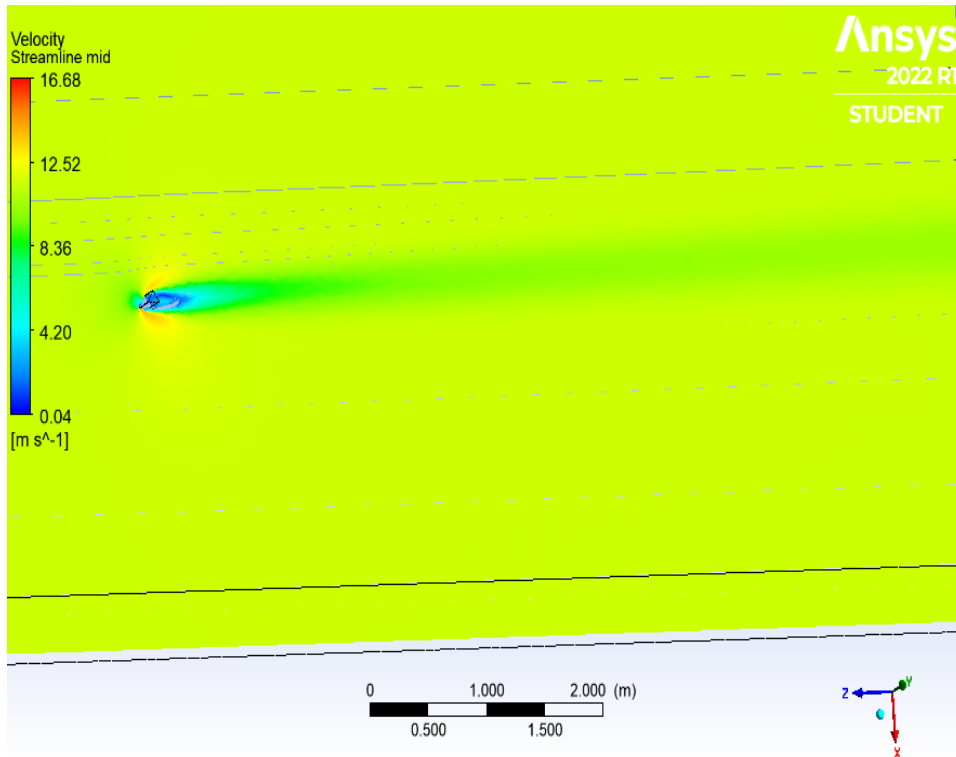


Fig. 4.40 Velocity streamline at 150° angle of wind incidence

7. 180° wind incidence

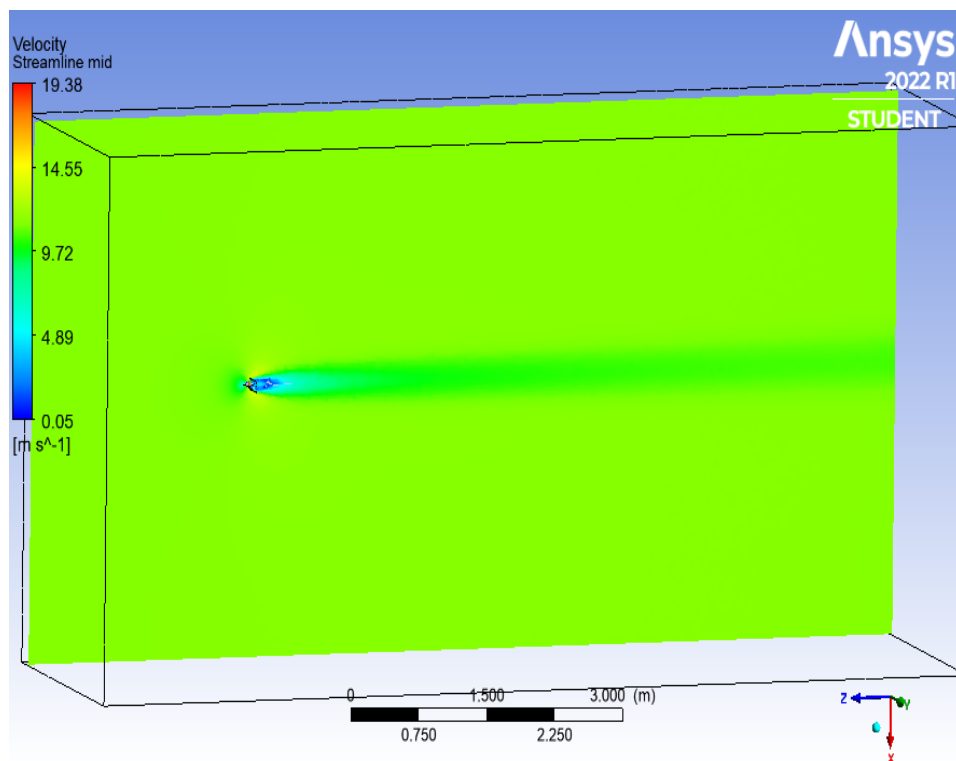


Fig. 4.41 Velocity streamline at 180° wind angle of wind incidence

4.3 Pressure Coefficient

- The variation in the pressure coefficient C_p value for various faces as a function of height. Therefore, the face average value of C_p for several models at various angles of incidence are evaluated.
- The pressure coefficient is defined as

$$C_p = \frac{\Delta P}{\frac{1}{2} \rho U_\infty^2}$$

Where,

$$\Delta P = P - P_o$$

P is the static pressure on the surface of the cylinder

P_o is the ambient pressure

ρ is the density of the air

U_∞ is the free stream velocity

Model 1 Square cross-section building

- Table 4-1 shows that the values of different faces for pressure coefficient C_p given in different standard codes.

Table 4.1: Value of C_p for different codes

Wind loading code	Face- A	Face-B	Face-C	Face-D
By ANSYS CFX	0.799	-0.45	-0.68	-0.9
ASCE 7-10	0.8	-0.5	-0.7	-0.7
AS/NZS-1170.2(2002)	0.8	-0.5	-0.65	-0.65
IS: 875 (part3) (2015)	0.8	-0.25	-0.8	-0.8

- Table 4.2 shows the values obtained in analysis of square cross section building using Ansys CFX.

Table 4.2: Pressure coefficient C_p for different faces at different angles

	0°	15°	30°	45°	60°	90°
Face A	0.799	0.78	0.74	0.69	0.63	-0.78
Face B	-0.45	-0.89	-0.86	-0.84	-0.80	-0.73
Face C	-0.68	-0.67	-0.64	-0.61	-0.58	0.65
Face D	-0.90	-0.92	-0.87	-0.83	-0.79	0.88

- A position on the windward face shows the highest Pressure coefficient of +0.79, and a place on the face parallel to the wind and close to the windward edge shows the lowest pressure coefficient of -0.92.

Model 2- Triangular cross-section building

- The wind pressure distribution on the surface of triangular shape model with fillet corners is found to be dependent on the direction of wind.
- Table 4.3 shows the values obtained in analysis of triangular cross section building using Ansys CFX.

Table 4.3: Pressure coefficient C_p for different faces at different angles

	0°	30°	60°	90°	120°	150°	180°
Face A	0.64	0.59	-0.52	-0.95	-0.66	-0.68	-0.8
Face B	-0.66	-0.95	-0.60	0.6	0.62	0.59	-0.36
Face C	-0.664	-0.68	-0.81	-0.68	-0.67	-0.97	0.59

- The results were also contrasted with those from (**Abdusemed and Ahuja 2015**), which found that at a 90° wind incidence angle, the front surface (Face-B) is subjected to varying pressure with a maximum C_p of 0.6, the leeward surface (Face-A) is subjected to varying suction with a minimum C_p of -0.68, and the side face (Face-C) is subjected to varying suction with minimum C_p of -0.95.
- By Ansys CFX a position on the windward face shows the highest pressure coefficient of +0.64 while a place near the windward face shows the lowest pressure coefficient of -0.97.

5.1 Summary

ANSYS The CFX tool is used to perform analysis by creating an atmosphere tunnel as a model. Airflow is considered to be the liquid that enters air tunnel (Domain). In this research, an analysis of two different cross-sections of the building has been done i.e. square and triangular cross-section building with fillet end corners. Current research is being conducted so to investigate the behaviour of the height of the building under the air load around the building for various angles of wind incidence and by using existing transformations.

Square cross-section building analysis are performed at different wind incidence angle (0, 15°,30°,45°,60° and 90°) while the triangular cross-section building analysis are performed at (0, 30°,60°,90°, 120°,150° and 180°). The pressure distributions for different faces of square and triangular plan buildings are also considered in this present study wind velocity around the square and triangular cross-section shape building are calculated and studied

5.2 Conclusion

This study proved that numerical models are accurate for predicting along wind components. The findings of this study have improved our understanding of the aerodynamic and response characteristics of tall structures with various wind incidence angles. It has been demonstrated that the numerical model's computational fluid dynamics simulations and the outcomes of experiments are accurately performed and studied in this study. The results are more reliable on the leeward face, sidewalls, and windward face. Several modifications to the fluid domain and meshing in models are required to get more converging results. The k-e turbulence model has performed superbly in computer simulations. According to this study, more accurate numerical simulations of the wind can be performed.

- Current research is being conducted so to investigate the behaviour of the height of the building under the wind load and around the building for various angles and by using existing transformations.

- The influence of wind orientations on wind pressure distribution on buildings and magnitude of pressure coefficients on triangular and square building models are identified by numerical study measurement of wind pressures on building models.
- Comparison is made for numerical simulation data with various codes.
- For triangular cross-section with fillet end corners, maximum pressure coefficient of +0.64 magnitude is observed at a point on windward face and minimum pressure coefficient of -0.97 is observed at a point on the face parallel to wind near windward edge.
- For square cross-section building, maximum pressure coefficient of +0.79 is observed at a point on windward face and minimum pressure coefficient of -0.92 is observed at a point on the face parallel to wind and near to windward edge.

5.3 Future scope

Structures have been designed in large part using wind force. So, while designing structures prone to wind forces, wind load has to be considered. More over with this research it is clear that wind load calculation while designing is very necessary. Further study can be done to find out the variations in pressure coefficient and pressure variations with increase in the height of the structures. Also work can be done in finding out the pressure coefficient and pressure variation with changes in the velocity of the wind. Further study can be done to find out the force coefficient for high rise building.

LITERATURE CITED

- Abdusemed, M.A., and Ahuja, A.K. 2015.** Wind Pressure Distribution on Triangular Shape Tall Buildings. *Int. j. innov. res. technol. sci. eng.*, 4(8):502-507.
- American Standard ASCE 7-02 2007.** Minimum Design loads for buildings and other structures, American Society of Civil Engineers, New York.
- Arya, U., Hussain, A. and Khan, W. 2014.** Wind Analysis of Building Frames on Sloping Ground. *Int. J. Sci. Res.*, 4(5):102-108.
- Australia and New Zealand AS/NZS 1170.2: 2021.** Structural Design Action, Part 2: Wind Actions, Australian, New-Zealand Standard, Sydney, Wellington.
- Bhattacharyya, B. and Dalui, S. K, 2015.** Along and Across Wind effects on Irregular Plan Shaped Tall Building. *Struct. Des. Tall. Spec. Build.*, 86(24): 72-80.
- British standard 6399- 2:1997:** Loading for building- Part 2: Code of Practice for wind loads; BS British Standard Institution, London.
- Chakraborty, S., Dalui, S. K. and Ahuja A. K. 2013.** Experimental and Numerical Study of Surface Pressure on '+' Plan Shape Tall Building. *Int. J. Concr. Struct. Mater.*, 8(11): 321-329.
- Dagneu, A. K., and Bitsuamlak, G. T. 2014.** Computational evaluation of wind loads on a standard tall building using LES. *Wind Struct. Int. J.*, 18(5): 567-598.
- Davenport, A.G. 1963.** The Relation to wind Structure to Wind Loading. *In: Proceedings of the Conference on Wind Effects on Buildings and Structures*, during June 1963 1 pp. 123-129.
- European Committee for Standardization EN 1991-1- 4:2005.** Eurocode 1: Actions on structures – Part 1–4: General actions – wind actions
- Frank, J., Hirsch, k., and Wright, N.G. 2004.** Recommendations on the use of CFD in wind engineering., *In: Conference on Urban Wind Engineering and Building Aerodynamics* at Atsugi, Japan, March 8-9 pp. 250-261.

- IS:456. 2000.** Indian Standard Plain and Reinforced Concrete - Code of Practice. Bureau of Indian Standard, New Delhi, India.
- IS:875, Part 1. 1987.** Indian Standard Code of Practice for Dead Loads for buildings and Structures. Bureau of Indian Standards, New Delhi, India.
- IS:875, Part 2. 1987.** Indian Standard Code of Practice for Imposed Loads for buildings and Structures. Bureau of Indian Standards, New Delhi, India.
- IS:875, Part 3. 2015.** Indian Standard Code of Practice for Design Wind Load on Buildings and Structures, Second Revision, New Delhi, India.
- IS-875, Part 4. 1987.** Indian Standard Code of Practice for Design Snow Loads for buildings and Structures. Bureau of Indian Standards, New Delhi, India.
- Javed, M. and Satish, K. 2020.** Enhancement of Tall Buildings Under the Wind Load. *Int. J. Eng. Res.*, 9(6): 184-186.
- Kumar, H. S. and Reddy, V. B 2017.** Pressure Measurement Studies on a 1:1.5:7 Rectangular High-rise Building Model under Uniform Flow. *In: IOP Conference Series Materials Science and Engineering* during. September 15-19 pp. 225-230.
- Li, Y., Li, Y. G., LI, Q.S. and Tee, K.F. 2018.** Investigation of wind effect reduction on square high-rise buildings by corner modification. *Adv. Struct. Eng.*, 1(13): 102-107.
- Liu, M. 2012.** 3D Numerical Simulation of Flow Perpendicular to One Face of a Cube in a Straight Rectangular Duct. *Appl. Mech. Mater.*, 130(21): 2681-2683.
- Mendis, P., Gunawardena, T., Karunaratne, R., and Ngo, T. 2017.** Prefabricated Construction Technologies for the Future of Sri Lanka's Construction Industry. *In: The 7th International Conference on Sustainable Built Environment*, at Earl's Regency Hotel, Kandy, Sri Lanka during. December 16-18 pp. 105-110.
- Meroney, R. N., Klein, P., Rau, M. and Leitzl, B. M., 1999.** Concentration and flow distributions in the vicinity of U-shaped buildings wind-tunnel and computational data. *J. Wind. Eng. Ind. Aerodyn.*, 67(12): 745-755.

- Muffassir, S. and Kalurkar, L.G. 2016.** Comparative Study on Wind Analysis of Multi-story RCC and Composite Structure for Different Plan Configuration. *j. mech. civ. Eng.*, 13(4): 42-49.
- Murakami, S., Mochida, A. and Hibi, K. 1988.** Three-dimensional numerical simulation of airflow around a cubic model by means of large eddy simulation. *J. Wind. Eng. Ind. Aerodyn.*, 25(10): 291-305.
- Raj, R., and Ahuja, A. K. 2013.** Wind Loads on Cross Shape Tall Buildings. *J. Acad. ind. res.*, 2(2): 100-108.
- Raj, R., Rukhaiyar, A. Jayant, B., Dahiya, K. 2022.** “CFD Analysis for wind flow characteristics of varying cross section tall building using ANSYS. *Research Square.*, 67(10): 568-573
- Reddy, K. R. C. 2015.** Along wind analysis of reinforced concrete chimneys. *Int. J. Eng. Res. Technol.*, 4(13): 87-94.
- Roy, K., and Kumar B. A. 2016.** Wind Pressure and Velocity Around Stepped Unsymmetrical Plan Shape Tall Building Using cfd Simulation - A Case Study. *Asian J. Civ. Eng.*, 17(8): 1055 To 1075.
- Sanyal, P. and Dalui, S.K. 2021.** Supervision Effects of internal angle between limbs of “Y” plan shaped tall building under wind load. *J. Build. Eng.*, 5(15): 56-89
- Sevaliaa, J.K., Desaib A. K. And Vasanwala, S. A. 2012.** Effect of Geometric Plan Configuration of Tall Building on Wind Force Coefficient Using cfd. *Int. J. Adv. Eng.*, 1(8):127-130.
- Tamura, T. and Kawai, H. 1997.** Numerical Prediction of Wind Loading on Structures and Buildings. *J. Wind. Eng. Ind. Aerodyn.*, 68(15): 671-685.
- Tang, J. W., Xie, Y. M., Felicetti, P., Tu, J. Y. and Li, J. D. 2013.** Numerical simulations of wind drags on straight and twisted polygonal buildings. *Struct. Des. Tall. Spec. Build.*, 56(14): 62–73.

Verma, S. K., Ahuja, A. K. and Pandey, A. D. 2013. Effects of wind incidence angle on wind pressure distribution on square plan tall buildings. *J. Acad. Indus. Res.*, 1(12): 234-242.

Yadav, V. and Jignesh A. B. 2016. Recent Advances in Civil Engineering for Global Sustainability. *Int. j. eng. res. dev.*, 8(16): 75-82.

2. Vaibhav Saxena and Astha Verma, Wind load on a Triangular Cross-Section Tall Building Using Ansys”, “International Journal of All Research Education and Scientific Methods (IJARESM)”, Volume 10 issue 7, July 2022

Software Skills: AutoCAD, Ansys.

Professional Skills: Communication and Motivational Skill.

Professional Affiliations (Membership, etc.): NIL

Awards/Honours/Achievement: NIL

Place: Pantnagar, Uttarakhand

Date: September, 2022



(Vaibhav Saxena)

Name : Vaibhav Saxena **Id No.** : 56974
Semester & year of admission : 1st sem, 2020-21 **Degree** : M.Tech (Civil Engg.)
Major : Structural Engineering **Department** : Civil Engineering
:
Thesis Title : “Effect of Wind Load on Various Geometrical Tall Buildings”
Page No. : 74 **Advisor** : Dr. Astha Verma

ABSTRACT

Square cross-section building analysis at different angle (0, 15°,30°,45°,60° and 90°) while the triangular cross-section building analysis at (0, 30°,60°,90°, 120°,150° and 180°). The pressure distributions for different faces of square and triangular plan buildings, wind velocity around the square and triangular cross-section shape building are calculated. To examine how the height of a building would behave when there is a wind load surrounding it from different angles and using pre-existing transformations. By measuring wind pressures on building models numerically, it is possible to determine how wind orientations affect the distribution of wind pressure on structures and the size pressure coefficients on triangular and square building models. For triangular cross-section with fillet end corners, Maximum pressure coefficient of +0.64 is observed at a point on windward face and minimum pressure coefficient of -0.97 is observed at a point on the face parallel to wind near windward edge. For square cross-section building, Maximum pressure coefficient of +0.79 is observed at a point on windward face and minimum pressure coefficient of -0.92 is observed at a point on the face parallel to wind and near to windward edge.



(Astha Verma)
Advisor



(Vaibhav Saxena)
Author

नाम	: वैभव सक्सेना	परिचयांक	: ५६९७४
सत्र एवं प्रवेश का वर्ष	: प्रथम सेमेस्टर, २०२०-२१	उपाधि	: एम.टेक (सिविल इंजीनियरिंग)
मुख्य विषय	: स्ट्रक्चरल इंजीनियरिंग	विभाग	: सिविल इंजीनियरिंग
शोध का शीर्षक	: “विभिन्न ज्यामितीय लंबा भवन पर पवन भार का प्रभाव”		
पृष्ठ संख्या	: ७४	सलाहकार	: डॉ आस्था वर्मा

सारांश

विभिन्न कोणों (0° , 15° , 30° , 45° , 60° और 90°) पर स्ववायर क्रॉस-सेक्शन बिल्डिंग विश्लेषण (0° , 30° , 60° , 90° , 110° , 130° और 160°) पर त्रिकोणीय क्रॉस-सेक्शन बिल्डिंग विश्लेषण। वर्ग और त्रिकोणीय योजना भवनों के विभिन्न चेहरों के लिए दबाव वितरण, वर्ग के चारों ओर हवा के वेग और त्रिकोणीय क्रॉस-सेक्शन आकार की इमारत की गणना की जाती है। यह जांचने के लिए कि विभिन्न कोणों से और पूर्व-मौजूदा परिवर्तनों का उपयोग करते हुए किसी भवन के चारों ओर हवा का भार होने पर भवन की ऊंचाई कैसे व्यवहार करेगी। मॉडल के निर्माण पर हवा के दबाव को संख्यात्मक रूप से मापकर, यह निर्धारित करना संभव है कि हवा का झुकाव संरचनाओं पर हवा के दबाव के वितरण और त्रिकोणीय और वर्ग निर्माण मॉडल पर आकार के दबाव गुणांक को कैसे प्रभावित करता है। पट्टिका अंत कोणों के साथ त्रिकोणीय क्रॉस-सेक्शन के लिए $+ 0.64$ का अधिकतम दबाव गुणांक विंडवर्ड फेस पर एक बिंदु पर देखा जाता है और $- 0.37$ का न्यूनतम दबाव गुणांक हवा के किनारे के पास हवा के समानांतर चेहरे पर एक बिंदु पर मनाया जाता है। स्ववायर क्रॉस-सेक्शन बिल्डिंग के लिए, विंडवर्ड फेस पर एक बिंदु पर $+ 0.79$ का अधिकतम दबाव गुणांक मनाया जाता है और $- 0.31$ का न्यूनतम दबाव गुणांक हवा के समानांतर और हवा के किनारे के पास चेहरे पर एक बिंदु पर मनाया जाता है।



(डॉ आस्था वर्मा)
सलाहकार



(वैभव सक्सेना)
लेखक